IN VIVO AND *IN VITRO* REGULATION OF PLASMINOGEN ACTIVATOR INHIBITOR TYPE-1.

by Dr. Mark R. Keeton (M.B.Ch.B.).

Thesis Presented for the Degree of

DOCTOR OF PHILOSOPHY

in the Department of Clinical Science and Immunology

UNIVERSITY OF CAPE TOWN

March 1992.

ABSTRACT.

The human leukaemic cell line, K562 can be induced to differentiate along the megakaryoblastic pathway by the addition of phorbol myristate acetate and, during this process, the cells switch from producing a mixture of active tissue plasminogen activator (t-PA) and urokinase (u-PA) to producing active u-PA alone. I performed a series of experiments designed to examine the mechanism of down regulation of t-PA activity that occurred with differentiation. The results of these experiments showed that, in the K562 system at least, differentiation-linked changes in t-PA activity are incidental to plasminogen activator inhibitor type-1 (PAI-1) synthesis and release and that the inhibitor is a critical regulatory protein in this model system.

I therefore chose to study the regulation of PAI-1 both *in vitro* and *in vivo*. To perform the *in vitro* regulation studies, DNA constructs derived from the PAI-1 promoter and 5' flanking sequence were cloned upstream of a luciferase reporter gene. These constructs were transfected into human hepatoma cells, the cells treated with TGFß for 24 hours after which luciferase activity was measured as a function of promoter activity. The active regions were also analyzed by gel retardation to investigate the transcription factors that bound to these regions. The functional data taken together with the DNA binding data supported the hypothesis that the response of the PAI-1 promoter to TGFβ was mediated by two conserved regions of the promoter and 5'

flanking sequence, both of which contain DNA sequences with homology to the activator protein-1 (AP-1) consensus sequence.

I then focused on a single region from the PAI-1 5' flanking region in an attempt to define the role of the AP-1-like sites in the TGFß response. The direct response of this region to AP-1 was assessed by co-transfection of plasmids containing the genes for c-fos and c-jun together with the PAI-1/reporter constructs. My data indicates that the full TGFß response of this region of the PAI-1 promoter is dependent on the interaction of two distinct binding sites. Although the first site has homology to the AP-1 site, it does not appear to bind AP-1. While this site does not appear to be essential, it is required for the full TGFß response of this region. The second site, located 5' to the AP-1 site, appears to be critical in the TGFß response. This site is 15bp in length and contains a motif that is present in both active regions of the PAI-1 promoter. This novel sequence does not appear to correspond to any previously described transcription factor binding site and may represent a new and specific binding site which is critical for a strong TGFß response.

My in vivo studies were aimed at determining the sites of PAI-1 synthesis in the normal mouse and then examining how these changed during diseases known to have a predisposition to thrombosis. I used an acute phase model in which mice were injected with endotoxin. *In situ* hybridization and immunhistochemical analysis revealed that the normal animal produced a low level of PAI-1 and this was confined

primarily to smooth muscles cells of the vessel wall. In contrast, following injection with endotoxin, there was a large increase in PAI-1 synthesis by vascular endothelium throughout the animal. I also studied the distribution of PAI-1 in a more chronic model of renal disease. This study of murine lupus nephritis (LN) demonstrated a number of unique features about the expression of PAI-1 in vivo. First of all, I found the chronic expression of PAI-1 in a disease in which coagulation is a prominent feature. I showed that many cell types express PAI-1, a fact that had been suggested by in vitro studies but not previously demonstrated in vivo. Finally, I demonstrated that the PAI-1 expression is localised to sites of active disease. All of this data is suggestive of a role for this potent anti-fibrinolytic molecule in the ongoing pathology of LN.

Acknowledgements:

This work represents a truly collaborative scientific effort. I have been fortunate to work with many excellent scientists during the course of my work and would like to thank everyone whose help and effort made this thesis possible.

I would like to extend my thanks to both Professor Eugene Dowdle and Dr David Loskutoff. They have supervised my work over the past years and I am very grateful for the guidance they have provided.

Professor Dowdle was responsible in many ways for my interest in research and I had many stimulating times during my learning period in his laboratory. He also gave me an introduction to computer science which has been useful in many other spheres of my life. Everyone in Professor Dowdle's laboratory was helpful and tolerant during my first months at the bench and I would like to mention a few people specifically. Jean Fletcher helped me on the unsteady path from tissue plasminogen activator to plasminogen activator inhibitor type-1 (PAI-1). I will always be grateful for her generous help and teaching. Bruno Orlandi taught me how much can be achieved with careful planning and an inventive mind. Lynn Wilson encouraged me during a less optimistic phase of my research and helped me achieve this goal. Paul Potter and Jill Finlayson were great friends and always provided me with helpful discussion and advice.

David Loskutoff was kind enough to offer me a post in his laboratory, at Scripps Clinic in La Jolla where I have had a productive and wonderful learning experience. Dave's knowledge and experience in the PAI-1 field helped me focus on some interesting aspects of this inhibitor and led to many fruitful collaborations. Once again I have been fortunate to work with some experienced and helpful people. Scott Curriden has been a wonderful friend and co-worker. We had a lot of fun with the regulation project. Heather Craig and Amy Wright provided excellent assistance and were both good friends. Karen Roegner was 'unlucky' enough to have to work through the in situ project with me and her cheerful, uncomplaining attitude helped the work progress successfully. Her successor, Terri Thinnes, also provided excellent work with the same cheerful and positive attitude. Mike Sawdey provided great inspiration by the example of his meticulous science much of which led the way to many of my projects. Curie Ahn taught me much of the background necessary for the renal projects and I am grateful for the help she provided. Alan McLachlan, Nigel Mackman and Anneke Raney were friends whose experience helped me through many sticky patches. Peggy Tayman deserves special mention since she has provided the excellent secretarial assistance in a calm and supportive fashion.

Finally I would like to thank my family who have always supported me and made the difficult times easier. More recently I would like to thank my fiance, Cara, who has had to live through the preparation and departure phase of this work. There are many people whose names are not listed here and who have all, in various ways, contributed to this work and I would like to thank them all.

Abbreviations

ABTS	2,2' azino-di (3-ethyl-benzthiozoline) sulphonic acid
AP-1	activator protein-1
CAT	chloramphenicol acetyl transferase
Ci	curies
CM	conditioned medium
CRE	cyclic AMP responsive element
DAB	diamino benzidine
DNA	deoxyribonucleic acid
EC	endothelial cell
ECM	extra cellular matrix
EGF	epidermal growth factor
ELISA	enzyme linked immunosorbant assay
EM	electron microscopy
GBM	glomerular basement membrane
GN	glomerulonephritis
HNF1	human nuclear factor-1
HUS	haemolytic uraemic syndrome
Kb	kilobase
LN	lupus nephritis
LUC	luciferase
NF-1	nuclear factor-1
oligo	oligonucleotide
PA	plasminogen activator
PAGE	polyacrylamide gel electrophoresis
PAI-1	plasminogen activator inhibitor type-1

PAI-2	plasminogen activator inhibitor type-2
PAP	Peroxidase anti-peroxidase
PAS	periodic acid schiff
PBS	phosphate buffered saline
PDGF	platelet derived growth factor
PMA	phorbol myristate acetate
RNA	ribonucleic acid
SLE	systemic lupus erythematosus
t-PA	tissue plasminogen activator
TGFß	transforming growth factor beta
TNFα	tumour necrosis factor-α
u-PA	urokinase activator
vWF	von Willerbrand factor

CHAPTER 1: INTRODUCTION

PLASMINOGEN ACTIVATOR INHIBITOR TYPE-1.

Plasminogen activation provides an important source of localized proteolytic activity in the blood during fibrinolysis, and in the tissues during a variety of normal and pathologic processes that in general involve invasive or degradative events (1,2). Precise regulation of plasminogen activator (PA) activity thus constitutes a critical feature of many biological processes and abnormalities in this regulation may lead to clinical problems (3-5). This control is achieved at many levels. These include regulation of synthesis of tissue-type PA (t-PA) and/or urokinase-like PA (u-PA) by cells of the vessel wall; and modulation of PA activity through interactions with cell surface receptors (6-10), components of the extracelluar matrix (11,12) or with specific PA inhibitors (PAIs). There are at least 3 immunologically distinct groups of PAIs (13). These include type-1 PAI (PAI-1) previously termed the "endothelial cell-type" PAI (14), PAI-2 previously termed the placental type inhibitor (15) and protease nexin (16) detected in cultured fibroblasts.

Gene structure and physical characteristics.

The structure of PAI-1 has been investigated using both the purified protein and its cDNA (reviewed in (17). The human PAI-1 gene is located on chromosome number

7 (18), close to the locus for cystic fibrosis (19). The entire PAI-1 gene was isolated and shown to be 12.2 Kb in length and to be organized into 8 introns and 9 exons (20). It specifies two distinct transcripts of 3.2 and 2.3 Kb which are co-linear from their 5'-end and appear to be formed by alternative polyadenylation. The 3.2 Kb cDNA contains a small 5' non-translated region, a region that codes for a 23 amino acid signal peptide, the coding region, and a rather large, 3' non-translated region which accounts for over 50% of the cDNA (18,21,22). The translated protein is a single-chain glycoprotein with an approximate molecular weight of 50,000 and an isoelectric point of 4.5-5.0. More precisely, the cDNA revealed that the mature human protein consists of 379 amino acids, three of which represent potential sites for the attachment of n-linked carbohydrate side chains. Carbohydrates constitute approximately 13% of the mass of the molecule. Comparison of the sequence of the PAI-1 cDNA with that of α_1-antitrypsin indicates that its reactive centre is located at the carboxyterminal end of the molecule, at Arg_{346}-Met_{347} (23), and that it is a member of the serine proteinase inhibitor (Serpin) gene family. It is noteworthy that PAI-1 lacks cysteine residues, a property that may account for its stability under reducing conditions.

During the initial characterization of PAI-1 it was apparent that this was an unusual protease inhibitor. For example, it migrated with β-mobility when analyzed by agarose zone electrophoresis (24) while most plasma protease inhibitors display α-mobility. Moreover, its activity was still apparent after SDS-PAGE and reduction

(25) treatments that irreversibly inactivate most other inhibitors. In spite of this unusual stability, the molecule was rapidly and efficiently inactivated by oxidants (26). Finally, an unexpected but rather consistent finding was that a latent form of PAI-1 exists in the conditioned medium of a large variety of cells and may also be present in platelets (27). The inactive form can be converted into the active inhibitor by treatment with denaturants (28), heat (29), negatively charged phospholipids (30) or vitronectin (31). Biologically relevant activators of latent PAI-1 in plasma and cells have not yet been identified and all detectable intracellular PAI-1 appears to be active (32,33) but labile, decaying to the latent form with a half-life of 2-3 hours after it is secreted (34). These observations are consistent with the simple idea that PAI-1 is produced in an active form but is inherently unstable and rapidly decays into the inactive form once secreted, perhaps because of conformational changes in the molecule (17). It is likely that denaturants activate latent PAI-1 by altering the 3-dimensional structure of the molecule, transiently re-exposing its reactive centre. Interestingly, PAI-1 is present in the extracelluar matrix (ECM) of a variety of cells (35-37) where it appears to be distributed as a rather homogeneous carpet under the cells (38). ECM-associated PAI-1 is active, not latent (39). It is bound to specific PAI-1 binding proteins that protect it from the spontaneous loss of activity observed in solution, increasing its half-life from under 3 hours to over 20 hours (40). These binding proteins thus stabilize PAI-1 in the active configuration (41). PAI-1 in plasma is also predominantly active and bound to a specific binding protein, an observation that suggests that the PAI-1 binding protein is an important regulator of PAI-1 activity.

The binding protein has been purified from both human (41) and bovine (42) plasma and shown to be vitronectin. The biological significance of the interaction between PAI-1 and vitronectin in plasma, which increases the half life of PAI-1 from 2 hours to 4 hours, remains unclear since the clearance time for PAI-1 *in vivo* is only 5-10 minutes (43).

Role of PAI-1 *in vivo*.

Naturally occurring complexes between single-chain t-PA and PAI-1, but not between t-PA and PAI-2, PAI-3 or protease nexin (44), can be detected in the blood, and the second order rate constant for the interaction of single-chain t-PA with PAI-1 is approximately 20,000 times higher than the constant derived for the interaction of t-PA with PAI-2 and protease nexin (45,46). These observations have led to the conclusion that of all the serpin inhibitors, the primary regulator of plasminogen activation may be PAI-1 (reviewed in (17) and that PAI-1 appears to be the physiological inhibitor of t-PA, at least in the blood. PAI-1 is a regulated protein. Its synthesis is stimulated by transforming growth factor beta(TGFβ), basic fibroblast growth factor, tumour necrosis factor, interleukin-1, endotoxin, phorbol myristate acetate(PMA) and dexamethasone (reviewed in (47) all of which cause an increase in gene transcription as demonstrated in nuclear run-on experiments (48). These data suggest that the regulatory region of the PAI-1 gene must be unusually complex,

containing DNA elements responsive to all of these molecules. Transfection experiments with 6.3kb of the PAI-1 promoter and firefly luciferase as the reporter gene have confirmed the presence of DNA elements responsive to dexamethasone (49), TGFβ (50) and PMA (unpublished data). Nucleotides -90 to +75 mediate a ten fold increase with dexamethasone and this element functions in both the forward and the reverse orientation suggesting that it is an authentic glucocorticoid responsive enhancer. Additional information on the response of the PAI-1 promoter to TGFß is presented in Chapters 3 and 4 of this thesis.

A number of recent observations attest to the clinical relevance of alterations in plasma levels of PAI-1 and it is now clear that patients with elevated PAI-1 levels have, or are at risk of developing, thrombotic problems. For example, the levels of PAI-1 increase 10 to 20-fold during gram negative infections (51)that have disseminated intravascular coagulation as one of their major clinical manifestations. Specific information on the identity of the cell types expressing PAI-1 in endotoxaemia and their localization is considered in Chapters 5 and 6 of this thesis.

Increased plasma PAI-1 activity has also been associated with deep vein thrombosis (52), myocardial infarction (53), angina pectoris (54) and pregnancy (55), all conditions with an increased thrombotic risk. The precise role of PAI-1 in coronary artery disease, however, is thrown into question by a recent angiographically monitored study that failed to show any correlation between the severity of the

disease and plasma PAI-1 levels (56). It is possible that the role of PAI-1 in the acute phase of coronary occlusive disease is distinct from its role in the chronic phase where persistently elevated PAI-1 levels may merely correlate with some other risk factor for myocardial infarction, such as raised triglycerides. This association has been demonstrated in a number of studies (53,54,57).

Raised PAI-1 levels have also been detected in critically ill patients with unrelated diseases such as pancreatitis, malignancy, and liver disease (58). Hepatic failure may affect plasma PAI-1 levels in various ways since, for example, PAI-1 is cleared from the circulation by the liver and it is perhaps not surprising that diseases such as chronic alcoholism, hepatitis or cirrhosis are associated with elevated plasma PAI-1 levels (41). Furthermore, PAI-1 is known to be produced by hepatocytes (59,60). In this regard it has been demonstrated that hyperinsulinaemia is associated with high PAI activity in cases of type-2 diabetes and obesity (61) an observation which correlates well with cell culture studies where insulin has been shown to stimulate PAI-1 synthesis in a number of different hepatoma cell lines (62).

PAI-1 activity in plasma frequently increases after major surgery and in response to acute trauma (63), suggesting that it is an acute-phase reactant. However the *in situ* hybridisation studies I present in Chapter 5 showed that PAI-1 is synthesized by endothelial cells of many organs in response to endotoxin. This observation suggests that PAI-1 in not a classical acute phase protein, since these proteins are generally

synthesized by liver hepatocytes (64,65).

The importance of PAI-1 regulation is further emphasized by the finding that patients with low plasma PAI-1 concentrations have bleeding disorders (5,66). An interesting example of the relationship between PAI-1 and haemostasis is provided by the case of activated protein C which stimulates the fibrinolytic activity of endothelial cells and plasma. This it does, not by increasing t-PA or u-PA production or by dissociating preexisting t-PA/PAI-1 complexes, but rather by decreasing PAI-1 itself (reviewed in (17)). It would seem that the net fibrinolytic activity of blood or cells reflects a balance between PA's and PAI-1, and that changes in the relative concentrations of either of these molecules may lead to thrombotic problems or to a bleeding diathesis.

Thesis aim.

Although the initial aim of my thesis (Cape Town) was to examine the mechanism of down regulation of tissue plasminogen activator (t-PA) activity during the differentiation of the leukaemic cell line K562, most of my subsequent work (La Jolla) was designed to investigate the *in vivo* and *in vitro* regulation of PAI-1. This change of emphasis arose from my initial observations with the K562 cells which showed that PAI-1 was a critical regulator of PA activity in this system.

Chapter 2 begins with a short outline of the work performed on the regulation of t-PA activity released by K562 cells in response to PMA. This work showed that t-PA activity was primarily regulated by PAI-1 levels and that PAI-1 secretion was highly regulated by changes in PMA concentrations. Much of the basic protein chemistry and molecular biology of PAI-1 had already been completed and I therefore chose to focus on two aspects of PAI-1 which may contribute to understanding the role of PAI-1 *in vivo*. Chapters 3 and 4 contain work in which I mapped regions of the PAI-1 promoter that were responsive to TGFß. I isolated a number of regions of the promoter that were TGFß responsive and from these regions focused on the minimal DNA sequences that were able to confer TGFß responsiveness. I also studied the role of the transcription factors AP-1 and NF-1 in the TGFß response of these regions.

Chapters 5 and 6 record the *in vivo* localization of PAI-1 mRNA synthesis in

normal mice and also in mouse models of human disease. Although clinical studies had suggested a role for PAI-1 in thrombotic disease, very little is known about the sites of synthesis or the regulation of PAI-1 *in vivo*. I therefore studied the localisation of PAI-1 using *in situ* hybridisation in both normal mice and in mice with diseases characterised by an increased incidence in thrombosis.

Chapter 7 contains a short summary.

CHAPTER 2: REGULATION OF PLASMINOGEN ACTIVATOR AND PAI-1 IN K562 CELLS IN RESPONSE TO PHORBOL MYRISTATE ACETATE.

Introduction:

The species of PA secreted by the leukocytes from patients with acute myeloid leukaemia has prognostic significance (67) and has been shown by Wilson et al to be a differentiation-linked process (68). Primitive myeloid cells secrete active t-PA while differentiated cells secrete active u-PA. A convenient experimental model for studying this process is presented by the human leukaemic cell line K562, which was established from the pleural effusion of a patient with chronic myeloid leukaemia (69). These cells are induced to differentiate along the megakaryoblastic pathway by the addition of phorbol myristate acetate (PMA (70) and, during this process, they switch from producing a mixture of active t-PA and u-PA to producing active u-PA alone and they show increased production of both transforming growth factor-ß (TGFß) and platelet derived growth factor. In this Chapter I describe the results of experiments designed to examine the mechanism of down regulation of t-PA activity that occurred with differentiation.

Methods:

Cell culture. K562 cells were grown in RPMI1640 (Flow Laboratory, McLean, VA) supplemented with 10% heat-inactivated fetal calf serum (FCS), penicillin and streptomycin (Whittaker, Walkersville, MD). Cells ($5x10^5$) were cultured for 48 hours

after which the serum-containing medium was replaced by serum-free RPMI or serum-free RMPI with 10ng/ml of PMA. The conditioned medium (CM) was collected after a further 24 hours, and centrifuged to remove the cells and debris and assayed immediately or stored at 4°C.

PA activity assay. PA in the CM was assayed as previously described (71). Briefly, plasminogen dependent lysis of insoluble ^{125}I-labelled fibrin was measured in Linbro multi well plates (Flow). The species of PA was established by incubating the CM with an excess of neutralizing antibodies to either t-PA or u-PA for 1 hour at 4°C before measuring residual PA activity.

PA inhibitor assay. To assay for an inhibitor of PAs, a known amount of t-PA was preincubated with the CM from K562 cells treated for 24 hours with 10ng/ml of PMA. The residual t-PA activity was quantitated in the PA activity assay as described above. SDS activation, a known property of the inhibitor PAI-1, was performed by incubating the conditioned medium sequentially with 0.2% SDS at 37°C for 30 mins followed by 1% Triton X-100, before incubation with a known amount of t-PA.

Fibrin-plasminogen zymography. Polyacrylamide gel electrophoresis (PAGE) and zymography were performed as described by others (72,73). Briefly the CM were run on 11% polyacrylamide gels containing 0.1% sodium dodecyl sulphate (SDS) and then washed in 2.5% Triton X-100 to remove the SDS. The gels were then laid on indicator gels consisting of 1.25% agar, human plasminogen (50ug/ml), thrombin (0.03U/ml) and fibrinogen (2mg/ml). Plasminogen dependent lysis was seen as clear zones in the opaque indicator gel.

ELISA assay for t-PA antigen. A 96-well ELISA tray was coated with 100ul polyclonal anti-t-PA at 0.1mg/ml in phosphate buffered saline pH 7.6 (PBS) and incubated at 4°C overnight. The residual serum in the polyclonal preparation was sufficient for blocking. The wells were washed twice with PBS. Samples (50ul) containing either t-PA standards or CM were added and incubated at RT for 1 hour. Recombinant t-PA, diluted in ELISA diluent (500 mmol NaCl, 10mmol Na_2HPO_4; pH 8.5 and 0.5% Triton-X100) containing 3% FCS, was used to construct a standard curve using 2-fold dilutions starting at 4ng/50ul. After incubation with the antigen the wells were washed five times with TST (150 mmol NaCl, 50 mmol Tris; pH 8.0 and 0.05% Tween 20) followed by sequential addition of 50ul of mouse monoclonal anti-t-PA (20ug/ml); 50ul of link Ab (sheep anti-mouse at 20ug/ml); 50ul of peroxidase anti-peroxidase (PAP at 135ug/ml) and ABTS/peroxide substrate. Absorbance readings were taken at 414nm, 0.5-2 hours after addition of the substrate. The assay was linear ($r = .997$) for a range of t-PA from 4ng/well to 0.1ng/well.

PAP was prepared by incubating peroxidase at 100ug/ml in PBS pH 7.6 with purified mouse anti-peroxidase at 2.7mg/ml. The enzyme substrate (40 mmol ABTS [2,2' azino-di (3-ethyl-benzthiozoline) sulphonic acid]) was made up in water and stored at -20°C. It was diluted 1:100 in citrate buffer pH4.0 and a 1:100 dilution of 30% hydrogen peroxide was added immediately before use.

Northern blot analysis. The total RNA was extracted from K562 cells that had been incubated for 24 hours in serum-free RPMI alone or containing 1ng/ml or 10ng/ml

of PMA. The acid/guanidium thiocyanate/phenol-chloroform method was used (74) and concentration was determined by measurement of sample absorbance at 260 nm. Total RNA (20 μg) was analyzed for PAI-1 mRNA by Northern blotting as described previously, employing a 1.3 kb human PAI-1 cDNA probe kindly provided by Dr D.Loskutoff(48). The probe was labelled by the random primer technique (75) employing α-^{32}P dGTP (>3000 Ci/mmol; Amersham, Arlington Heights, IL). Equal loading and transfer of the RNA was confirmed by inspection of the ethidium bromide-stained RNA in the nylon membrane following transfer. Autoradiography was performed at -80°C employing Kodak XAR-5 film with intensifying screens.

Results.

PA activity released by K562 cells in response to PMA treatment. The CM from control cells (serum free medium) and from cells treated with increasing doses of PMA in serum free medium was assayed for PA activity and the species of PA determined by titration with neutralizing antibodies. The control cells (Fig.1: SF) secreted both active t-PA (cross hatched bars) and active u-PA (solid bars). Treatment of the cells with 0.01ng/ml or 0.1ng/ml of PMA (Fig.1) caused a large increase in the secretion of t-PA and u-PA. In contrast, cells treated with 1ng/ml or 10ng/ml of PMA released decreased amounts of PA activity and the residual activity was all due to u-PA (Fig.1).

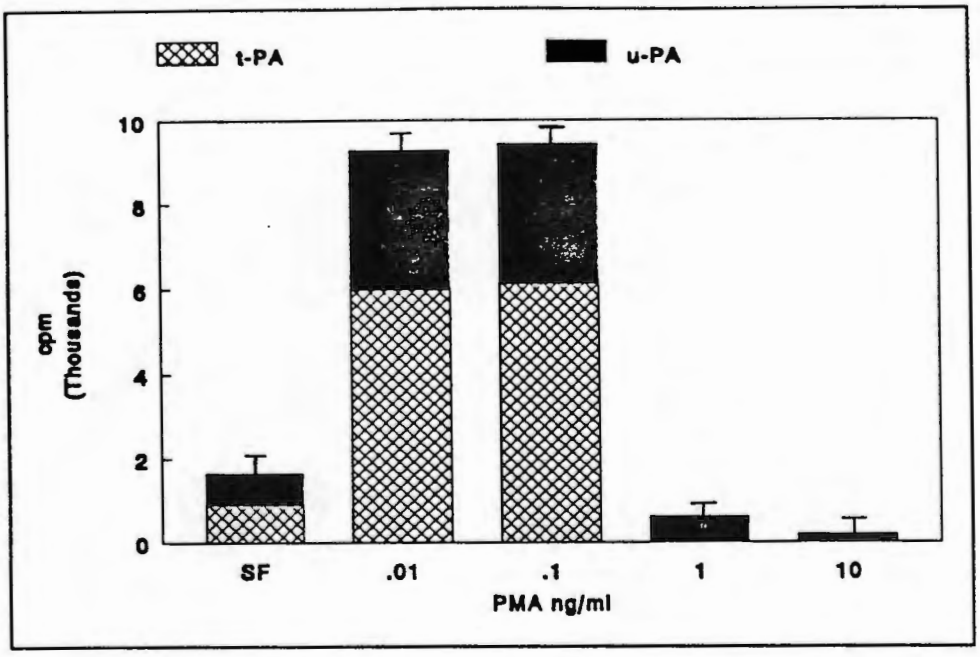

Figure 1. PA activity assay. The PA activity and species was measured using the fibrin lysis assay as described in the method. t-PA is represented by cross hatched bars and u-PA by solid bars. The PMA concentration is on the x-axis and solubilized ^{125}I fibrin cpm are on the y-axis. These results represent the average of three experiments each performed in duplicate.

t-PA antigen released by K562 cells in response to PMA treatment. The CM from control cells and from cells treated with PMA was assayed in the t-PA ELISA assay as described in the methods. The control cells (Fig.2: SF) secreted low amounts of t-PA antigen. Treatment of the cells with PMA led to an increase in the amount of t-PA antigen secreted for all amounts of PMA used (Fig.2). Unlike the t-PA activity which was decreased in response to 10ng/ml of PMA, the t-PA antigen was increased (compare Fig.1 to Fig.2).

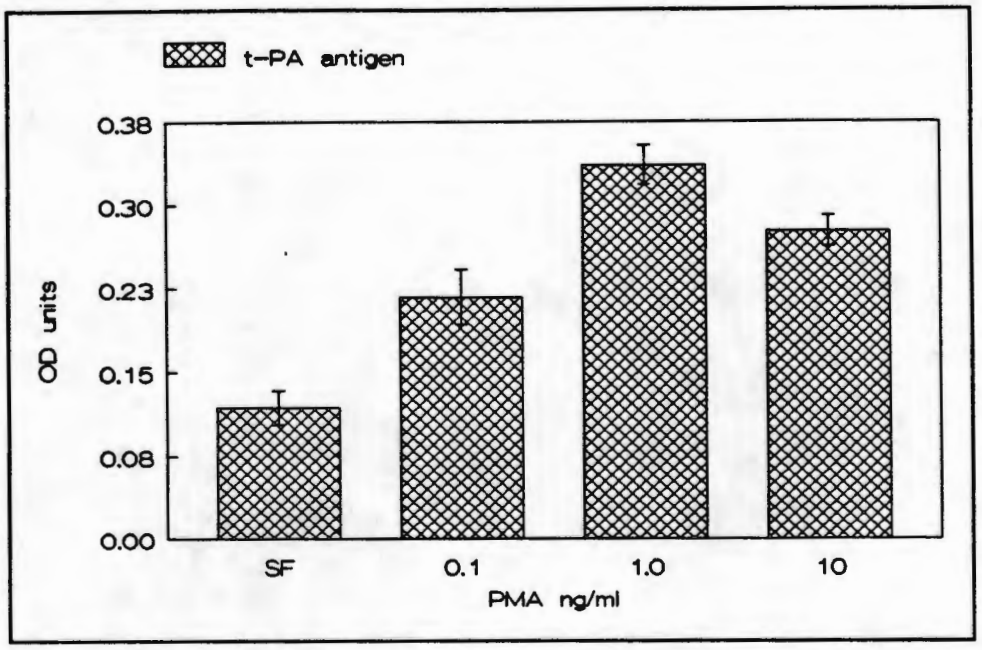

Figure 2. The t-PA antigen from K562 cells treated with PMA. PMA concentration is on the x-axis and the absorbance at 414nm is on the y-axis. These results represent the mean of three experiments +- SD.

Inhibition of t-PA by CM from K562 cells treated with 10ng/ml PMA. CM from K562 cells that had been treated with 10ng/ml of PMA was added to a known amount of t-PA (1ng), the mixture was incubated for 30 min at 37°C and then assayed for residual PA activity. This assay was performed in the presence of the neutralizing antibody to u-PA so that only t-PA lysis and inhibition was measured.

RPMI alone, or RPMI treated sequentially with 0.2% SDS and 1% Triton X-100 were added to 1ng t-PA without effect on the residual t-PA activity (Fig.3). When CM from K562 cells treated with 10ng/ml of PMA was added, there was a greater than

50% reduction in residual t-PA activity (Fig.3). When CM treated with SDS to unmask latent PAI-1 as described in the methods was added the residual t-PA activity was reduced to less than 1%.

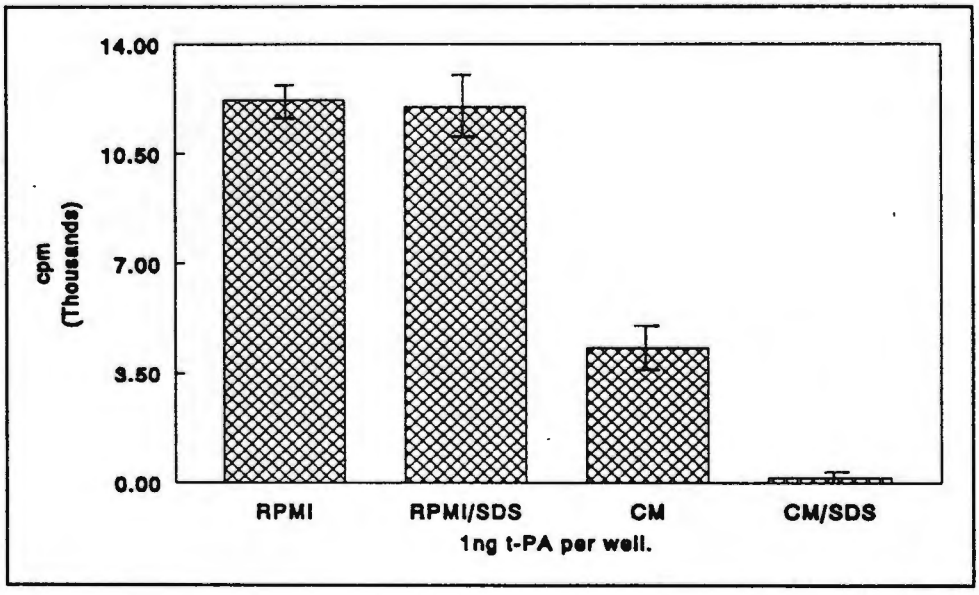

Figure 3. Assay for t-PA inhibitor. was performed by pre-incubating a known amount of t-PA with CM from K562 cells treated for 24 hours with 10ng/ml of PMA. The residual PA activity was quantitated in a fibrin lysis assay. The effect of treatment of the CM with 0.2% SDS was also studied. These results represent the mean of three experiments.

Inhibition of t-PA and u-PA by CM from K562 cells treated with 10ng/ml PMA.

The ability of the CM to inhibit t-PA or u-PA was also tested by using fibrin

autography. The CM alone (10ul) showed a small zone of lysis at the same molecular weight (55 000 MW) as the proenzyme form of u-PA (Fig.4: lane 1). t-PA alone showed a lysis zone of a higher molecular weight (70 000 MW; Fig.4: lane 2) and this was completely inhibited by pre-incubation of the t-PA with 10ul of CM (Fig.4: lane 3). u-PA alone showed 2 zones of lysis consistent with the two chain and the single chain form of u-PA (55 000 MW and 30 000 MW) as indicated by the arrow heads (Fig.4: lane 4) which again showed inhibition after pre-incubation with CM (Fig.4: Lane 5).

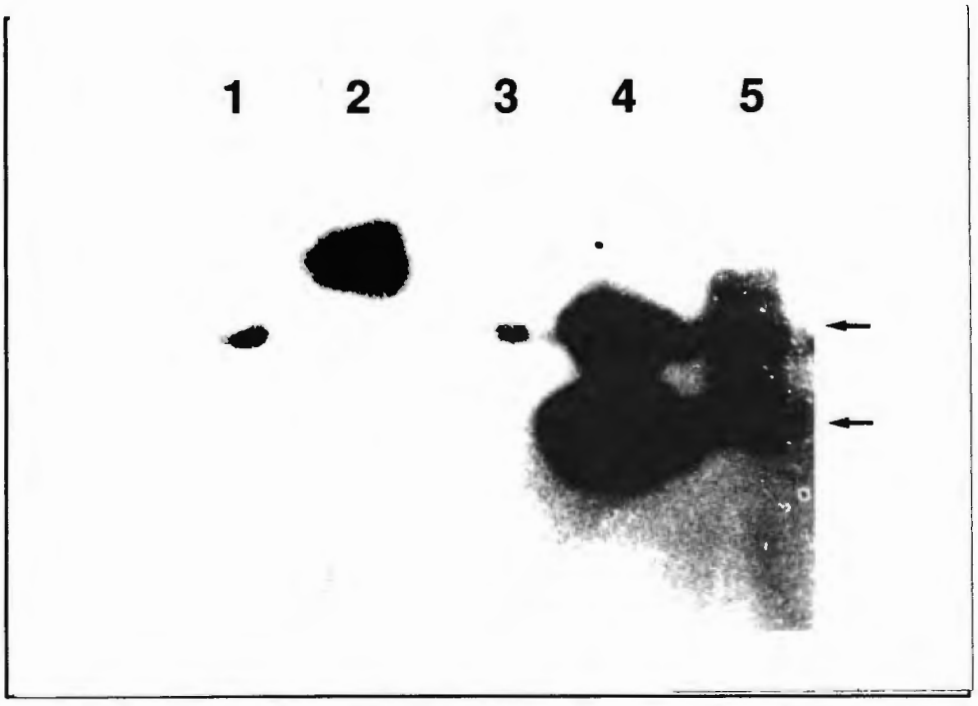

Figure 4. Fibrin-plasminogen zymography was performed as described in the methods section on CM alone (1); t-PA alone (2); t-PA + CM (3); u-PA alone (4) and u-PA + CM (5). Dark bands: lysis zones in the indicator gel.

Northern blot analysis of K562 for PAI-1 mRNA. Total RNA was extracted from K562 cells after treatment with serum free medium (Fig.5 lane-1) or serum free medium containing 0.1ng/ml PMA (Fig.5 lane-2) or 10ng/ml PMA (Fig.5 lane-3). Panel A shows the northern hybridization signal and Panel B shows the same gel stained with ethidium bromide before hybridization to determine equal loading of the lanes. Two species of mRNA were detected for PAI-1 mRNA of control cells (Panel A: lane-1) which represent the 3.2Kb and the 2.3Kb mRNAs for PAI-1 as described by others (21). After treatment with 0.1ng/ml of PMA, there was a slight increase in the signal

for PAI-1 mRNA (Panel A: lane-2). There was a large induction in PAI-1 mRNA after treatment with 10ng/ml of PMA (Panel A: lane-3).

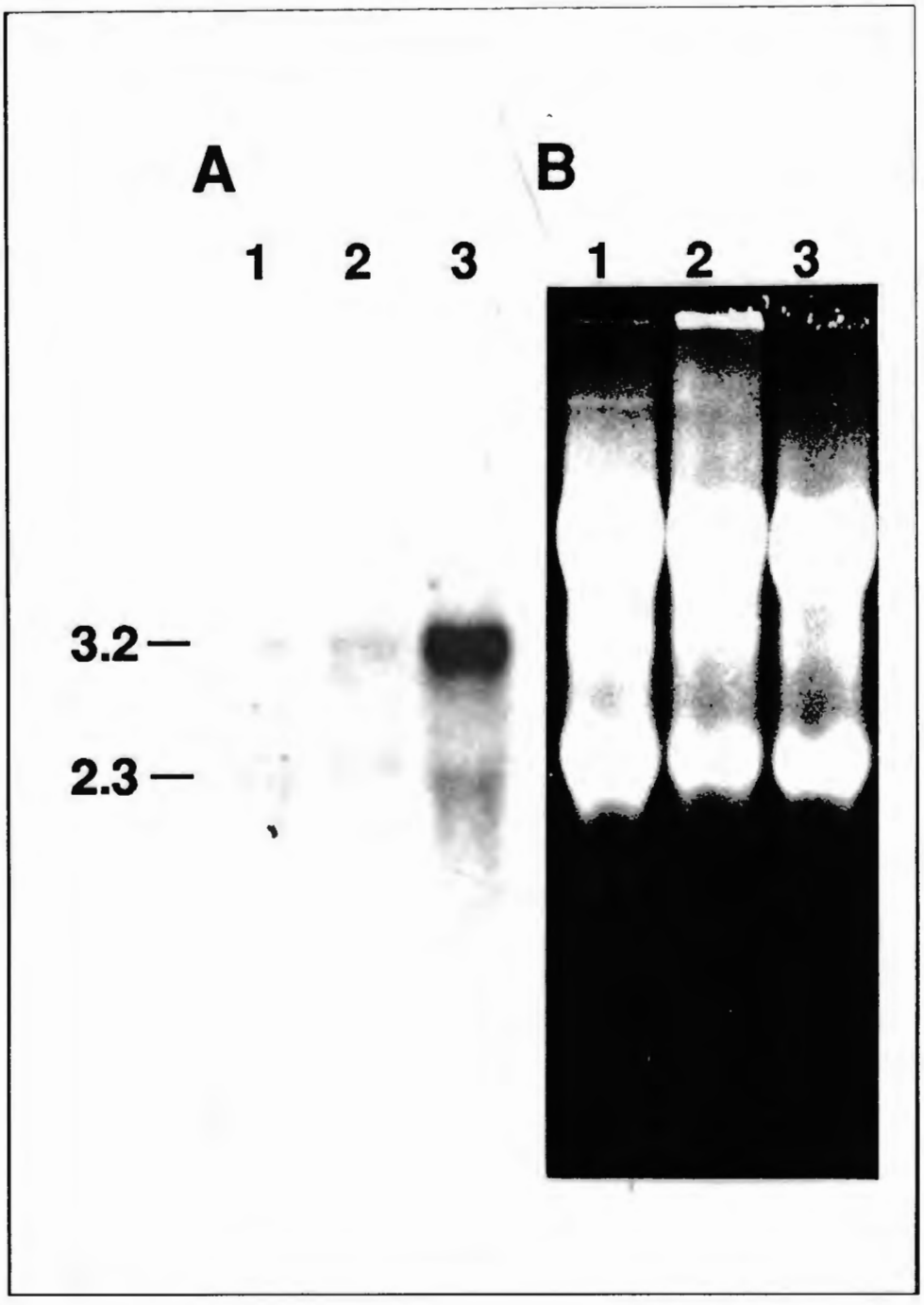

Figure 5. Induction of PAI-1 mRNA by PMA. Panel A shows the results of a Northern hybridization for PAI-1 MRNA using a ^{32}p labelled PAI-1 cDNA probe on control cells (lane-1) and cells treated with 0.1ng/ml PMA (lane-2) and 10ng/ml PMA (lanes-3). Both the 3.2Kb and the 2.3Kb PAI-1 mRNA species are detected. Panel B shows the same gel stained with ethidium bromide prior to hybridization as a control for equal loading of the lanes.

Discussion.

It has previously been shown that normal bone marrow progenitor cells release t-PA activity which changes to u-PA as the cells differentiate and mature. The mechanism of this switch in enzyme type has not been elucidated. K562 cells secreted both t-PA and u-PA and responded to PMA with a change in the amount of active t-PA in the CM (Fig. 1). K562 cells thus show a pattern of PA regulation that is similar to that of bone marrow cells in as much as the phenotypic changes induced by PMA can be equated with "differentiation" or "maturation".

Treatment with 0.1ng/ml of PMA caused an increase in both t-PA and u-PA activity but 10ng/ml of PMA completely abolished t-PA activity and decreased levels of u-PA could be measured (Fig.1). The fall in release of t-PA activity caused by high concentrations of PMA proved to be due, not to decreased release of active enzyme, but rather to concomitant induction of inhibitor release since t-PA antigen levels in CM were induced by high, medium and low concentrations of PMA (Fig.2). Moreover, when the conditioned medium from these cells was analyzed, I was able to show that an inhibitor of t-PA was being induced by PMA treatment (Fig.3 and 4). The activity of this inhibitor was increased by treatment with SDS, a known property of the inhibitor, PAI-1 (25).

Using a cDNA probe for PAI-1 (48) I was able to show the specific induction of

PAI-1 mRNA in K562 cells by 10ng/ml of PMA (Fig.5). The increase in PAI-1 synthesis induced by 10ng/ml of PMA was thus sufficient to inhibit completely the t-PA that was also induced by the PMA. The small amounts of active u-PA (detected by the ^{125}I fibrin lysis assay and by zymography) in CM from cells treated with 10ng/ml of PMA can be explained by the fact that PAI-1, while it inhibits two-chain u-PA, has no effect upon the single chain form (76). During the assay, therefore, single chain u-PA was probably converted into active two-chain enzyme by traces of plasmin, and this was not inhibited by the PAI-1 which had decayed to the latent form in the interval that elapsed between secretion and the assay. This explanation is consistent with the report by Andreasan et al (77) of their ability to measure u-PA activity in the presence of PAI-1 and with the fact that the decay of active PAI-1 is rapid (32).

The results of these experiments thus show that, in the K562 system at least, differentiation-linked changes in t-PA activity are incidental to PAI-1 synthesis and release and that the inhibitor is a critical regulatory protein. Whether or not the increase in PAI-1 secretion was due to a direct effect of PMA is uncertain, since phorbol ester is known to increase TGFß and PDGF levels in these cells (70,78) and TGFß causes large increases in PAI-1 synthesis by a variety of cultured cell types (48,79,80).

These initial observations were extended, to include the assay of intracellular levels of these components. These results were published in *Blood, Vol 74, No 4*

(September), 1988: **Regulation and secretion of Plasminogen Activators and Their Inhibitors in a Human Leukaemic Cell Line (K562) by L. J. Oliver, M. Keeton and E. L. Wilson.**

Acknowledgements. I would like to thank Jean Fletcher for excellent technical assistance and for teaching me many of the techniques used in this work.

CHAPTER 3: IDENTIFICATION OF REGULATORY SEQUENCES IN THE TYPE-1 PLASMINOGEN ACTIVATOR INHIBITOR GENE RESPONSIVE TO TRANSFORMING GROWTH FACTOR ß

Introduction.

PAI-1 is the primary inhibitor of both tissue-type plasminogen activator (t-PA) and urokinase-type plasminogen activator (u-PA) (46), and as such is a potent anti-fibrinolytic molecule. PAI-1 synthesis by cultured cells *in vitro* is induced by a number of molecules including cytokines (81,82), growth factors (48,83,84), hormones (49,62), and a variety of other agents such as endotoxin (85) and phorbol myristate acetate (86). Nuclear transcription run-on assays have shown that the regulation of PAI-1 by many of these agents occurs primarily at the level of transcription (48,50). This observation, together with the wide spectrum of effector molecules now known to regulate PAI-1 gene expression (87), indicates that the PAI-1 promoter is precisely regulated, and suggests that it is also highly reactive to various trans-acting pathways.

Increased levels of plasma PAI-1 have been demonstrated in a number of human conditions frequently associated with a predisposition to thrombosis, including myocardial infarction (53), deep vein thrombosis (52) and pregnancy (55). Plasma PAI-1 has also been shown to be elevated in patients with sepsis and endotoxaemia, a disease associated with disseminated intravascular coagulation (51). These observations suggest that PAI-1 gene expression is also highly regulated *in vivo*, and

that abnormal expression of this inhibitor may contribute to the pathogenesis of these disorders. One molecule of particular importance in this setting may be transforming growth factor beta (TGFß), a molecule released from activated platelets and leukocytes at sites of inflammation and thrombosis (88). The release of TGFß from activated platelets appears to induce PAI-1 in endothelial (89) and hepatoma (80) cells, and also increases the level of plasma PAI-1 when infused into rabbits (80).

Although the mechanism of action of TGFß remains unclear (88), its effect on several promoters has been studied. For example, the autoinduction of the TGF-β1 promoter suggests a feedback loop designed to amplify the response to TGFß under certain conditions (90). This response appears to involve specific AP-1 binding sites. AP-1 is a heterodimeric complex of Fos and Jun protein subunits which binds to specific DNA enhancer sites which have the consensus sequence TGAg/cTCA (91). AP-1 is believed to mediate the transcriptional effects of the tumour promoting phorbol esters (92). In contrast to these results, the TGFβ response sequence in the promoter for type 1 collagen, has been localized to a sequence with homology to a nuclear factor 1 (NF-1) binding site (93). A number of different consensus sequences for the NF-1 DNA binding site have been proposed including TGG(n7)GCCAA (94) and TGGCA (95,96).

The PAI-1 promoter and 5'-flanking region contains several sequences which are similar to both NF-1 and AP-1 consensus binding sites. I report here the results

of transfection experiments which indicate that regions containing AP-1-like elements appear to be critical for TGFβ inducibility. Deletion of NF-1-like sequences has no effect on induction of the PAI-1 promoter by TGFβ in this system.

General Methods.

DNA preparation. Plasmid DNA was isolated using anion exchange chromatography with a Qiagen pack 500 kit (Qiagen,Studio City, CA). Enzyme reaction conditions were as recommended by suppliers. DNA fragments were isolated from agarose gels using a silica matrix (Geneclean II kit; Bio 101, La Jolla, CA). DNA sequencing was performed by a modification of the dideoxy chain-termination procedure with a Sequenase kit (United States Biochemical; Cleveland, OH).

Plasmid construction (Fig.1). The starting constructs had identical 3' ends (the EcoRI cleavage site at +75 in the 5' non-translated region of the PAI-1 cDNA (49)) but extended upstream to -800, -549 and to -100 respectively. p39LUC was constructed in the same way and contains the sequence from +75 to -39 of the PAI-1 promoter. Specific fragments consisting of the sequences between -595 to -800,-595 to -636 and -636 to -800 were subcloned at the -39 position of p39LUC. A 5' deletion series through the region -636 to -800, starting from -800, was constructed using Bal-31 slow exonuclease (International Biotechnologies; New Haven, CN). A 3' deletion series through the same region starting from -636, was also constructed using Bal-31. p800LUC/mutXhoI, which has a 10 bp substitution containing an XhoI

restriction site at -39, was linearized at -636, digested with Bal-31 exonuclease and then cleaved at the XhoI site to remove the intervening sequence between -636 and -39. The ends were filled using the Klenow enzyme and the plasmid was ligated with T4 DNA ligase.

Cell culture. Hep3B human hepatoma cells obtained from ATCC (HB8064; Rockville, MD) were maintained in DMEM/HAMs F-12 (Whittaker;Walkersville, MD) supplemented with 10% fetal bovine serum (Hyclone; Logan, UT), glutamine, sodium pyruvate, non-essential amino acids and penicillin/streptomycin (Whittaker). For transfection experiments, semiconfluent cells in 6-well (10 cm^2 per well) tissue culture plates (Corning; Corning, NY) were washed twice with serum free media (DMEM/F-12) then incubated in serum free media. A mixture containing lipofectin (GIBCO, Grand Island, NY; 12.5ug/well) and DNA constructs (2.5ug/well) in water was added to each well (50 μl/well) and the plates were incubated for 18hrs. After lipofection, plates were incubated an additional 24hrs in the absence or presence of 1ng/ml TGFß1 (a generous gift of Berlix Biosciences, South San Francisco, CA). The monolayers were washed and then extracted into 0.25% Triton X-100. An internal control plasmid (pSV2CAT) was co-transfected with the luciferase fragments and CAT activity was used to correct for differences in DNA uptake when using different constructs. In addition to this control, each construct was tested with at least 2 independent DNA preparations in order to rule out any effects related to differences in DNA preparation. For each experiment, two independent transfections were performed with each

construct. The fold induction calculated for Figs. 2-6 represents the average of four or more experiments.

Luciferase and CAT assays. Cells were extracted into Triton X-100 (0.25% in 0.1MKPO4/1mM DTT/pH7.8) and then assayed for luciferase as described (97) by using a Monolight 2010 luminometer (Analytical Luminescence; San Diego, CA). CAT assays were performed as previously described (98) and the results were expressed as the percentage of acetylated chloramphenicol over the total labelled chloramphenicol in each sample.

Gel retardation. Gel retardation experiments were performed (99,100) using oligonucleotides homologous to the regions between -66 to -87 (5'-AGA GCC AGT GAG TGG TGG GGC-3') and between -650 to -674 (5'-GTG GGG AGT CAG CCG TGT ATC ATC G-3'). The oligonucleotides (100ng) were end-labelled using 6.25uCi of gamma ^{32}P ATP and 20U T4 polynucleotide kinase for 30 mins at 37°C. The free label was removed by 2 cycles of ethanol precipitation in the presence of 2.5M ammonium acetate. Hep3B nuclear extract was prepared (101) and then 5 μg was incubated in the presence or absence of a 50-fold molar excess of the cold competitor oligonucleotides (50ng) for 15 mins on ice (The sequence of the AP-1 competitor = 5'-GGG GGT TGA ATC ACT GGG GTG AGT CAC CCC C-3' and the sequence of the non specific competitors = 5'-AGC TTG AGC TCA GAT CT-3' or 5'-CCG AGT TGA TAC CGG G-3'). The mixtures were then incubated with 20,000 cpm of the labelled

oligonucleotide (1ng) in the presence of 1ug of poly dI-dC (Boehringer Mannheim, West Germany) in gel shift buffer (25mM HEPES pH 7.4, 40mM KCl, 7.5% glycerol, 0.125mM EDTA, 0.75mM DTT and 5mM $MgCl_2$) for 30 mins on ice and then at room temperature for 15 mins. The reaction mixture was loaded on a 6% non-denaturing polyacrylamide gel system using a 5mM Tris/380mM glycine/2mM EDTA buffer pH 8.5. The gels were run at 150V for 4 hours, dried and then autoradiographed on XAR-5 film (Kodak; Rochester, NY).

Results.

Identification of PAI-1 5' flanking sequences responsive to TGFß. A series of overlapping fragments (-800, -549, -100 and -39) with identical 3' ends (+75), containing the start site of transcription at +1 as well as a perfect TATA box at -23 to -28 (102), were cloned into the multiple cloning site of p19LUC. These plasmids were then transfected into Hep 3B cells and assayed for response to TGFß as described in Materials and Methods (Fig. 1). Deletion of the region between -800 and -549 reduced the TGFß response from 54-fold to 11-fold, and the remaining response disappeared when sequences between -100 and -39 were deleted. Thus, two areas in the PAI-1 5' flanking sequence appear to mediate the response of the PAI-1 gene to TGFβ. Figure 1 also shows the response when sequences between +7 and +75 in the 5' untranslated region were deleted. This region contains a perfect NF-1

consensus sequence ((94); TGG(n7)GCCAA) at +15 to +29, and NF-1 has been implicated in the TGFß response of the type 1 collagen promoter (93). This deletion had no effect on the TGFß response of the proximal 100 bp region.

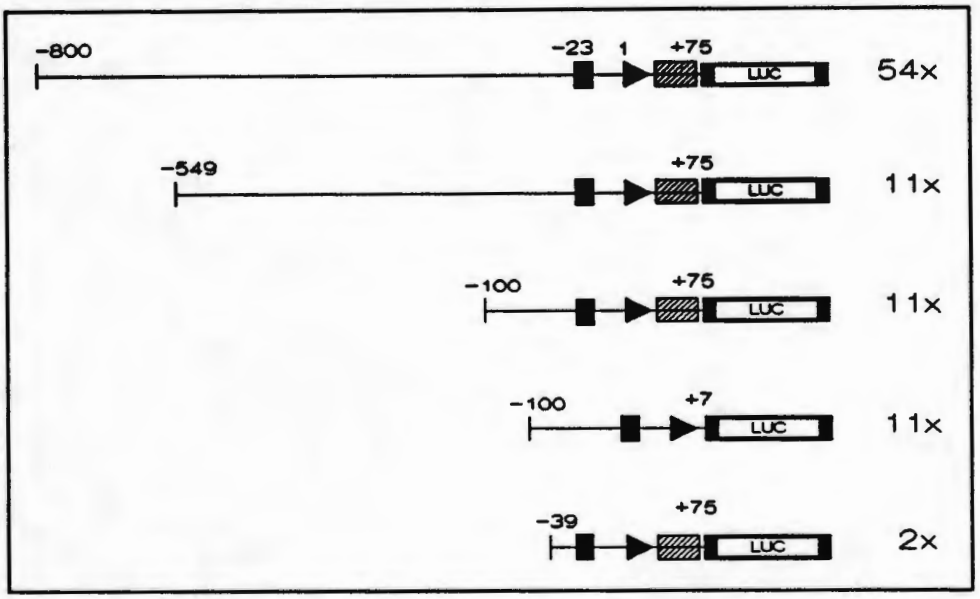

Figure 1. 5' deletion series of 800 bp of the PAI-1 promoter and 5' flanking region. A series of overlapping fragments of the 5' flanking region of the PAI-1 gene were transiently transfected into Hep3B hepatoma cells using lipofection, treated with 1ng/ml of TGFß for 24 hours, and then cell lysates were prepared and assayed for luciferase activity as described in the methods. The 5' boundaries are indicated to the left top of each construct. The fold increase in luciferase activity following TGFß treatment is presented to the right of each construct. The ratios are representative of changes in promoter activity and have been corrected for minor differences in DNA uptake by co-transfection of pSV2 CAT. The solid box (■) at position -23 represents the "TATA" box. The arrow (▸) at position 0 indicates the location and direction of transcription initiation. The open box denotes the coding sequence for the luciferase reporter gene. The cross hatched box (□) at position +7 to +75 contains an NF-1 consensus sequence (TGGn7GCCAA)between +15 to +29.

5' deletional analysis of proximal region. A more detailed analysis of the proximal promoter region (-100 to -39) was performed by transfecting Hep 3B cells with overlapping 5' deletion fragments starting at -100 (Fig.2). The response (11-fold

induction with TGFß) was lost when the sequence from -87 to -49 was deleted. As is shown in the lower part of the figure, this region contains an AP-1-like consensus sequence in the reverse orientation at -75 to -81 (underlined twice) as well as a CRE consensus sequence at -51 to -58 (underlined once).

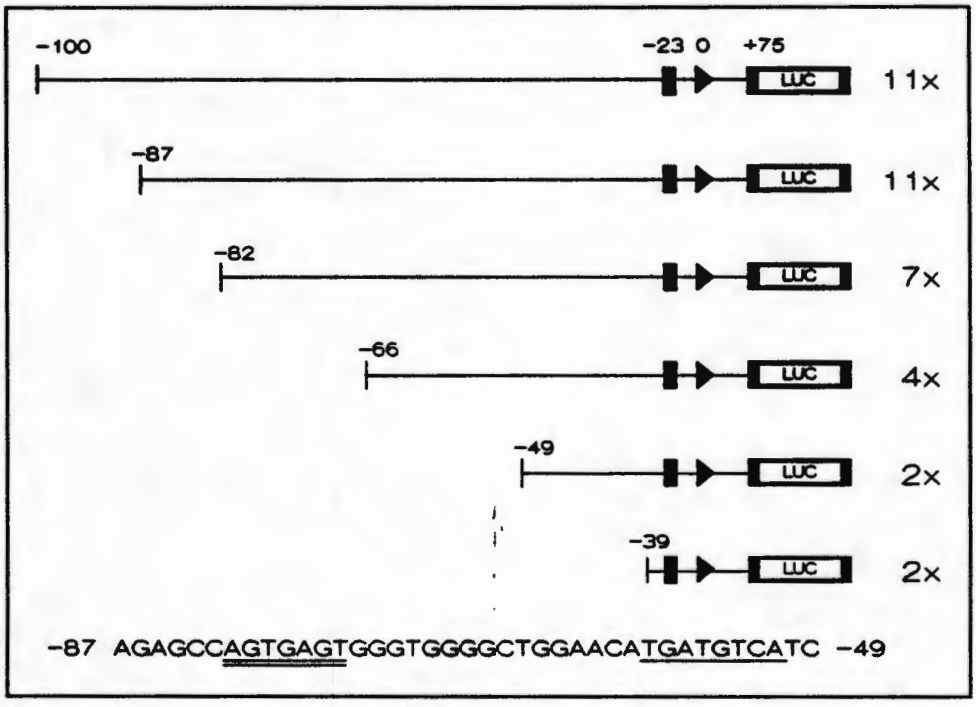

Figure 2. 5' Deletion analysis of the proximal region. A 5' deletion series between -100 and -39 was assayed for luciferase induction following treatment with 1ng/ml of TGFß as described in the legend to Fig.1. The 5' boundaries are indicated on the top left of each construct and the fold-induction after treatment with TGFß is indicated to the right of each construct. The sequence of the region between -87 and -49 is displayed at the bottom of the figure with the AP-1-like site in the reverse orientation underlined twice and the CRE like site underlined once.

Deletional analysis of distal region. The distal region contains an NF-1-like sequence between -595 and -636 (Fig.3, underlined once) as well as three AP-1-like sequences between -636 and -800 (Fig. 3, underlined twice). To begin the analysis of this region, I cloned the sequence between -595 and -800 into p39LUC and assayed this construct for TGFß induction. This 206 bp fragment showed strong (37-fold) induction in response to TGFß (Fig. 3). I then subcloned the NF-1 containing region between -595 and -636 into p39LUC and assayed this construct for response to TGFß. This 46 bp region showed little or no induction with TGFß (less than 2-fold) suggesting that it was not involved in the TGFß response of the PAI-1 gene. I tested the remaining AP-1 containing sequence between -636 and -800 for TGFß induction. This 165 bp sequence showed strong (50-fold) induction with TGFß despite the fact that the NF-1 containing sequences were removed.

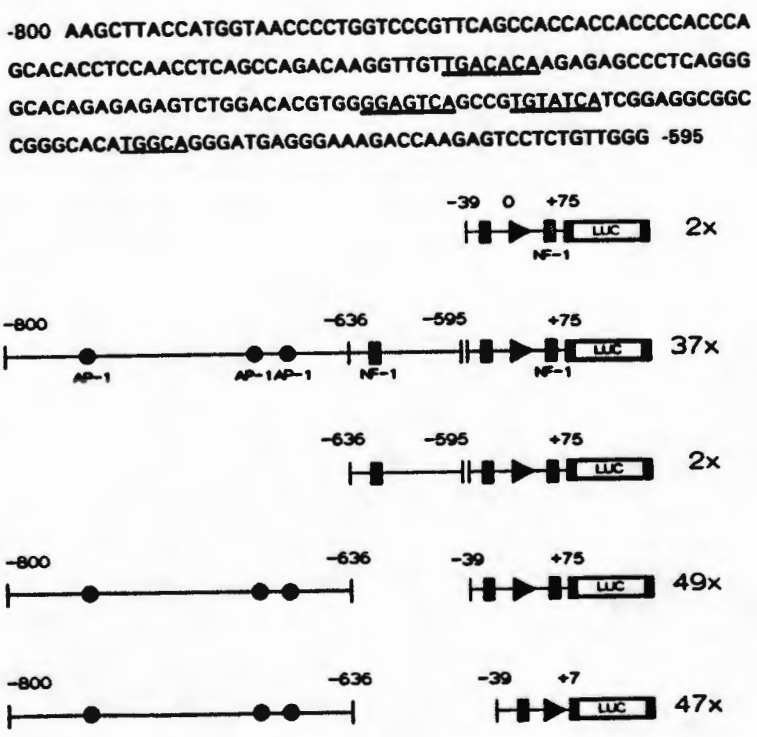

Figure 3. Deletional analysis of distal responsive region. The region containing both the distal NF-1-like sequence (cross-hatched box between -636 and -595) and distal AP-1-like sequences (cross-hatched circles between -800 to -636) was cloned into P39LUC. Then the regions containing either the distal NF-1 consensus sequence or the distal AP-1 consensus sequences were cloned into p39LUC. Finally a construct lacking the proximal NF-1 consensus sequence (cross-hatched box at +7 to +75) was also cloned. These constructs were assayed for induction after treatment with TGFß as described in Figure 1 and the fold induction is indicated to the right of each construct. The sequence between -595 and -800 is displayed at the top of the figure with the AP-1-like sites underlined twice and the NF-1-like site underlined once.

Finally, a dose response experiment was performed to compare directly the TGFß sensitivity of the NF-1 and AP-1 containing fragments (Fig.4). The fragment containing the AP-1 sequences responded to TGFß in a dose dependent manner showing a greater than 50-fold increase at 1ng/ml of TGFß, while the fragment containing the NF-1 sequence showed no response even at doses up to 5ng/ml. Figure 4 (inset) shows the CAT assays for both of these constructs in the absence of

TGFß (lane 1 and lane 3) and in the presence of 5 ng/ml TGFß (lane 2 and lane 4). Quantitation of the CAT assay revealed that all samples in this assay had conversions between 31% and 33%. This control experiment indicates that DNA uptake was equal for both constructs at all doses of TGFß used in this assay. I again deleted the NF-1 containing sequence in the 5' untranslated region (between +7 and +75) to ensure that it was not playing a role in the TGFß response of the distal region. No change in the level of induction of this fragment with TGFβ was observed (Fig.3, last construct). Thus, the sequence between +7 and +75 does not seem to contribute to the TGFβ response of this distal region.

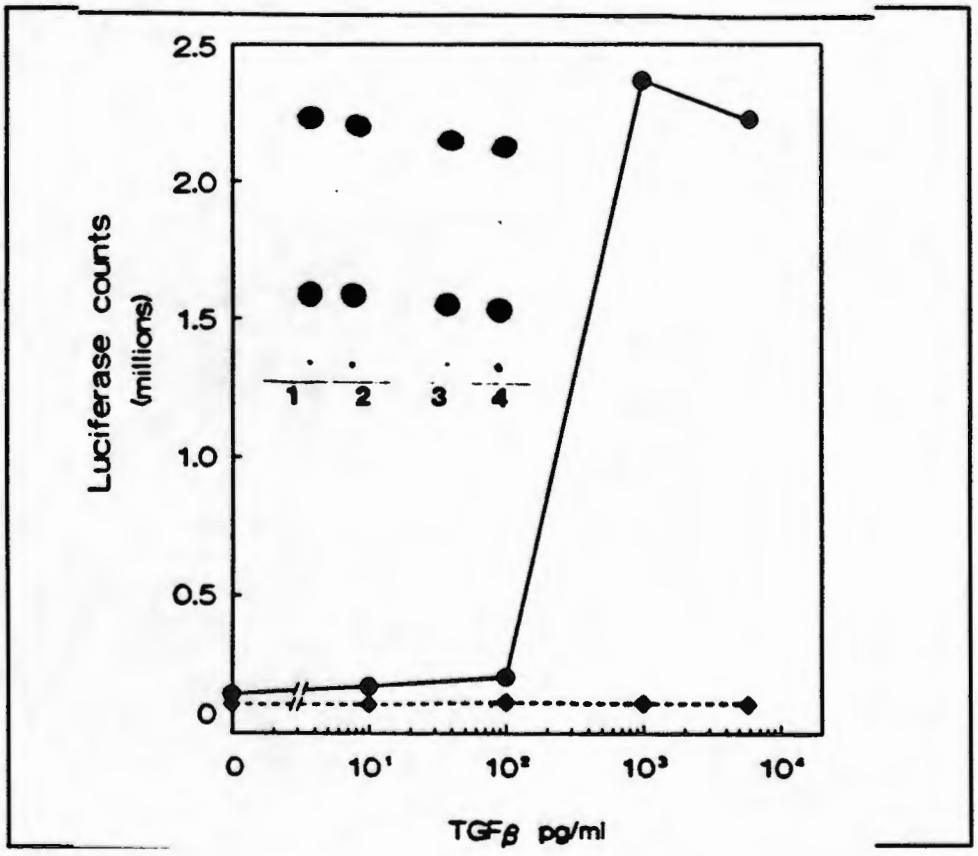

Figure 4. Dose response of distal AP-1 and NF-1 regions with TGFß. The constructs containing either the distal AP-1-like sequences or the distal NF-1-like sequences were transfected into Hep3B cells as described in Fig.1. The cells were then treated with increasing amounts of TGFß for 24 hours and assayed for luciferase activity as described in the legend to Figure.1. The fold induction is plotted on the y-axis (linear scale) against the concentration of TGFß on the x-axis (logarithmic scale). The inset contains the CAT assay for the NF-1 containing region at both 0 pg/ml (lane 1) and 5000pg/ml (lane 2) and for the AP-1 containing region at both 0 pg/ml (lane 3) and 5000pg/ml (lane 4). Quantitation of this assay gave conversions of between 31% and 33% for all of the constructs used in this assay.

In order to define the TGFβ response sequence between -636 and -800, I made several progressive 5' deletions through this region (Fig.5). Fragments lacking the region -740 to -800 were fully responsive to TGFβ. However, when sequences between -740 and -703 were deleted, the level of TGFß induction fell from 50-fold to

4-fold. The remaining 4-fold induction was still present at -674. These experiments showed that two sequences within the distal region were responsive to TGFß, the first between -740 and -703 and the second between -674 and -636. To confirm the above results, I also performed a 3' deletion series through this region (Fig.5). Deletion of the region between -648 and -678 reduced the TGFß response approximately 4-fold (i.e., from 50-fold to 12-fold). This is the same region that still showed 4-fold induction in the 5' deletion series. The remaining 12-fold induction was lost when sequences between -703 and -732 were deleted. This is the same region localized by the 5' deletion series. Thus, both the 3' and the 5' deletion series localized the same two regions of activity.

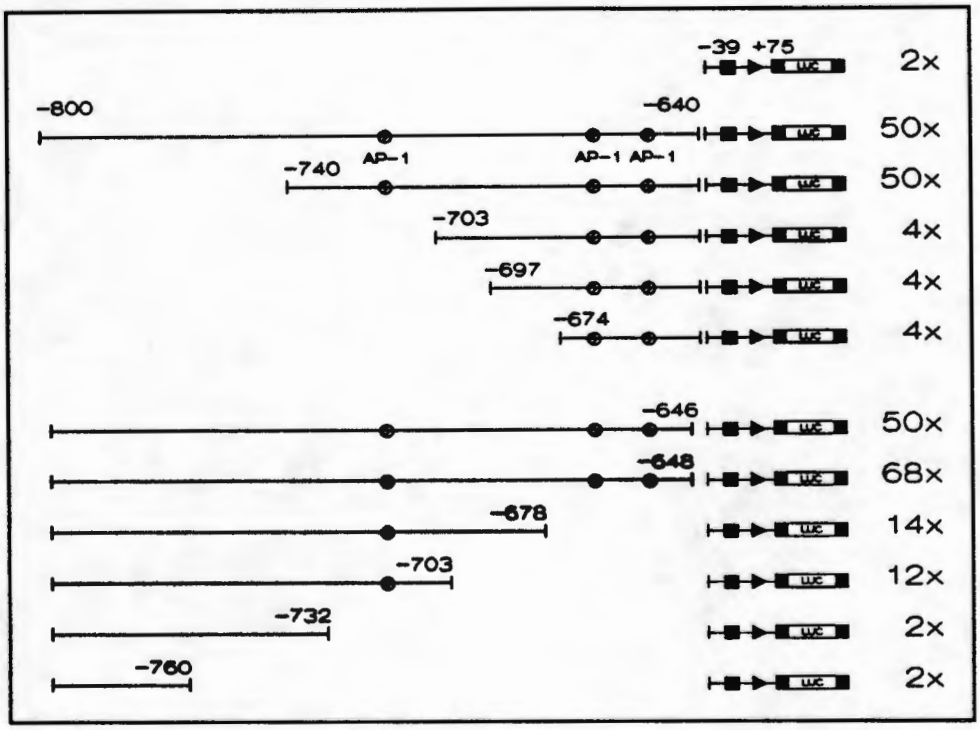

Figure 5. Deletional analysis of the distal region. A 5' and a 3' deletion series through the region between -636 and -800 were assayed for induction in response to 1ng/ml of TGFß as described in Fig.1. The 5' boundaries are indicated to the top left of each construct and the 3' boundaries to the top right of each construct. The cross hatched circles represent AP-1-like sequences. The fold induction in response to 1ng/ml of TGFß is represented to the far right of the figure.

Gel retardation analysis. Gel retardation experiments (99,100) were performed using synthetic oligonucleotides as described in the Methods, to assess whether the responsive sequences in the promoter proximal and distal regions were able to bind a common nuclear protein. The first oligonucleotide was from the proximal region (-66 to -88) and it appeared to bind a single specific protein (Fig.6 lane-1) when analyzed in this manner. Binding was eliminated by the presence of a 50-fold molar excess of

cold oligonucleotide of the same sequence (Fig.6 lane-2), but was only weakly reduced by using a 50-fold molar excess of two different non specific oligonucleotides (Fig.6 lanes 5 and 6). A 50-fold molar excess of an oligonucleotide that contained 2 AP-1 consensus sequences, also eliminated the formation of this complex (Fig.6 lane-4) indicating that AP-1 or an AP-1 like protein was binding to this oligonucleotide. Finally, the unlabeled cold oligonucleotide from the distal responsive region (-650 to -674) also competed for the binding to this protein (Fig.6 lane-3). These results suggest that both regions may be binding the same protein. This conclusion is supported by the observation that the second oligonucleotide from the distal responsive region (-650 to -674) also showed a single specific band (Fig.6, lane-7) which ran at the same molecular weight as the band from the proximal region. The formation of this radiolabeled complex was eliminated by the presence of a 50-fold excess of cold oligonucleotide of the same sequence (Fig.6 lane-8), but was only weakly reduced by a 50-fold excess of two different non specific oligonucleotides (Fig.6 lanes 11 and 12). Again, this complex was not detected in the presence of a 50-fold excess of either the consensus AP-1 oligonucleotide (Fig.6 lane-10), or of the proximal (-66 to -88) oligonucleotide (Fig.6 lane-9). The two oligonucleotides used for the non-specific competition both contain a TGA sequence (see Materials and Methods) which may account for the slight competition seen in these assays (103).

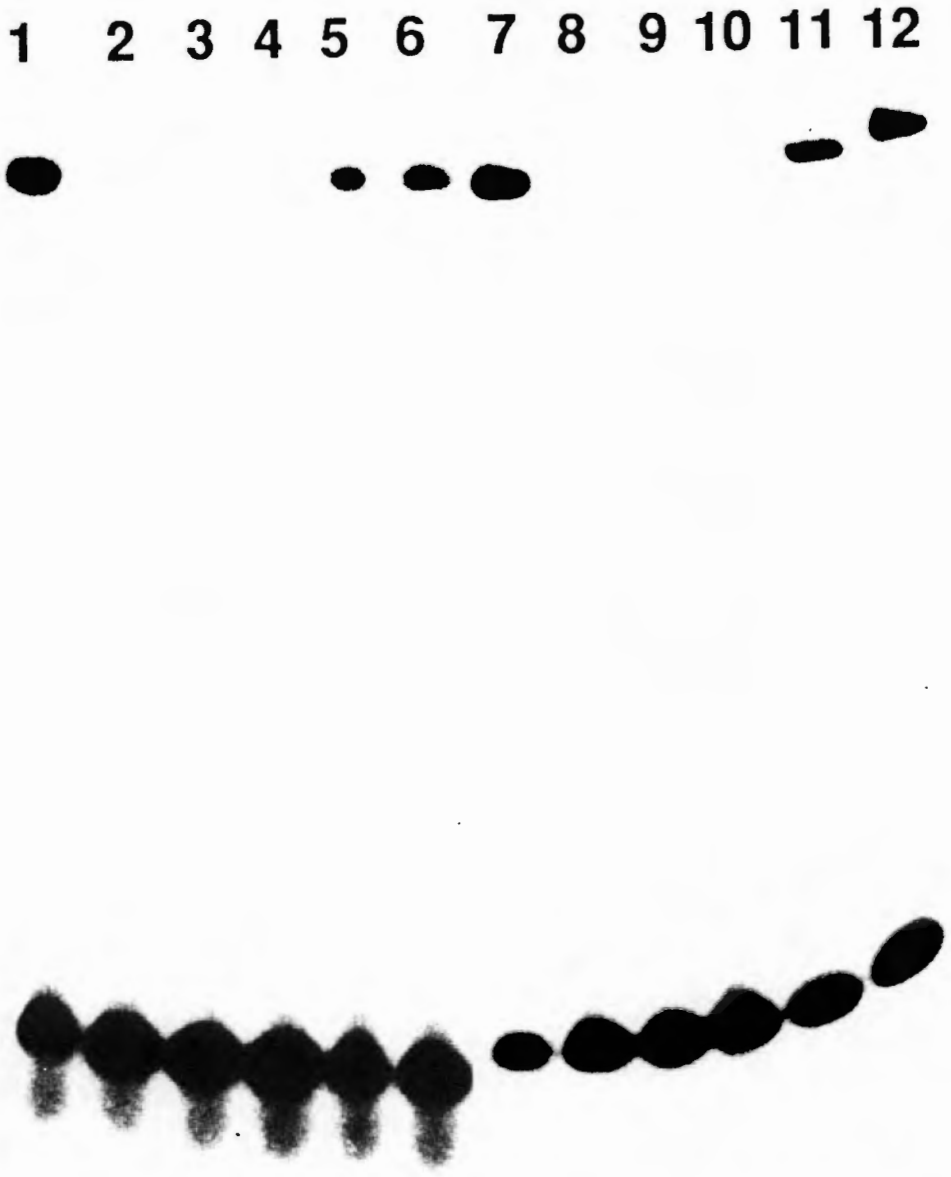

Figure 6. Gel retardation analysis. Labelled oligonucleotides (^{32}P: 20,000cpm per lane) containing the distal responsive sequence (-650 to -674) in lanes 1 to 6, and proximal responsive sequence (-66 to -87) in lanes 7 to 12 were incubated with 5ug Hep3B nuclear extract in the presence and absence of competitor oligonucleotides (i.e., a 50-fold molar excess of unlabelled oligonucleotide). The arrow head indicates the position of the complexes. Lanes 1 and 7, no competitor; lanes 2 and 8, competition with oligonucleotide of the same sequence; lanes 3 and 9, competition with an oligonucleotide containing two consensus AP-1 sequences; lane 4, competition with sequence from proximal promoter (-66 to -87) ; lane 10, competition with sequence from distal region (-650 to -674); lanes 5,6 and 11,12, competition with non-specific oligonucleotide.

Discussion.

TGFβ is a homodimeric molecule that belongs to a family of structurally related peptides. It has been called a "multifunctional signaling molecule" (104) since, for example, it inhibits the growth of endothelial cells in culture (84) and yet acts as a potent angiogenic agent *in vivo* (105). It has also been shown to stimulate the production of extracellular matrix proteins including PAI-1 (84,106). I have studied the regulation of the PAI-1 promoter and 5' flanking sequence by TGFß and have shown that the response lies within two separate regions (107). The first of these is in the proximal promoter at -49 to -87 and mediates an 11-fold induction with TGFß (Fig.2). The second is in the distal 5' flanking sequence at -636 to -800 and mediates 50-fold induction. These are the same two general regions that mediate the response of the PAI-1 promoter to dexamethasone (49). Comparative analysis of the human, mouse and bovine promoters shows a high degree of homology in these two regions (108). This observation suggests that these sequences have been conserved between species, most likely because of their functional importance for the regulation of this gene *in vivo*. Kim et al demonstrated that autoinduction of the TGFβ gene was mediated by AP-1 sequences (90), and both the proximal and distal regions of the PAI-1 promoter contain responsive sequences with homology to the AP-1 consensus binding site (Fig.4). The proximal region contains an AP-1-like binding site in the reverse orientation at -75 to -81 (TGAGTGA) as well as a cAMP binding sequence at -58 to -51 (TGATGTCA). The distal region contains 3 AP-1-like binding sites located

between -636 and -800. Two of these sites have a single base pair mismatch from the consensus sequence (-664 to -670 = GGAGTCA; -711 to -717 = TGACACA), and the third one has a 2 bp mismatch (-659 to -653:TGTATCA). Based on sequence homology, all of the AP-1-like sites are expected to be active except for the one at -664 to -670 (GGAGTCA) which has a T to G substitution of the first base. This change has been shown to decrease the binding affinity for AP-1 (91).

To test whether AP-1 or an AP-1-like protein was binding to any of these responsive sequences I end labelled two oligonucleotides from these regions and tested them in a gel retardation binding assay. The first oligonucleotide spanned the region from -66 to -87 (i.e., the region containing the AP-1-like site in the proximal promoter), while the second (-650 to -674) contains 2 of the 3 AP-1-like sites from the distal promoter. I found that each of these 2 oligonucleotides had a common specific band that could be completely competed with a 50-fold molar excess of an oligonucleotide containing 2 AP-1 consensus sequences. Thus, AP-1 or an AP-1-like protein binds to the regions that mediate the TGFß response. Furthermore, competition studies between these two regions indicated that they could compete with one another for binding of the same protein. These results suggest that both regions may mediate the TGFß response, at least in part, by binding a related nuclear factor.

The distal region (-636 to -800) which shows the strongest response to TGFß,

appears to have two responsive sequences that function cooperatively with one another to account for the full activity seen in this region. The relative activities of these two sequences appear different in the 5' deletion series compared to the 3' deletion series (Fig.5). A possible explanation for this difference may be that 3' deletions are accompanied by rotation of upstream binding sites about the DNA helix and by changes in the distance of upstream sequences from the TATA box, both of which can affect the activity of an upstream binding site (109). However, in spite of the differences in relative activity seen in the 5' and the 3' deletion series, the localization of the responsive sequences is the same.

Westerhausen et al (50) have recently shown that two regions mediate the TGFß response of the PAI-1 promoter in another cell line, Hep G2. The first, a 259 bp region (between -546 and -804) includes the sequence in which I find two separate 40 bp responsive sequences (i.e., between -636 and -740). However, the second region (between -186 and -328) which mediates a 2-fold induction in their study, was inactive in my analysis. Another difference between the two studies is that I detected significant activity in response to TGFß in the region between -39 and -100 (11-fold induction) whereas this region was inactive in the Westerhausen et al study. These differences may be due to quantitative differences in the transcription factors present in the cell lines employed in the two studies, or alternatively to differences in the sensitivity of the assay systems.

A nuclear factor-1 (NF-1) binding sequence (TGG(n6)GCCAA) has been shown to mediate the TGFß response of the alpha-2 (type-1) collagen promoter (93) and the PAI-1 promoter has a number of sites with homology to the consensus sequence for NF-1 (94-96). However in my study, none of these sequences appeared to mediate the response of the PAI-1 promoter to TGFß. For example, there is an NF-1-like binding sequence located in the 5' untranslated sequence of the PAI-1 cDNA at +15 to +29. This site has the sequence : TGG(n7)GCCAA which was shown by Shaul et al. to be a high affinity binding site for NF-1 (94). I therefore deleted sequences between +7 and +75 to create a construct which lacks this NF-1 consensus sequence (Fig.2). This deletion had no effect on the TGFß response of the proximal 100 bp region. I also deleted the same NF-1 site (deletion from +7 to +75) to ensure that it was not playing a role in the TGFß response of the distal region and observed no change in induction. (Fig.4). Finally, in my analysis of the distal region, an NF-1-like binding site located between -629 and -634 (TGGCA (95,96)) showed no activity in response to TGFß. These mapping experiments suggest that the NF-1 binding sites present in both the proximal and the distal promoter are not responsible for the TGFß induction in my system.

In summary, the functional data taken together with the DNA binding data support the hypothesis that the response of the PAI-1 promoter to TGFβ is mediated by two conserved regions of the promoter and 5' flanking sequence, both of which contain DNA sequences with homology to the AP-1 consensus sequence.

Acknowledgments. I would like to thank Anton van Zonneveld whose intial work in this field set an excellent background for my studies, Dr.s A. McLachlan and N. Mackman for helpful discussion.

These results were published in *Journal of Biological Chemistry, Vol 266, No 34, 23049-23052, (December), 1991*: **Identification of regulatory sequences in the type-1 plasminogen activator inhibitor gene responsive to transforming growth factor ß by M. Keeton, S. A. Curriden, A. J. van Zonneveld and D. J. Loskutoff.**

CHAPTER 4: A NOVEL SEQUENCE IN THE 5' FLANKING REGION OF THE PAI-1 GENE MEDIATES INDUCTION BY TRANSFORMING GROWTH FACTOR BETA.

Introduction.

PAI-1 synthesis by cultured cells in vitro is induced by a variety of molecules including cytokines (81,82), growth factors (48,83,84), hormones (49,62), and other agents such as endotoxin (85) and phorbol myristate acetate (86). Nuclear transcription run-on assays demonstrate that the regulation of PAI-1 by many of these agents, including TGFß, occurs primarily at the level of transcription (48). TGFß is a homodimeric molecule that belongs to a family of structurally related peptides, and is interesting because it has such a diverse number of biological functions. For example, it inhibits the growth of endothelial cells in culture (84) and yet acts as a potent angiogenic agent *in vivo* (105). TGFß released from platelets may be an important negative regulator of the fibrinolytic system of the vessel wall since the TGFß in releasates of thrombin activated platelets causes large increases in PAI-1 synthesis by endothelial cells (89). This increased PAI-1 synthesis may account for the resistance of platelet-rich thrombi to thrombolytic therapy (110). The PAI-1 that accumulates in the extracellular matrix in response to TGFß protects matrix proteins from proteolytic degradation (111). Thus, the induction of PAI-1 by TGFß may also play a role in both wound healing and fibrotic responses.

Because the induction of PAI-1 and other genes by TGFß appears to affect a number of biological systems, the mechanism of transcriptional regulation by this growth/differentiation mediator has been extensively studied (50,107). For example, the autoinduction of the TGF-β1 promoter suggests a feedback loop designed to amplify the response to TGFß under certain conditions (90). This response was shown to involve specific AP-1 sites (90). AP-1 is a heterodimeric complex of Fos and Jun protein subunits which binds to specific DNA enhancer sites which have the consensus sequence TGAg/cTCA (91). AP-1 is believed to mediate the transcriptional effects of the tumor promoting phorbol esters (92). In contrast to these results, the TGFß response sequence in the promoter for type 1 collagen, has been localized to a sequence with homology to a nuclear factor 1 (NF-1) binding site (93). A number of different consensus sequences for NF-1 have been described and these include the sequences TGGn7GCCAA (94) and TGGCA (95,96). In preliminary experiments, I (Chapter 3) and others (50) studied the effect of TGFß on the PAI-1 promoter and demonstrated that the responsive regions contain sequences with homology to the AP-1 consensus sequence. I was unable to demonstrate a role for NF-1 sites in the TGFß response of the PAI-1 promoter in Hep3B cells.

To investigate the role of AP-1 in the regulation of the PAI-1 promoter in more detail, I compared the effect of both TGFß and AP-1 itself on the activity of a 25bp fragment from the PAI-1 promoter. This fragment contains one of the AP-1 like sequences and responds to TGFß. I show that, although the AP-1 like sequence

influences the response to TGFß, its function does not appear to be related to its ability to bind AP-1. Gel shift and functional analysis of the AP-1 like site suggests that a protein binds in this region and that this protein has a higher affinity for the wild type sequence in PAI-1 than it does for the consensus AP-1 site. Furthermore, a second sequence close to this site appears critical for the TGFß response and this sequence shows no functional activity in response to AP-1. Thus, it appears that a protein unrelated to AP-1 is critical to the TGFß response of the PAI-1 gene, and that the AP-1-like site enhances but is not essential for this response.

Materials and methods.

DNA preparation, cell culture and luciferase assays were performed as described in Chapter 3.

Plasmid construction. A fragment of the PAI-1 promoter (i.e., between -39 and +71), which had previously been shown to have low basal activity and only minimal response to TGFß (average induction of 2.7-fold), was used as a minimal promoter in these studies. Double-stranded blunt-end oligonucleotides were cloned into the -39 position of this promoter and the sequences confirmed by double-stranded sequencing methods. A minimal promoter construct derived from the Hepatitis B viral promoter (a generous gift from Dr. A. McLachlan, The Scripps Research Institute) was used

as a heterologous promoter to test some of the same oligonucleotides. This promoter contained from -188 to +145 of the Hepatitis B promoter and in experiments not shown, demonstrated only 4-fold induction in response to TGFß.

Gel retardation analysis. Gel retardation experiments were performed as previously described (99,100). The oligonucleotides employed in these studies were homologous to the regions between -732 to -708 (5'-GCC AGA CAA GGT TGT TGA CAC AAG A-3') and between -732 to -716 (5'-GCC AGA CAA GGT TGT-3'). The oligonucleotides (100ng) were end-labelled using 6.25uCi of gamma ^{32}P ATP and 20U T4 Polynucleotide kinase for 30 mins at 37°C. The free label was removed by 2 cycles of ethanol precipitation in the presence of 2.5M ammonium acetate. Hep3B nuclear extract was prepared (101) and then 5 μg was incubated in the presence or absence of a 50-fold and 100-fold molar excess of the cold competitor oligonucleotides in the presence of 5ug of poly dI-dC (Boehringer Mannheim, West Germany) in gel shift buffer (25mM HEPES Ph 7.4, 40mM KCl, 7.5% glycerol, 0.125mM EDTA, 0.75mM DTT and 5mM $MgCl_2$) for 15 mins on ice. The mixtures were then incubated with 50,000 cpm of the labelled oligonucleotide (1ng) for 30 mins on ice and then at room temperature for 15 mins. The reaction mixture was loaded on a 6% non-denaturing polyacrylamide gel using a Tris/borate buffer pH 7.4. The gels were run at 150V for 4 hours, dried and then autoradiographed on XAR-5 film (Kodak).

Results.

TGFß responsiveness of three synthetic oligonucleotides. Previous deletion mapping of the PAI-1 promoter demonstrated that three separate regions (-49 to -87, -636 to -674 and -703 to -740) were important in the TGFß response (Chapter 3). Based on these observations, I synthesized oligonucleotides containing the AP-1 like sites from each of these regions, cloned them into the plasmid containing the minimal promoter, and tested their response to TGFß (Fig.1). The first oligo was 16bp in length, corresponded to -56 to -41 of the PAI-1 gene (region A), and conferred, approximately 10-fold induction on the minimal promoter. The second oligo was 25bp in length and corresponded to -674 to -650 (region B). It conferred 56-fold induction on the minimal promoter. The last oligo was 36bp long and corresponded to -743 to -708 (region C) and led to a 25-fold induction in the promoter. Regions A and C contain only a single AP-1 like sequence whereas region B contains 2 AP-1 like binding sequences. Thus, oligonucleotides containing AP-1 like sequences from each region were able to confer TGFß responsiveness to a non-responsive minimal promoter (Fig.1).

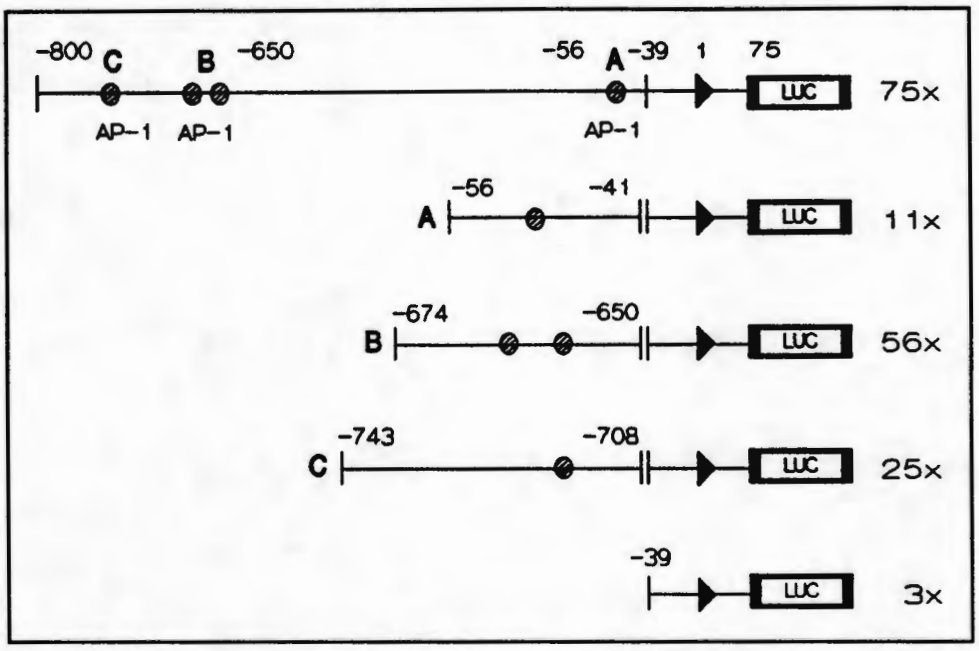

Figure 1. Localization of TGFß resposive regions of the PAI-1 promoter. A series of oligonucleotides from the PAI-1 promoter were cloned into a minimal promoter construct and tested for response to 1ng/ml TGFß after transient transfection in Hep3B cells as previously described. The minimal promoter contains a perfect TATA box at -23 and the start site of transcription (▸) fused to the firefly luciferase reporter gene (LUC). These oligonucleotide sequences were derived from the proximal promoter (Region A: -56 to -41) and from the distal 5' flanking sequence (Region B: -674 to -650 and Region C: - 743 to -708) of the PAI-1 gene. Each region showed a specific response to TGFß when compared to the background response of the minimal promoter (3-fold) and the results (fold induction in respose to TGFß) are indicated on the far right of the figure. These and all subsequent results represent the average of at least 4 indepedent experiments, each performed in duplicate.

Responsiveness of regions A,B and C to c-fos/c-jun. In order to test directly the responses of these sequences to AP-1 itself, I co-transfected them with plasmids containing the mouse genes for c-fos and c-jun under the control of the RSV promoter. I found that all three of these regions showed a dose-dependent response to increasing amounts of transfected c-fos/c-jun (Fig.2), with maximum responses seen at 0.1ug per well.

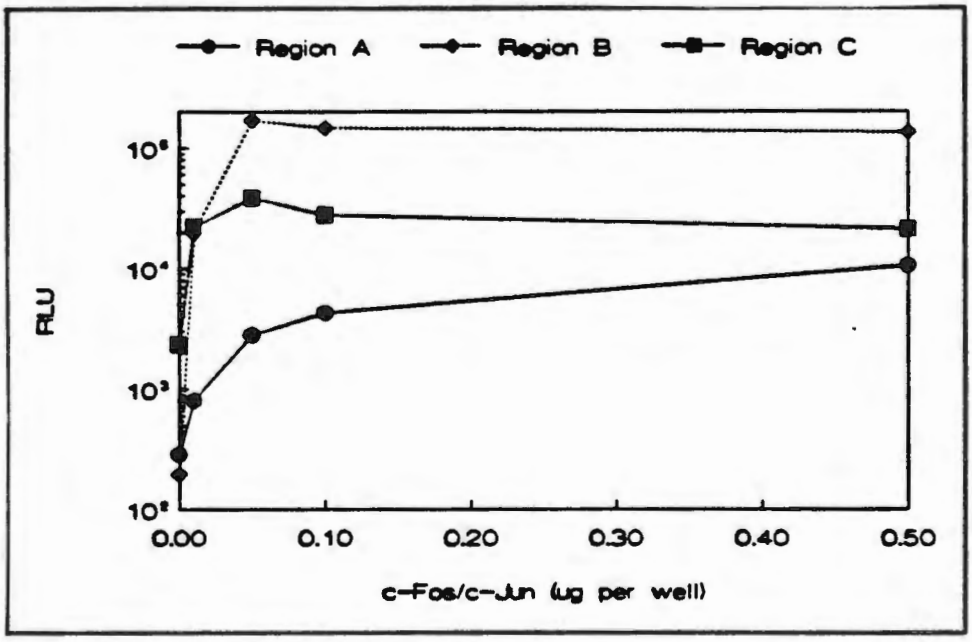

Figure 2. Dose response of regions A to C to co-transfected RSV c-fos/c-jun. **Co-transfection experiments were performed in which the constructs to be tested were transfected together with the plasmids containing the genes for mouse c-fos and c-jun under the control of the RSV promoter. The x-axis reprents the concentration in ug/well of each of the c-fos/c-jun plasmids added to 2.5ug of each of the reporter constructs (region A (●), region B (■) and region C (♦). The y-axis represents the luciferase light units in a log scale.**

using 0.1 ug/well of c-fos and c-jun plasmids. This response was dependent on co-transfection of both plasmids since neither c-fos or c-jun alone was able to cause this induction (data not shown).

Detailed analysis of the TGFß responsive sequence of region C. To examine the role of the AP-1 like sequences in the TGFß response, I chose to study region C since it contains only a single AP-1 site and shows relatively strong induction by TGFß

Although the expression plasmids for c-fos and c-jun contained cDNAs derived from mouse genes, I did not anticipate any problems using these proteins in a human cells system in view of the extremely high degree of conservation of these proteins between species. Transcription factors have been shown by others to operate in an extremely wide variety of species (Mitchell, P. and Tjian, R. Science 245, 371-378, 1989.).

Detailed analysis of the TGFß responsive sequence of region C. To examine the role of the AP-1 like sequences in the TGFß response, I chose to study region C since it contains only a single AP-1 site and shows relatively strong induction by TGFß (Fig.2). To find the minimal TGFß responsive sequence in this region I constructed 2 oligonucleotides, the first from the 3' side of region C which contained the AP-1 like sequence (C2: -708 to -723) and the second from the remaining 5' sequence (C3: -727 to -743). When I tested the responsiveness of these oligonucleotides to TGFß I found that neither sequence showed maximal induction as compared to region C itself (Fig.3; compare C1 with C2 and C3). This result raised the possibility that I may have deleted a portion of a binding site located between -723 and -727. I therefore progressively extended the 5' side of C2 to include bases between -723 to -728 (Fig.3; C4) but found that this only slightly improved the TGFß response. However, when this region was extended another 4bp there was a dramatic increase in the TGFß response to 63-fold induction (Fig.3, C5) suggesting that this region was crucial for the response.

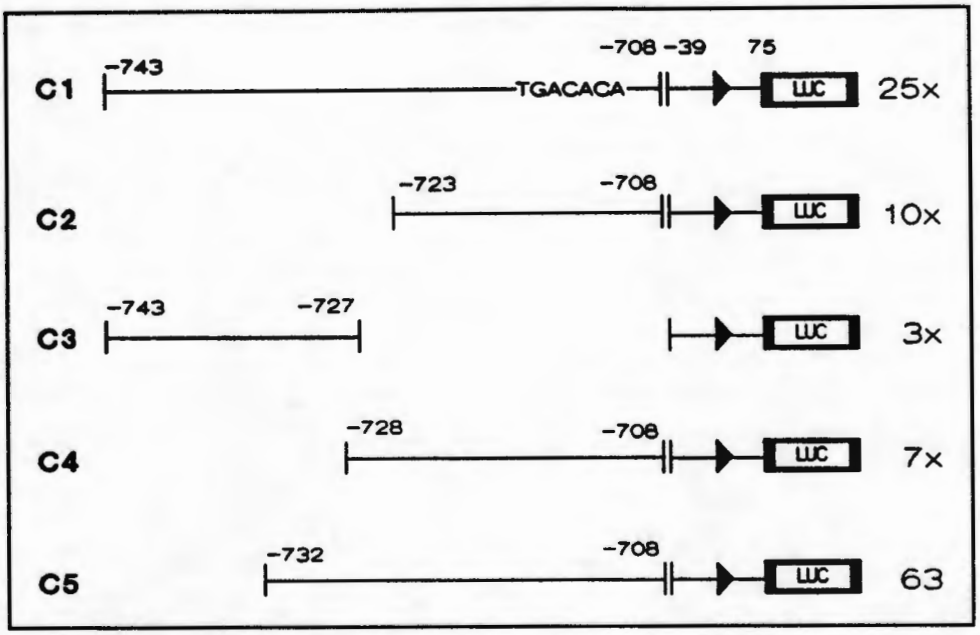

Figure 3. Localization of minimal TGFß responsive sequence in region C. Four constructs (C2: -723 to -708; C3: -743 to -727; C4: -728 to -708; and C5: -732 to -708) derived from region C1 were cloned into the minimal promoter and tested for response to 1ng/ml of TGFß as previously described. The fold induction is indicated to the right of the figure.

Functional analysis of region C5 to localize the TGFß and AP-1 (F/S) responsive regions. In preliminary studies, I determined the response of the minimal promoter to direct stimulation with c-fos/c-jun. It showed approximately 10-fold induction with AP-1 compared to only 3-fold induction with TGFß (Fig.4, bottom line). When I tested C5 itself in a similar manner, there was only a 2-fold increase above the vector background induced by c-fos/c-jun compared to a greater than 20-fold increase above background seen with TGFß (i.e., C5 itself showed 63-fold induction with TGFß). Thus, although the wild type AP-1-like site in C5 was a relatively poor responsive sequence for c-fos/c-jun, this region still showed a strong response to TGFß. I therefore mutated the AP-1 site to produce a consensus AP-1 sequence (converting

TGACACA to TGAGTCA) and again compared the responseness of this construct to both c-fos/c-jun and TGFß. This mutation increased the AP-1 response from 19-fold to 105-fold but did not improve the TGFß response (Fig.4: C5 and C6). In fact, there was a consistent decrease in the TGFß response following this mutation (compare 63-fold induction with TGFß for the wild type AP-1 like site (Fig.4 C5) to 27-fold for the consensus AP-1 site (Fig.4 C6). I then mutated the AP-1-like site by changing the critical TGA bases, a change shown by others to decrease the activity of the AP-1 binding site. Although this mutation had the expected effect of abolishing the AP-1 response, it did not completely abolish the response of this construct to TGFß (i.e., C7 showed a 10-fold induction with c-fos/c-jun [i.e. vector background] whereas it still showed 13-fold induction with TGFß [i.e. 5-fold above vector background]).

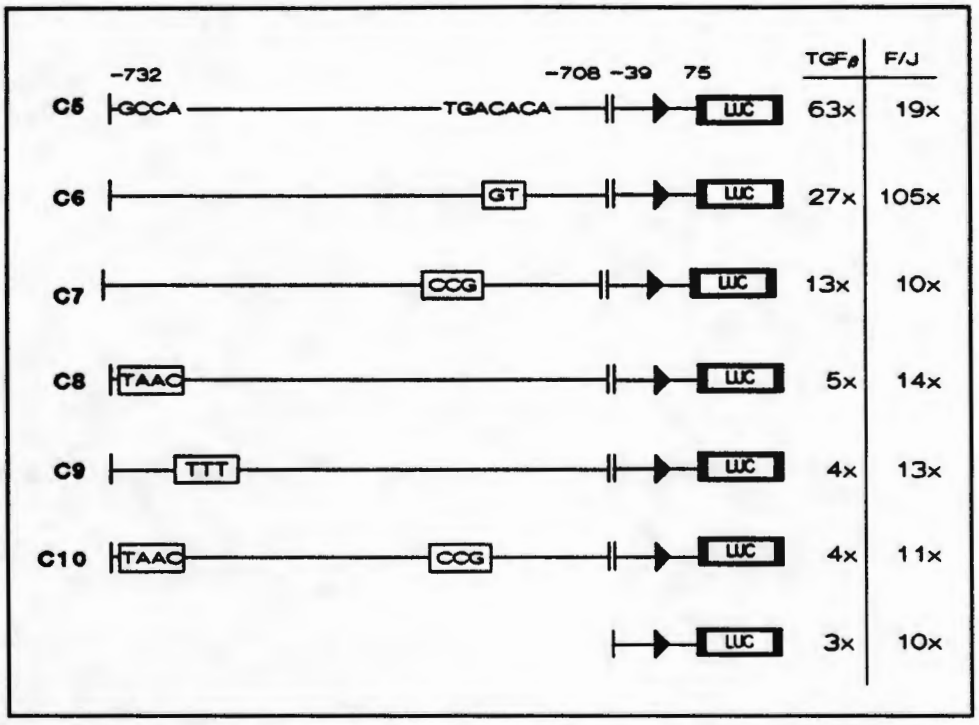

Figure 4. Site directed mutagenesis to localize the TGFß and AP-1 (F/J) responsive regions of C5. Five mutants derived from C5 were tested for their response to 1ng/ml of TGFß or to transactivation by AP-1. The altered bases in each case are indicated in the box for each construct (C6: CA to GT; C7: TGA to CCG; C8: GCCA to TAAC; C9: AGA to TTT; C10: TGA to CCG; and GCCA to TAAC). The fold inductions are indicated to the right of the figure.

This result once again suggested that the 5' portion of C5 was also important in mediating the TGFß response. To further test this hypothesis, I mutated the 4bp sequence between -728 and -732 (C8) since the previous deletion results (Fig.3; C4 compared to C5) suggested that this sequence was critical to the TGFß response. I also mutated 3bp between -726 and -728 (C9). As expected, both of these 5' mutations caused dramatic reductions in the response of C5 to TGFß, reducing the 65-fold response of C5 to vector background levels. These changes also reduced the AP-1 response from 19-fold to 13-14-fold (Fig.4: C8 and C9). Finally, I created a

double mutation of both of these sites and these changes abolished both the TGFß and the AP-1 responses (Fig.4 C10).

Heterologous promoter induction. To test whether the 25bp oligonucleotide (C5) was able to activate a heterologous promoter, I cloned it into a hepatitis B viral promoter. In control experiments, I tested from -188 to +145 of the viral promoter itself and demonstrated that this construct alone showed 28-fold induction with fos/jun (Fig.5). However, the viral promoter showed only 4-fold induction with TGFß. Thus, even though the hepatitis B viral promoter had active AP-1-like sites, these were not sufficient for a strong TGFß response. I then cloned the region between -708 and -732 of the PAI-1 promoter (C5) into the viral promoter and tested this construct as above. This 25bp PAI-1 fragment was able to increase the TGFß response of the viral promoter from 4-fold to 47-fold (Fig.5, second line) but did not significantly alter the AP-1 response (25-fold compared to 28-fold). Again, mutation of bases between -728 and -732 of the PAI-1 oligonucleotide reduced the TGFß induction of this fragment but did not lower the response to AP-1 (Fig. 5, third line).

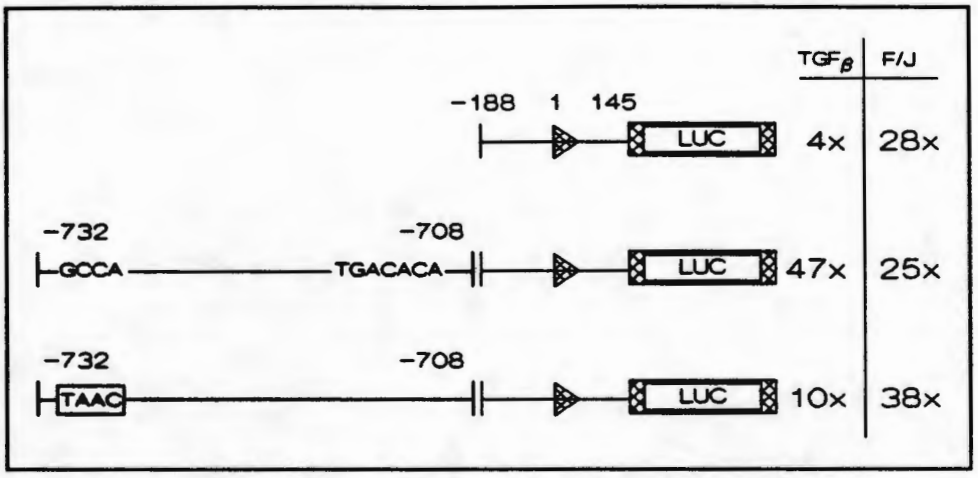

Figure 5. Heterologous promoter response to C5. The Hepatitis B viral promoter from -188 to +145 was tested for response to both TGFß and to transactivation in response to AP-1. C5 (-732 to -708 of the PAI-1 promoter) and C8 (mutation of bases -728 to -732 from GCCA to TAAC) were cloned at position -188 and then these constructs were also tested for response to both TGFß and AP-1. The fold induction is indicated to the right of the figure.

Gel shift analysis of C5. To identify the nuclear proteins that bind to regulatory regions of the PAI-1 gene, I performed gel shift studies using double-stranded oligonucleotides corresponding to position -708 to -732 and nuclear proteins from Hep3B cells. When labelled oligonucleotide C5 was incubated in the absence of any competitor oligonucleotides, I observed 2 specific shifted bands (Fig.7; lane 1, B1 and B2). In the presence of a 50 (lane 2) and, 100-fold (lane 3) excess of cold competitor of the same sequence, this shift was greatly reduced (band B1) or abolished (band B2). I then tested the ability of the mutated oligonucleotides to compete for binding to these proteins. I found that changing the sequence of the AP-1 like site to a consensus AP-1 site reduced the efficiency of competition for both bands B1 and B2 (Fig.7, lanes 4 and 5), even though functionally this mutation improved the response

to AP-1 by an order of magnitude (Fig.4: C6). Similarly, when the TGA of the AP-1 site was changed to CCG (C7), this oligonucleotide was still able to compete weakly for the binding of both B1 and B2 (lanes 6 and 7), even though functionally this site was no longer active in response to AP-1 (Fig.4: C7). This result suggested that although a protein bound to the AP-1 like site it was not competing in the manner expected of AP-1. When an oligonucleotide with a 4bp mutation between -728 and -732 was used in the competition assay (C8), it was as efficient in competing for bands B1 and B2 (lanes 8,9) as the wild type sequence (Fig.4:C8). Thus, the proteins in the shifted bands B1 and B2 appear to be binding in the region of the AP-1-like site and not to the 5' end of this oligonucleotide. Finally, the double mutant (C10) showed no specific competition of either band (lanes 10,11) as did a control oligonucleotide (lanes 12, 13) containing the HNF-1 binding site (Fig.4 C10 and HNF-1).

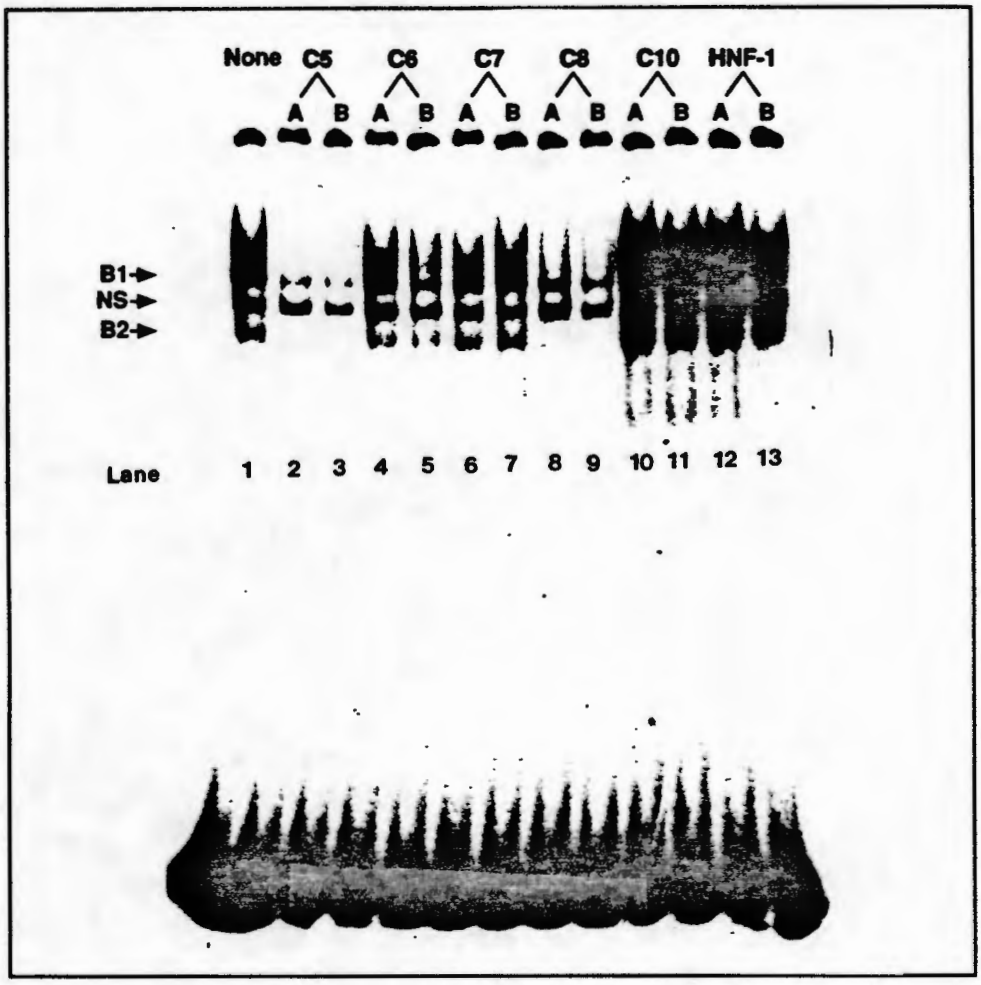

Figure 7. Gel retardation analysis. Labelled oligonucleotide (C5 ^{32}P: 50,000cpm per lane) containing the sequence from -732 to -708 of the PAI-1 promoter was incubated with 5ug Hep3B nuclear extract and 5ug of dIdC in the presence and absence of competitor oligonucleotides (i.e., a 50-fold (A) and 100-fold (B) molar excess of unlabelled oligonucleotide). The arrow head at B1 and B2 indicate the position of the specific complexes. The arrow head at NS represents a non-specific complex. Lane 1 no competitor; lanes 2 and 3, competition with oligonucleotide of the same sequence (C5); lanes 4 and 5, competition with the oligonucleotide containing the consensus AP-1 sequence (C6); lane 6 and 7, competition with the oligonucleotide containing the mutant AP-1 site (C7); lane 8 and 9, competition with the oligonucleotide with 4bp mutation at -732 to -728 (C8); lanes 10 and 11, competition with the double mutant (C10) and lanes 12 and 13, competition with non-specific oligonucleotide containing the sequence of the HNF1 binding site.

Discussion.

The TGFß response of both the PAI-1 promoter and the TGFß promoter (90) has been localized to regions containing specific AP-1 like sites. The simplest interpretation of this data is that TGFß acts by increasing the level of AP-1 in the cell to cause increased transcription of these promoters. However, when I examined two regions of the PAI-1 promoter that displayed similar levels of induction by TGFß (about 60-fold; Figure 1: region B and Figure 3: C5) I observed that one region showed 2000-fold transactivation with AP-1 (Figure 2: region B) whereas the other (Figure 4: C5) showed only about 19-fold transactivation. Thus, the TGFß response did not appear to correlate with the ability of these sequences to respond to AP-1. I examined the role of the AP-1-like sequences in the TGFß response more directly by using site directed mutagenesis. I found that although mutation of the AP-1-like site in C5 to a consensus AP-1 sequence increased transactivation by fos/jun from 19-fold to greater than 100-fold, this same change decreased the response to TGFß (Figure 4: region C6). This observation suggested that the AP-1-like site was important in the TGFß response but that its role was not apparently related to the ability of this sequence to respond to c-fos/c-jun. This hypothesis is supported by the observation that gel shift analysis demonstrated that the protein bound to the AP-1-like site did not show a competition pattern consistent with AP-1 (Figure 4). For example, the construct which contained the consensus AP-1 site was a relatively poor competitor for proteins bound to the wild type AP-1-like site (Figure 7: lanes 4 and 5), in spite of

the fact that it was functionally far more active in response to AP-1 (Figure 4: C6). Moreover, a mutant that was functionally inactive in terms of its response to AP-1 (Figure 4: C7), still showed specific competition (Figure 7: lanes 6 and 7) compared to a non-specific competitor (Figure 7: lanes 12 and 13). These results indicate that a protein binds to the wild type AP-1-like sequence that is functionally important in the TGFß response. However, both the binding and the functional data indicate that this protein is not AP-1. This protein may be derived from the large family of AP-1 like proteins (91) and may have slightly different sequence specificity when compared to c-fos/c-jun.

Examination of the published data on the TGFß promoter reveals that it contains three AP-1 like sites all of which appear to play a role in the autoinduction of this gene (90). The first site is located at -365 to -371 and mediates an approximately 10-fold induction with TGFß. The other two sites are located between +102 to + 289, and together mediated about 4-fold induction in response to TGFß. Moreover, each TGFß responsive region was also shown to be responsive to AP-1. Again, comparison of the level of transactivation by AP-1 to the level of induction by TGFß, reveals a similar discrepancy as I observed with the PAI-1 promoter. For example, one region (-453 to +11) showed approximately equal responses to AP-1 and TGFß (8.5-fold induction with TGFß and 12.7-fold response to AP-1), whereas a second region (+102 to +289) showed much greater response to AP-1 than to TGFß (4.7-fold induction with TGFß compared to 19-fold with AP-1). This result again suggests that TGFß induction

is not simply due to an increase in AP-1 in the cell.

Finally, it is interesting to note that there is a T to A substitution at the fifth position of the AP-1-like sites in the most TGFß response sequences of both the PAI-1 promoter and the TGFß promoter (TGA(n)TGA to TGA(n)ACA [PAI-1 promoter: -717 to -711 = TGACACA; -659 to -653 = TGATACA; TGFß promoter: reverse orientation: -365 to -371 = TGAGACA]). These sequences are distinct from the consensus sequence for AP-1 (TGA(g/c)TCA (92). It is possible that the T to A substitution may lower the binding affinity of this sequence for c-fos/c-jun resulting in a sequence that preferentially binds another protein. This possibility is consistent with the functional data on the AP-1-like site of the PAI-1 promoter (Figure 4: C5 between -711 to -717) since the wild type sequence is a poor AP-1 binding site and yet is still important in the TGFß response.

Analysis of the 25bp sequence derived from the wild type PAI-1 promoter (-708 to -732) suggested that the 5' side of the oligonucleotide may contain a second binding site of importance in the TGFß response (Figure 4: C5 compared to C8). In fact, mutation of the 5' side of this region almost completely abolished the TGFß response even though the AP-1 region was intact (Figure 4: C8). Moreover, this sequence alone was able to act independently of the AP-1 site and confer strong TGFß induction to the normally unresponsive minimal promoter (data not shown). These results indicate that this second site on the 5' side of C5 is also important for the

TGFß response in this system. The full TGFß response, however, seemed to be dependent on the functional activity of both the AP-1 like site and the 5' site.

The analysis of the critical bases involved in the TGFß response of this sequence is complicated by the fact that a partial NF-1 site (reverse orientation from -729 to -732: TGGC, Figure 4: C5) is found on the 5' side of this active region. A number of features suggest that this NF-1 site may not be functionally important. In the first instance, several other NF-1 sites of similar sequence are found in regions of the PAI-1 promoter that are not responsive to TGFß. For example, two other perfect NF-1 sites situated between -100 and -595 showed no response to TGFß (TGGCA: Chapter 2, Figure 1). Furthemore, the sequence between -595 and -636 contains a similar NF-1 site (TGGCA; -633 to -629) and also does not show any response to TGFß, when tested independently (Chap 2, Figure 3). The lack of activity of these other NF-1 sites may however be related to the context of the surrounding DNA, and it is possible that the bases adjacent to the site uniquely arranged so as to activate this NF-1 site. Secondly, mutation of the sequence adjacent to this NF-1 site (Figure 4: C9) which only affects the first base of the site still completely reduced the TGFß response.

When I compared the sequence of the 5' 15bp construct (-718 to -732) to the other region of the PAI-1 promoter which showed strong TGFß induction (region B = 60-fold), I found a high sequence similarity between these two regions (75%

homology). This region of homology contains only first base of the NF-1 site which further argues that the activity of this site may be independent of the NF-1 site. I performed a homology search on the TGFß promoter and detected a high degree of homology between the active regions of the PAI-1 promoter and a region between -365 to -371 of the TGFß promoter (75% homology). Interestingly, this is not only the same region of the TGFß promoter that shows the strongest TGFß induction, but it also has the AP-1-like sequence (TGAnACA) identical to those seen in responsive regions of the PAI-1 promoter.

In summary, the TGFß response of both the PAI-1 promoter and the TGFß promoter was localized to specific AP-1 like sites. However my data indicates that the full TGFß response of this region of the PAI-1 promoter is dependent on the interaction of two distinct binding sites. Although the first site has homology to the AP-1 site, it does not appear to bind AP-1. While this site does not appear to be essential, it is required for the full TGFß response of this region. The second site, located 5' to the AP-1 site, appears to be critical in the TGFß response. This site is 15bp in size and contains a motive that is present in both active regions of the PAI-1 promoter as well as in the most responsive region of the TGFß promoter. The 5' side of this 15bp sequence also contains a partial NF-1 site which our data suggests is probably not involved in the TGFß response of the sequence, but this conclusion still needs to be rigoursly tested. This novel region of homology between the active regions of the PAI-1 and TGFß promoters does not appear to correspond to any previously described

transcription factor binding sites and may represent a new and specific binding site which is critical for a strong TGFß response.

This work is currently being prepared for submission to the Journal of Biological Chemistry.

Title: A novel sequence in the 5' flanking region of the PAI-1 gene mediates induction by transforming growth factor beta.

Authors: M. Keeton, S. A. Curriden, H. Craig, A. Wright and D. J. Loskutoff.

CHAPTER 5: CELLULAR LOCALIZATION OF TYPE-1 PLASMINOGEN ACTIVATOR INHIBITOR mRNA AND PROTEIN IN MURINE RENAL TISSUE.

Introduction.

Increased levels of plasma PAI-1 have been demonstrated in a number of clinical conditions associated with a predisposition to thrombosis, such as myocardial infarction (53), deep vein thrombosis (52) and pregnancy (55). Plasma PAI-1 activity may also be elevated in patients with sepsis and endotoxemia, a condition frequently associated with disseminated intravascular coagulation (51). These observations suggest that increased rates of PAI-1 synthesis or release may contribute to the increased risk of thrombosis associated with these conditions.

We have been interested in the role of PAI-1 in renal disease since increased plasma PAI-1 levels also correlate with the active phase of a variety of human renal disorders, including the nephrotic syndrome (112) and the hemolytic uraemic syndrome (113). Moreover, a large increase in plasma PAI-1 was observed in an experimental model of glomerulonephritis (GN) in which rats were injected with anti-glomerular basement membrane (anti-GBM) antibodies (82). Microscopic examination of renal tissue from these animals showed fibrin thrombi in glomeruli. Direct administration of tumor necrosis factor alpha (TNFα) also caused large increases in plasma PAI-1, and concomitant administration of both the nephrotoxic antibody and

TNFα caused superinduction of plasma PAI-1 levels. The increase in PAI-1 was again associated with an increase in fibrin thrombi.

In spite of the potential importance of PAI-1 in human thrombotic disease, the cellular site(s) of synthesis of this important inhibitor *in vivo* is unknown. In most instances, measurements of PAI-1 have been confined to plasma and the origin of plasma PAI-1 also remains speculative (87). In this study, I investigate the site of renal PAI-1 production in control and endotoxemic mice. I show by Northern blot analysis that while PAI-1 mRNA expression is barely detectable in the control kidney, large amounts can be detected following administration LPS. Although cell culture studies suggest that endothelial cells may be the primary site of synthesis of PAI-1 *in vivo* (for a review see; (87)), little PAI-1 could be detected in the endothelium of untreated, control animals. Analysis of renal tissue from LPS-treated mice by *in situ* hybridization revealed that PAI mRNA was synthesized primarily by endothelial cells located throughout the kidney. The localization of PAI-1 production to the endothelium in this model may have relevance to the formation of fibrin thrombi in certain renal diseases like HUS and lupus nephritis.

Material and methods.

Tissue preparation. Twelve age matched CB6 mice (BalbC/ByJ x C57Bl6/J; Scripps Clinic Rodent Breeding Colony) between the ages of 2 months and 8 months received intraperitoneal injections of either 50ug of LPS in normal saline or saline alone. Three hours later the mice were killed by overdose inhalation anaesthesia using metofane and perfused for 5 minutes with 30ml of cold 4% paraformaldehyde injected through the left ventricle. Organs were removed and immersed in freshly prepared 4% cold paraformaldehyde. The tissues were fixed at 4°C overnight, embedded in paraffin blocks,and sectioned at 2-5um thickness using a microtome. The tissue sections were mounted onto polylysine slides and stored at room temperature, until analyzed. The results (see below) were consistent from animal to animal in both the control and the LPS treated groups.

Riboprobe preparation. A full length mouse PAI-1 cDNA (114) subcloned into the vector pBS+ (Stratagene) was provided by Drs. L.Diamond and M. Cole (Princeton University). An EcoRI/SphI fragment containing from nucleotide 1 to nucleotide 1085 of the mouse PAI-1 cDNA was cloned into pGEM -3Z (Promega). This vector was linearized with the restriction enzyme EcoRI and used to make an antisense riboprobe labelled with ^{35}S-labeled UTP (specific activity ,1200 Ci/mmol; Amersham) by *in vitro* transcription using SP6 RNA polymerase (Promega). The DNA

template was removed by digestion using RQ1 DNAse for 15 minutes at 37°C and the riboprobe purified by phenol extraction and ethanol precipitation. This vector-insert construct was also used to make a sense control probe by linearizing with the restriction enzyme HindIII and *in vitro* transcription using T7 RNA polymerase.

In situ hybridization. *In situ* hybridizations were carried out essentially as described (115). Briefly, prior to hybridization, the paraffin sections (2-5um) were pretreated sequentially with xylene (three 5 min washes), with 2x SSC (one 10 min wash; 1x SSC = 150mM NaCl/15mM sodium citrate, pH 7.0), with 4% paraformaldehyde (10 min at 4°C), and with proteinase K at 1ug/ml in 500mM NaCl/10mM Tris-HCl pH8.0 (10 min at room temperature). The slides were then prehybridized for 1-2hrs in 100ul of prehybridization buffer (50% (wt/vol) formamide/0.3M NaCl/20mM Tris-HCl, pH8.0/5mM EDTA/0.02% polyvinylpyrrolidone/0.02% Ficoll/0.02% bovine serum albumin/10% (wt/vol) dextran sulphate/10mM dithiothreitol) at 42°C. The hybridizations were started by adding 600,000 cpm of the ^{35}S-labeled riboprobe in 20ul of prehybridization buffer containing 2.5mg/ml of t-RNA, and were carried out at 55°C overnight. The sections were then washed with 2x SSC (two 10 min washes), treated with RNase A (20ug/ml in 500mM NaCl/10mM Tris-HCl for 30 mins at room temperature), washed in 2x SSC (two 10 min washes), and then washed at high stringency in 0.1x SSC at 60°C for 2hr. This wash temperature is considerably higher than other commonly described methods (e.g., 52°C; (115), and combined with RNAse A treatment, which reduces non-specific

hybridization by more than 8-fold (116), results in very high stringency conditions. All SSC solutions up to this point of the procedure contained 10mM 2-mercaptoethanol and 1mM EDTA to reduce non-specific binding of the probe. The sections were washed in 0.5x SSC without 2-mercaptoethanol (two 10 min washes), dehydrated by immersion in a graded alcohol series containing 0.3M NH_4Ac, dried, coated with NTB2 emulsion (Kodak; diluted 1:2 in water), and exposed in the dark at 4°C for 2-12 weeks. Slides were developed for 2 min in D19 developer (Kodak), fixed, washed in water (three 5 min washes) and counterstained with hematoxylin and eosin. Parallel sections were analyzed using a sense probe as the control for non-specific hybridization and in no instance was a specific signal detected even after 12 weeks exposure (data not shown).

Northern blot analysis. Total RNA was extracted from renal tissue of CB6 mice by the acid/guanidium/thiocyanate phenol-chloroform method (74) and its concentration determined by measurement of sample absorbance at 260 nm. Total RNA (20 μg) was analyzed for PAI-1 mRNA by Northern blotting as described previously (48), employing a 1.3 kb human PAI-1 cDNA probe. The probe was labeled by the random primer technique (75) employing α-^{32}P dGTP (>3000 Ci/mmol; Amersham). Equal loading and transfer of the RNA was confirmed by inspection of the ethidium bromide-stained RNA in the nylon membrane following transfer. Autoradiography was performed at -80°C., employing Kodak XAR-5 film with intensifying screens.

Antibodies. The full length mouse PAI-1 cDNA was cloned into a protein A expression vector (pRIT2T, Pharmacia). The fusion protein was expressed in E-coli (N4830-1, Pharmacia) and purified by passing the cell lysate over an IgG Sepharose (Pharmacia) column, and then over a heparin-Agarose (TypeII, Sigma) column. Rabbits were immunized with 0.4mg of the fusion protein and then boosted three times with 0.4mg at 2 week intervals. The IgG fraction of the resulting antiserum was isolated with Protein A-Sepharose (Bio-Rad), using the low salt method (117). The resulting IgG fraction contained antibodies to both PAI-1 and protein A. Therefore the anti-protein A specific IgG was removed by applying the total IgG fraction to a Protein A-Sepharose column. In order ensure that only the anti-protein A antibodies bound to this column, the Fc binding capacity of the column was first blocked with cross-linked normal rabbit IgG. The pass-through was then applied to a PAI-1-Sepharose column and the anti-PAI-1 IgG was eluted with 0.1M glycine, pH 2.5, and used for the immunohistochemistry. After these purification steps it could be demonstrated that this fraction of the antibody was specific for PAI-1 and had no non-specific binding to protein A (data not shown). The IgG fraction of rabbit anti-human vWF (118,119) was purified using protein A-sepharose affinity chromatography from antisera kindly provided by Dr Z. Ruggeri of this institution.

Immunohistochemistry. Immunohistochemical staining was carried out as described in the HISTOSTAIN-SP Kit (Zymed). Paraffin embedded, paraformaldehyde fixed sections were deparaffinized with xylene at 37°C (3x5 min), treated with 3%

hydrogen peroxide for 10 min at room temperature to quench endogenous peroxidase activity, and rehydrated with a graded series of ethanol. After washing with 0.05 M Tris-HCl, 0.15 M NaCl, pH 7.4 (TBS) for 10 min, the sections were treated with a graded series (0.2, 0.5, 1%) of Triton X-100 in TBS for permeabilization (10 min each at room temperature). The sections were then incubated with prewarmed 0.23% (wt/vol) pepsin (2830 U/mg, Worthington Bioche. Corp.) in 0.01 N HCl at 37°C for various times. Times were optimized for each antigen. For example, 3 min was the optimal time to unmask PAI-1 tissue antigens, while 8 min was optimal for vWF. The tissue sections were rinsed with cold distilled water, washed with 0.2% Triton-TBS (2x3 min), and incubated with 10% (wt/vol) normal goat serum in TBS for 30 min at room temperature. Incubation with primary rabbit antibodies was performed in a humidified box for 16-18 h at 4°C followed by 1 hr at room temperature. I used 5 μg/ml of immunopurified anti-mouse PAI-1 or 10 μg/ml of affinity-purified anti-human vWF, in TBS, containing 0.1% (wt/vol) bovine serum albumin (BSA). After washing with 1% Triton-TBS (3x3 min), the second antibody (biotinylated goat anti-rabbit IgG, Zymed diluted 1:100 with TBS containing 0.05% Tween 20) was added and allowed to react for 15 min at room temperature. The tissue sections were washed again with 1% Triton-TBS (3x3 min), incubated with streptavidin-peroxidase conjugate prepared according to the manufacturer's instructions for 10 min at room temperature, washed with 1% Triton-TBS (3x3 min), and then treated with a freshly prepared amino ethylcarbazole (AEC) chromogen containing 0.03% hydrogen peroxide at room temperature for 15 min. After rinsing in distilled water for 3 min, the sections were

counter-stained with Mayer's hematoxylin for 3 min at room temperature, rinsed well with tap water and mounted in GVA-mount (Zymed).

In control experiments, tissue sections were stained with antisera previously depleted of the specific antibodies. In the case of PAI-1, immunoadsorption was performed by adding a 20-fold molar excess of PAI-1 antigen over antibody to the immunopurified rabbit anti-mouse PAI-1 solution, and the mixture was incubated overnight at 4°C. This mixture was then used instead of the primary antibody for immunohistochemical staining. No specific staining was apparent in these control experiments. Tissues incubated with preimmune (normal) rabbit IgG instead of primary antibody also failed to stain. Cultured mouse 3T3 cells produce PAI-1 following incubation with 1 ng/ml phorbol 12-myristate 13-acetate (PMA) in serum-free media for 24 h (unpublished data). These cells were used as a positive control for immunohistochemical staining of PAI-1. Human umbilical vein ECs were cultured as described previously (120) and used as a positive control for immunohistochemical staining of vWF (121).

Immunoelectron microscopy. Staining for PAI-1 antigen was performed using avidin-biotin method with slight modifications. Sections (30um) of renal tissue from mice treated with 50ug LPS for 3 hours were first fixed in 4% paraformalderhyde for 1 hour at 4°C and then incubated in blocking buffer (10 mM TRIS-HCl, 2% BSA and 0.02% saponin, pH 7.5) for 1 hour at RT. The tissue sections were incubated with the primary antibody (rabbit anti-PAI-1) diluted 1:100 overnight at 4°C, washed,

incubated with biotinylated goat anti-rabbit IgG (1:100) for 4 hours at RT, and then with avidin-peroxidase complexes (1:200; prepared according to the directions of the Vectastatin Elite ABC Kit (Vector Lab)) for 4 hours at RT. All reagents were made in reagent diluent (0.05 M TRIS-HCl, 0.15M NaCl, 2% BSA, 1% heat inactivated human serum 0.02% saponin, pH 7.5) and between each step the sections were washed with reagent diluent three times for 15 minutes at RT. For color development, diaminobenzidine (2 mg/ml) in TBS were used at RT for 45 min.

The sections were then transferred into 0.1M cacodylate buffer, pH 7.4 for 15 to 60 min and dehydrated in graded ethanol, and then embedded in Epon 8 12 Resin (TAAB Lab Equipment LTD, England). Ultrathin sections were cut on an Ultratome III (LKB Instruments Inc., Gaithergurg, MD) and mounted on a 200 mesh bare grids. Osmium or lead acetate that might have obscured the diabenzidine reaction product were not used. The sections were examined and photographed with an HU 12A electron microscope (Hitachi Ltd., Tokyo, Japan) at a 75-kV excitation power using a 20-um objective aperture.

Results.

Northern blot analysis of renal PAI-1 mRNA. Examination of total RNA from control and endotoxin treated mice by Northern blot analysis using a human PAI-1 cDNA probe (48) revealed a single transcript of 3.2 Kb, in agreement with the size of mouse PAI-1 mRNA (114). Although only a relatively weak signal could be detected in RNA prepared from control mice (Fig.1 A), a strong signal was detected in RNA

from endotoxin-treated animals (Fig.1 B). These results agree with previous dose-response and time course studies in which nuclease protection assays were employed to demonstrate maximum (93-fold) induction of PAI-1 mRNA, in murine tissues 3 hours after LPS administration (122). Endotoxin also stimulates renal PAI-1 in rats (123).

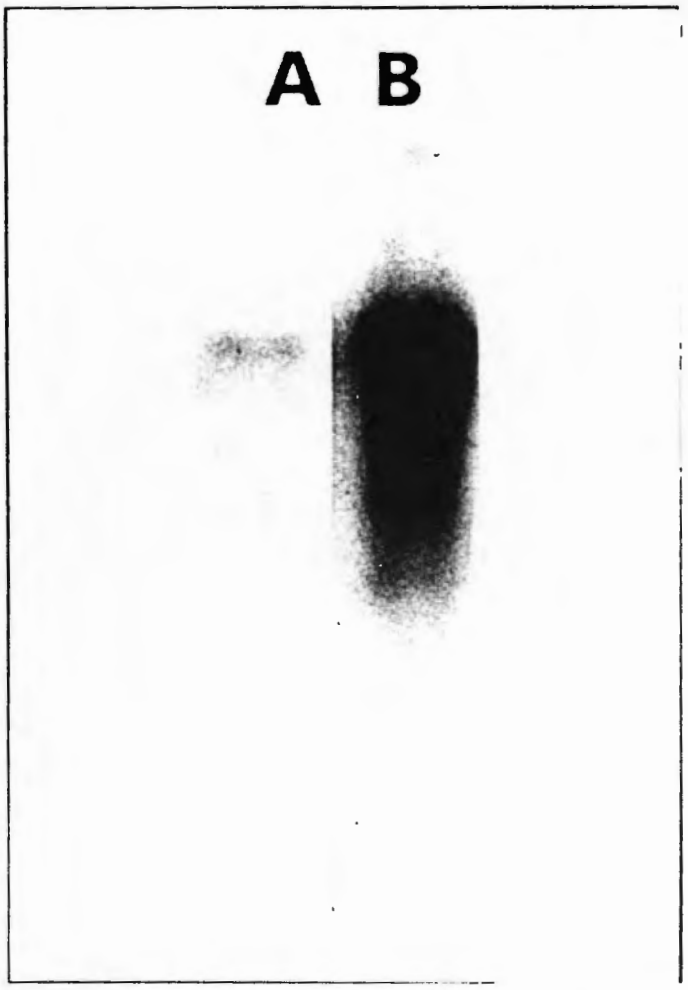

Figure 1. Northern blot analysis of PAI-1 mRNA in control and endotoxemic mice. Mice received intraperitoneal injections with saline (Lane **A**) or 50ug of LPS (Lane **B**) as described in the methods. Three hours later total kidney RNA was extracted, and 20 µg was fractionated by agarose gel electrophoresis, transferred to nitrocellulose and hybridized to a ^{32}P labelled human PAI-1 cDNA probe. The membranes were exposed for 3 days at -80^{o}C. Even loading and quality of the RNA was verified by ethidium bromide staining of the agarose gel. The estimated size of the positive band relative to the 18S and 28S RNA is 3.2Kb.

Localization of PAI-1 mRNA and antigen in the renal cortex. No PAI-1 mRNA was detected when the renal cortex from control mice was examined by in situ

hybridization (Fig.2 A), even alter 12 weeks exposure (not shown). However, after LPS administration, a strong hybridization signal was apparent both in the glomeruli, and in the peritubular region in close proximity to the tubules (Fig.2 B). Tubular epithelial cells were negative, and remained negative even after the long exposure time (not shown). This pattern of hybridization was relatively uniform throughout the cortical region. Examination of the glomeruli at higher magnification revealed that many of the positive cells had the morphologic appearance of glomerular endothelial cells (Fig.2 C; the arrow head marks a possible EC). The pattern of PAI-1 mRNA expression was similar to that obtained by immunohistochemistry for PAI-1 antigen since no staining of the renal cortex was apparent in control mice (Fig.2 D), but strong staining of the glomerulus and peri-tubular region was seen following LPS administration (Fig.2 E). No PAI-1 antigen could be detected in tubular epithelial cells (Fig.2 E and 2F). Examination of the glomerulus at high magnification once again revealed that the positive cells had the appearance of ECs (Fig.2 F: arrow). The staining pattern of these cells appears most dense over the cell bodies due to the blue color of the nuclear stain used to counter stain these sections; however, staining of the thin rim of cytoplasm can also be observed in these sections (Fig.2 F). To confirm the possible endothelial cell origin of the PAI-1 producing cells, serial sections from the renal cortex were stained with an antibody to vWF which is specific for ECs (124). The staining pattern observed with this antibody was almost identical to that seen with antibodies to PAI-1 (Fig.2 G: compare to Fig.2 F). The staining intensity of vWF in renal tissue from LPS-treated mice was slightly greater than that in control mice,

although the difference was much less marked than that observed for PAI-1 (data not shown).

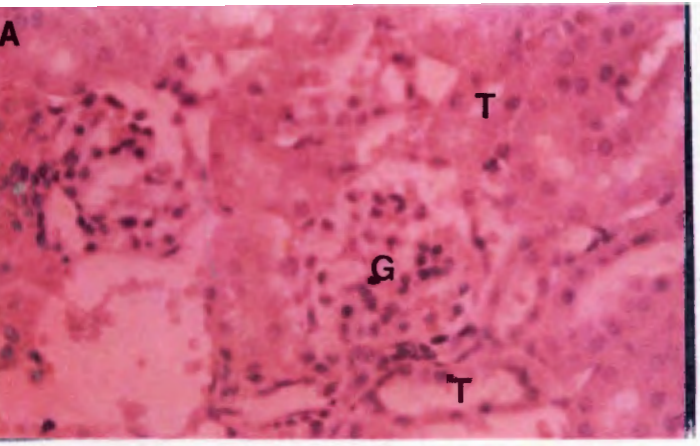

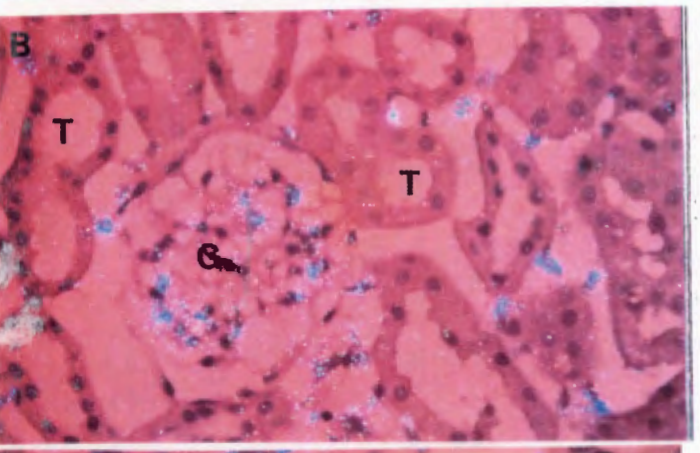

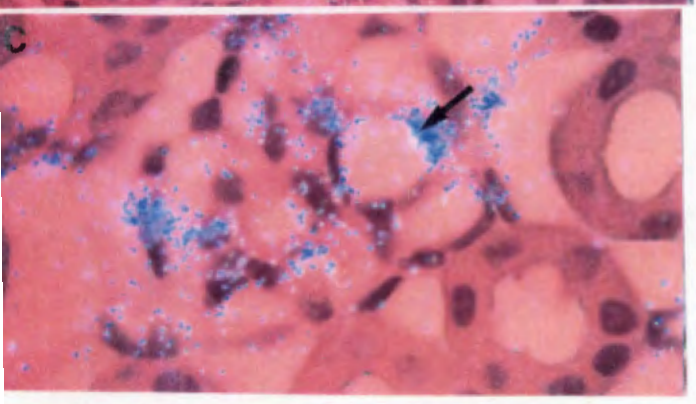

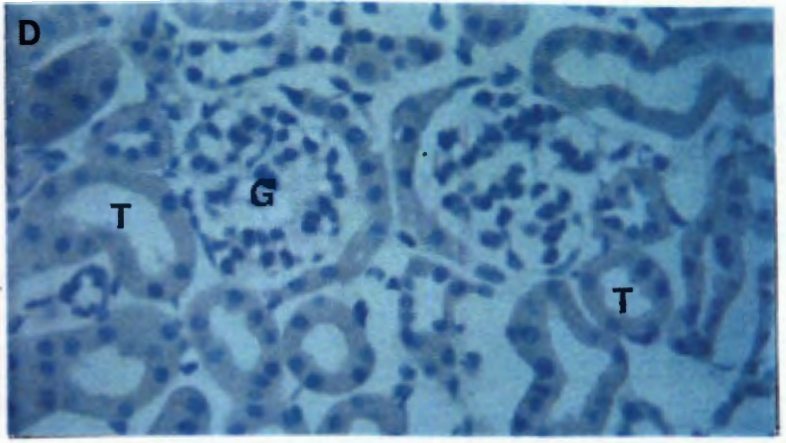

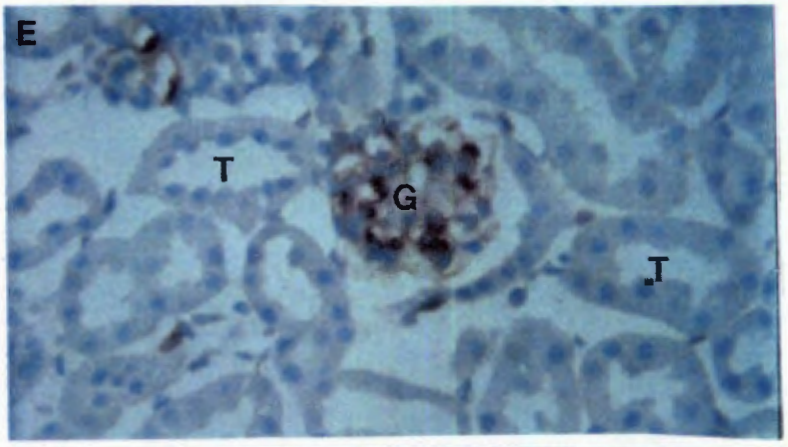

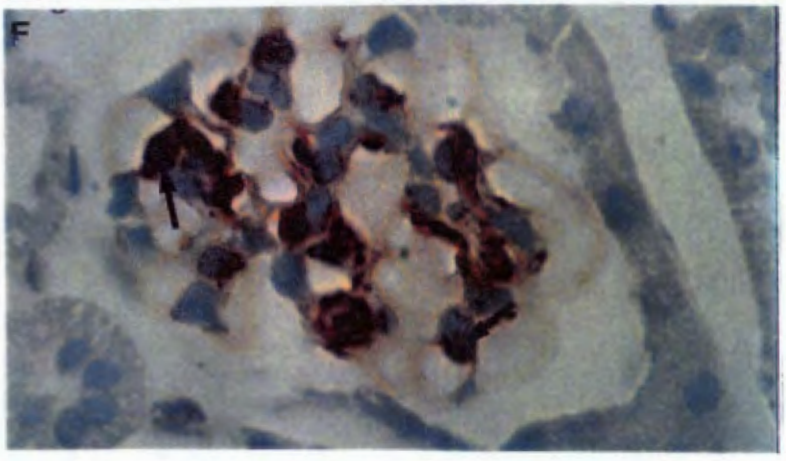

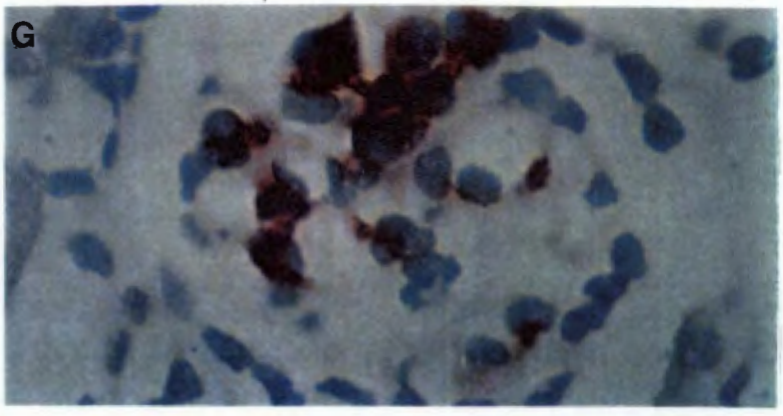

gure 2. Localization of PAI-1 in the renal cortex. Panels -C show paraffin sections from the renal cortex of control -400x mag) and LPS (50 μg) treated (B-400x mag and -1000x mag: Arrow denotes what appears to be an EC ucleus) mice after they were analyzed by in situ ybridization as described in the methods using a ^{35}S belled mouse PAI-1 antisense riboprobe. Panels D-G show arallel sections that were analyzed by mmunohistochemistry using antibodies to either PAI-1 (D: ntrol mice, 400x mag; E: endotoxin-treated mice, 400x ag; F: endotoxin-treated mice, 1000x mag: Arrow denotes EC nucleus) or to vWF (G: endotoxin-treated mice, 00x mag). Photographs were taken using bright field or larized light epiluminescence. G denotes a glomerulus d T denotes a tubule.

Localization of PAI-1 antigen in the glomerulus by immunoelectron microscopy. Sections from the renal cortex of mice injected with LPS were processed for PAI-1 antigen. Low power scanning EM showed the presence of positive staining in the cytoplasm of endothelial cells (Fig.3 A). A high power view of a positive region showed the basement membrane with foot processes of podocytes on one side and the cytoplasm of an endothelial cell on the other side (Fig.3 B). The positive staining in the endothelial cell is indicated by the arrow head.

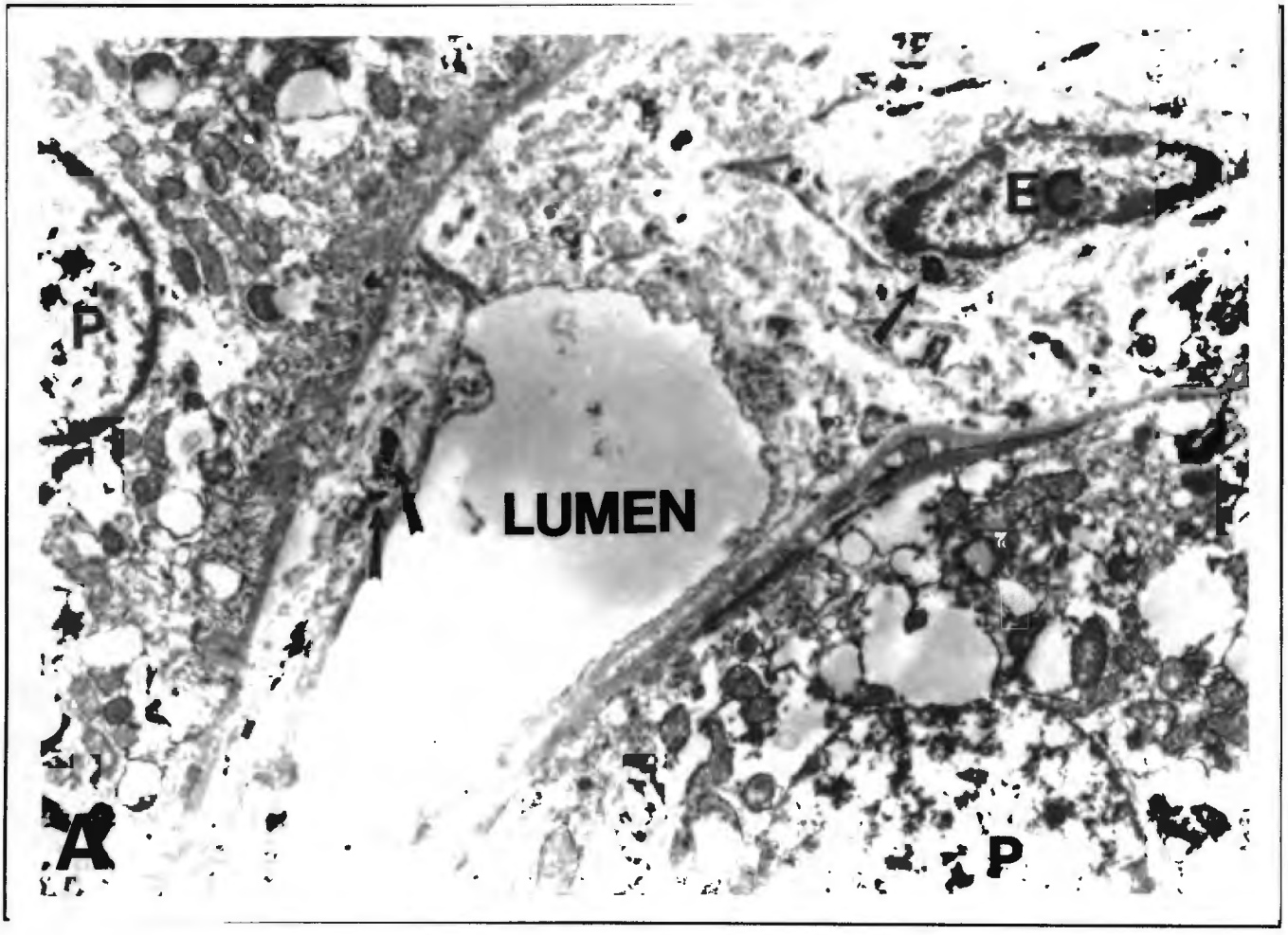

Figure 3: Panel **A.**

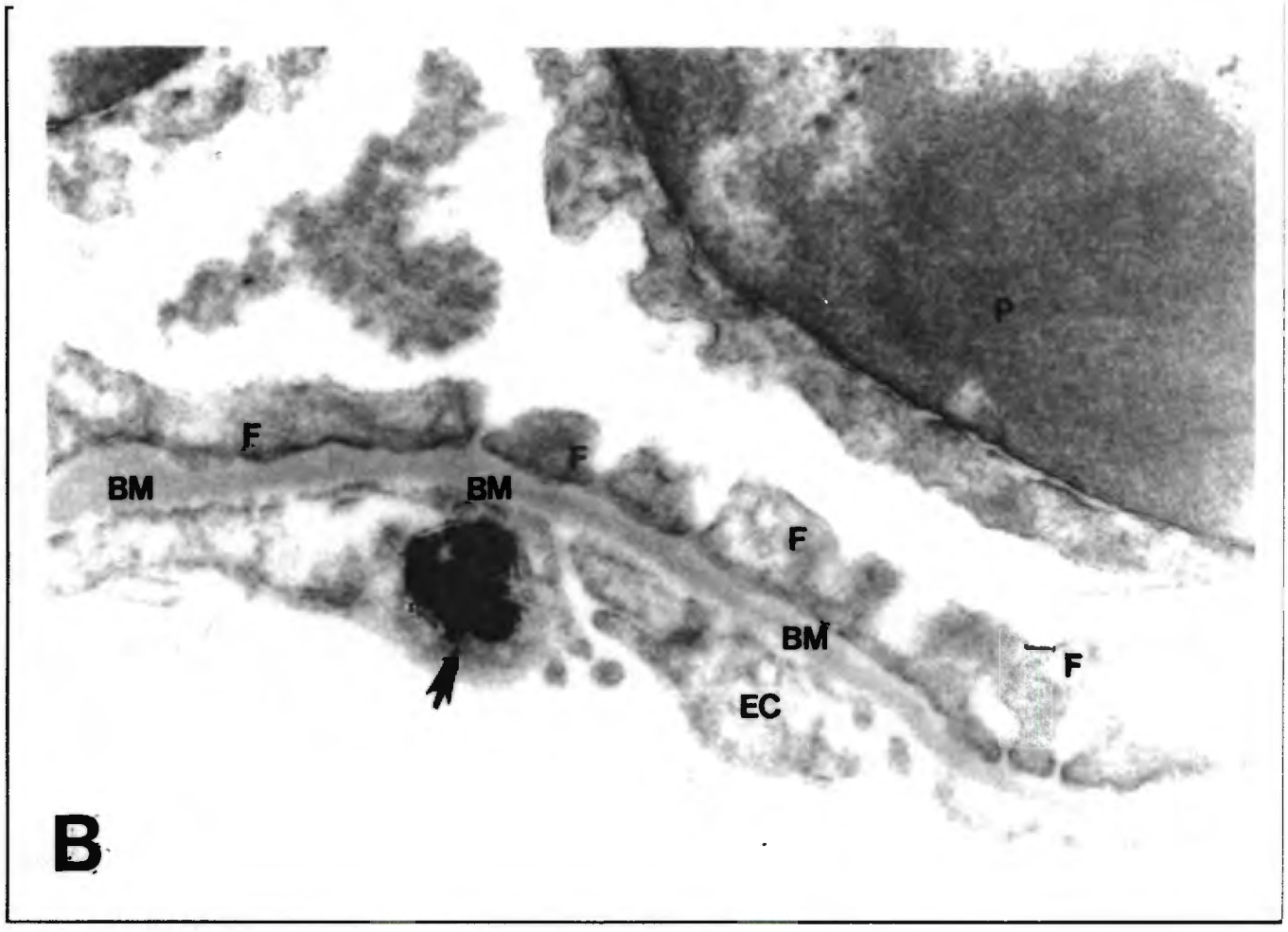

Figure 3: Panel B.

Immunoelectron microscopy for PAI-1 in the renal cortex. Sections from the renal cortex of LPS treated mice were processed for PAI-1 antigen using diaminobenzidine staining. Panel A shows a low power (2000x mag) view of a glomerulus with positive DAB staining (black) in the cytoplasm of both the endothelial cells seen in the field as indicated by the arrow heads. Panel B shows a high power (7000x mag) view with the foot processes (F) of the podocytes (F) seen above the basement membrane (BM) and the diaminobenzidine reaction product in the cytoplasm of the endothelial cells (EC) indicated by the arrow.

Localization of PAI-1 mRNA and antigen in the renal medulla. No PAI-1 mRNA was detected in the renal medulla of control mice (Fig.4 A). However, 3 hr after LPS administration, peri-tubular cells throughout the medulla hybridized strongly for PAI-1

mRNA (Fig.4 B). Examination of a distal tubule at high magnification suggested that the positive cells may again be peri-tubular ECs. (Fig.4 C: arrow). Again, the pattern of PAI-1 antigen distribution was similar to that of PAI-1 mRNA in that no PAI-1 antigen could be detected in the control renal medulla (Fig.4 D), a relatively strong signal was observed following LPS administration (Fig.4 E), and this signal seemed to be localized to ECs (Fig.4 F: The arrow marks a possible EC nucleus). Tubular epithelial cells of the medulla were negative for PAI-1 mRNA (Fig.4 B, C) and antigen (Fig.4 E, F). The PAI-1 mRNA and antigen staining patterns were uniform throughout the renal medulla. This pattern of staining was similar to that seen with vWF (Fig.4 G) confirming that the PAI-1 producing cells were ECs. Again, a slight increase in vWF staining was detected after LPS treatment (data not shown).

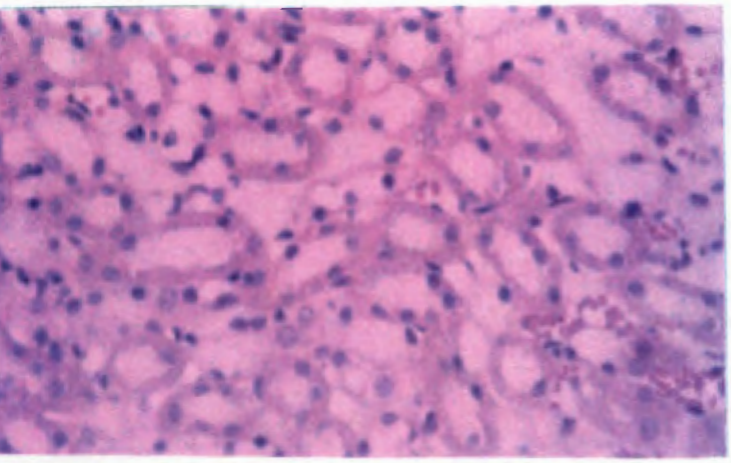

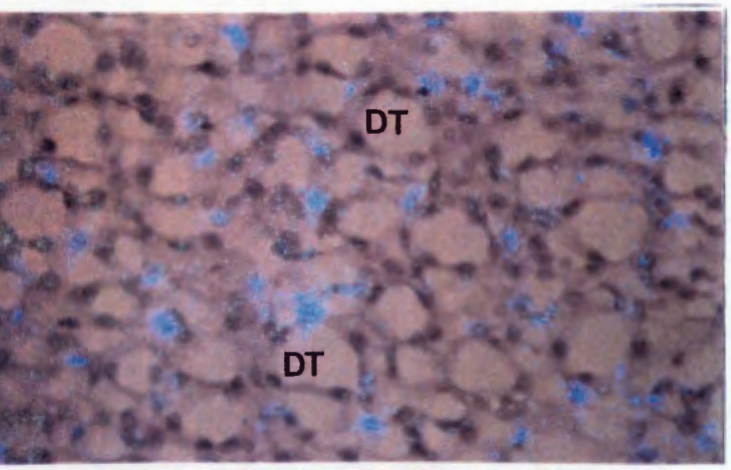

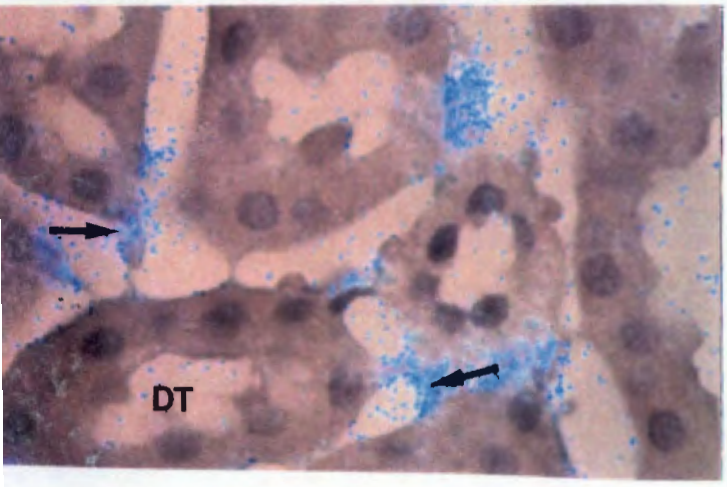

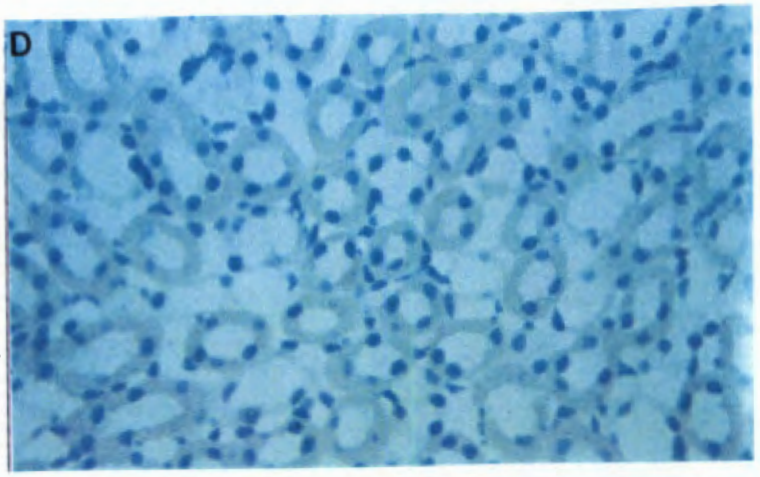

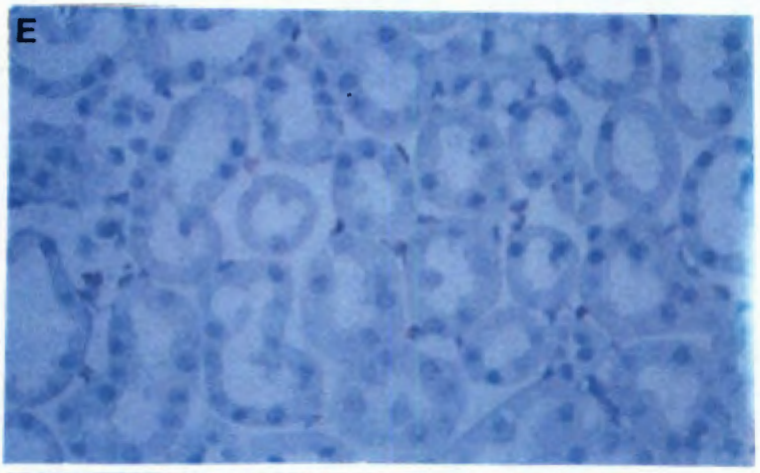

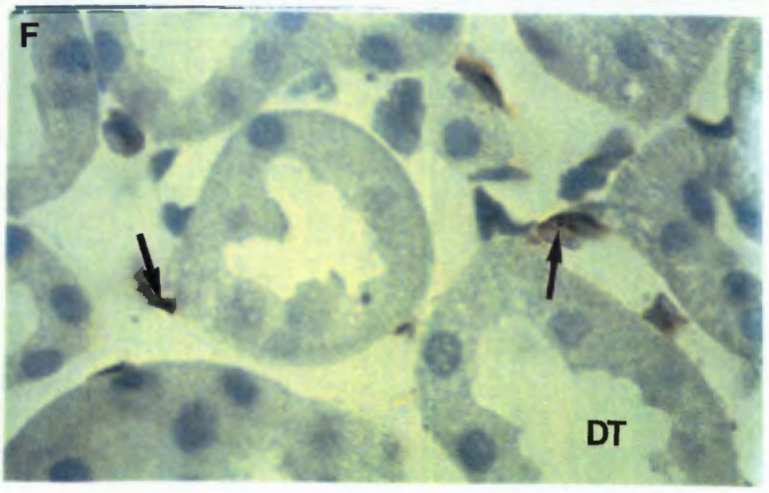

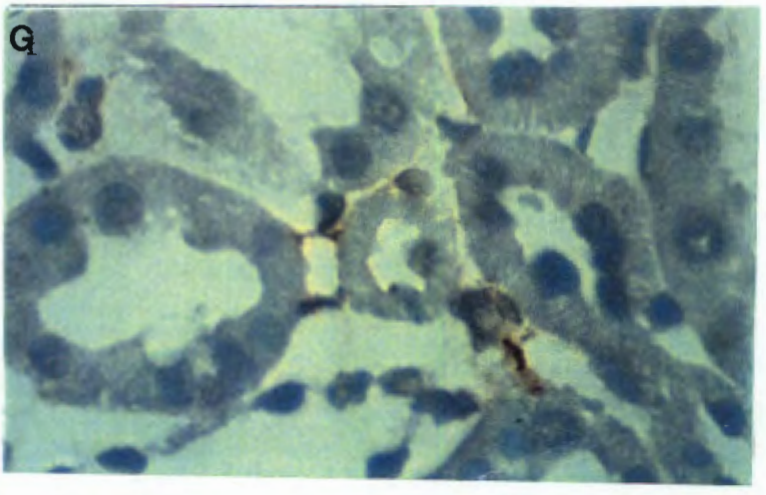

gure 4. Localization of PAI-1 in the renal medulla . nal medullary sections were analyzed by in situ bridization for PAI-1 as described in Fig.2 (Panel **A**: ntrol mice, 400x mag; Panel **B**: endotoxin-treated mice, 0x mag; Panel **C**: endotoxin-treated mice, 1000x mag: row denotes an EC nucleus). Slides were exposed for 2 eks. Serial sections were also analyzed by munohistochemistry for either PAI-1 (Panel **D**: control ce, 400x mag; Panel **E**: endotoxin-treated mice, 400x g; Panel **F**: endotoxin-treated mice, 1000x mag: Arrow notes an EC nucleus) or vWF (Panel **G**: endotoxin-treated ce, 1000x mag). Photographs were taken using bright ld or polarized light epiluminescence. **DT** denotes a distal bule.

Localization of PAI-1 mRNA and antigen in the renal papilla. The renal papilla in the control animal showed a weak but specific *in situ* hybridization signal for PAI-1 mRNA (Fig.5 A). However, this signal was only apparent after 12 weeks exposure of the slides, in contrast to the signal in the LPS-treated animals which was strongly positive at 2 weeks (Fig.5 B). The cell type involved in this response has yet to be determined. This signal seen in the renal papilla may account for the low level of PAI-1 mRNA that is detected following northern hybridization of total renal RNA. A stronger signal was detected at 2 weeks in the renal papilla following LPS treatment (Fig.5 B), and again the positive cells seemed to be ECs. No PAI-1 mRNA was detected in epithelial cells of the tubules at this level in the kidney. These results with PAI-1 mRNA were similar to those obtained with PAI-1 antigen (data not shown).

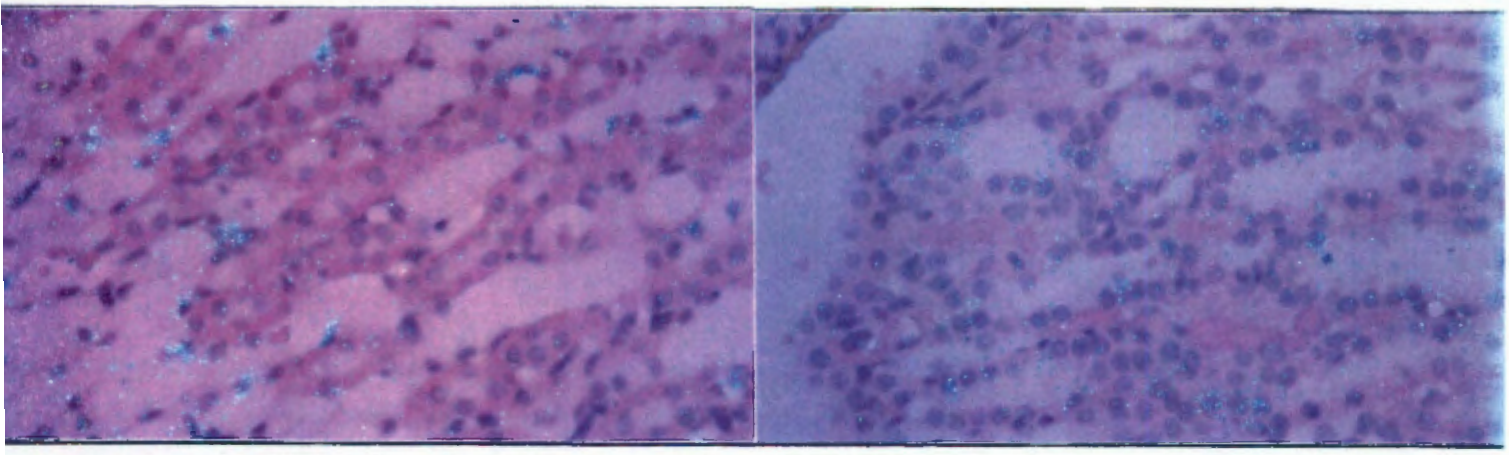

Figure 5. Localization of PAI-1 in renal papilla. Renal papillary sections from control (**A**) or LPS-treated (**B**) mice were analyzed by in situ hybridization for PAI-1 as described in Fig.2; 400x mag. The slide in panel A was exposed for 12 weeks, the slide in panel B for 2 weeks.

Localization of PAI-1 mRNA and antigen in the renal vasculature. Except for the renal papilla, the only other region in the untreated control kidney in which PAI-1 mRNA could be detected was in the muscular wall of vessels (Fig.6 A). Endothelial cells in these normal vessels were entirely negative, in contrast to the LPS treated mice where ECs of vessels throughout the kidney were strongly positive for PAI-1 mRNA (Fig.6 B). Interestingly, LPS-treatment seemed to reduce the level of PAI-1 mRNA detected in the medial layer of the muscular wall. The hybridization signal in these vessels was once again similar to the immunohistochemical staining pattern where a specific EC stain was seen in both arteries and veins of the LPS treated kidney (Fig.6 C).

Localization of PAI-1 mRNA in the perinephric fat. No PAI-1 mRNA was detected in perinephric fat from untreated control mice (Fig.6 D) whereas perinephric fat from the LPS-treated animals was strongly positive for PAI-1 mRNA (Fig.6 E). The cell type involved in this response has yet to be determined. No PAI-1 antigen was detected when perinephric fat from control mice was analyzed by immunohistochemical staining (not shown), while strong PAI-1 staining was detected in the LPS-treated mice (Fig.6 F).

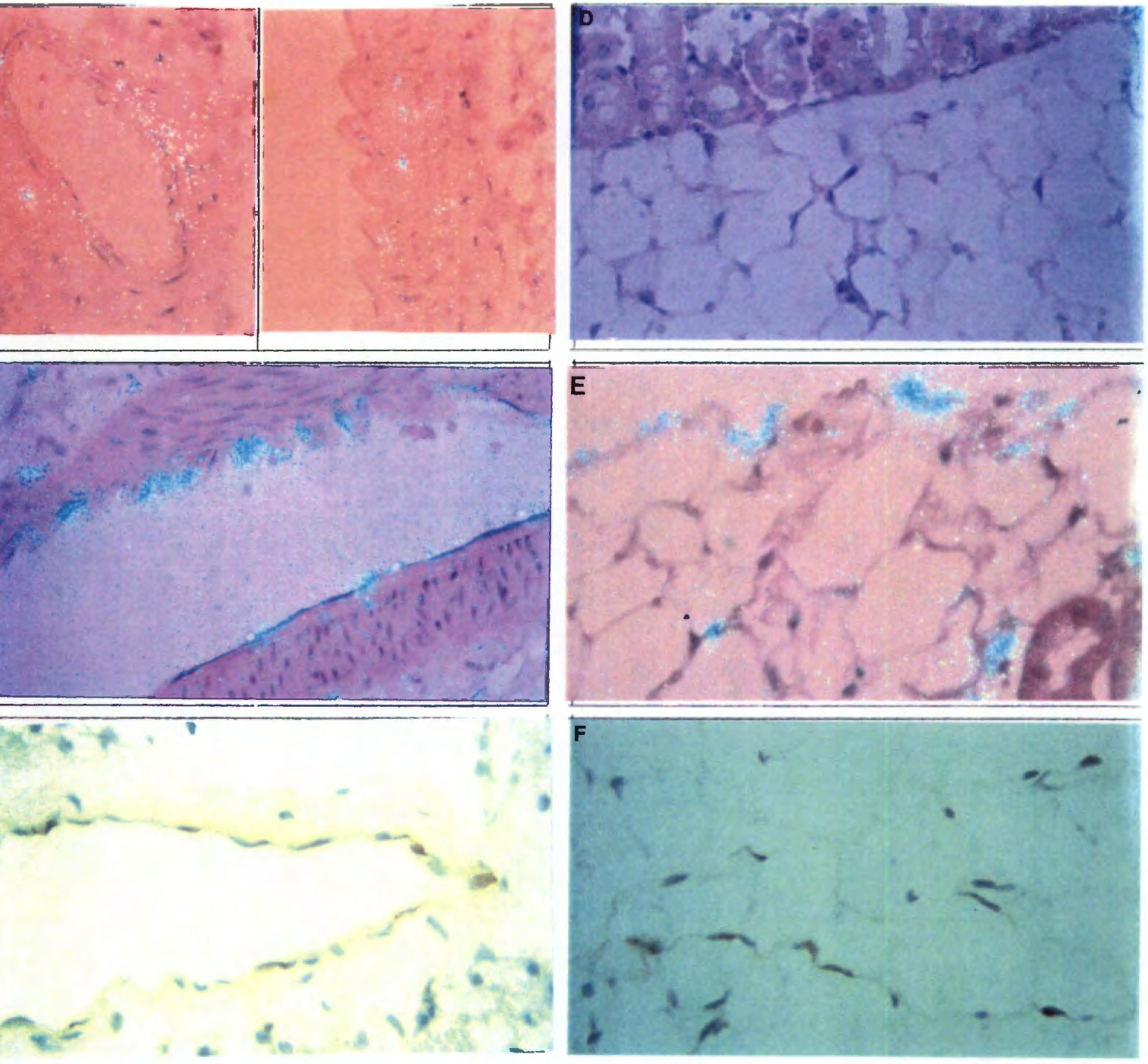

Figure 6. Localization of PAI-1 in renal vasculature and peri-nephric fat. Sections containing renal vasculature from control (**A**) or LPS-treated (**B**) mice were analyzed by in situ hybridization for PAI-1 as described in Fig. 2. Slides were exposed for 12 weeks. Serial sections from endotoxemic mice also were analyzed by immunohistochemistry for PAI-1 (Panel **C**). Sections containing perinephric fat from control (**D**) or LPS-treated (**E**) mice were analyzed by in situ hybridization for PAI-1. Slides were exposed for 2 weeks. Serial sections from endotoxemic mice were analyzed by immunohistochemistry for PAI-1 (Panel **F**). All photographs are shown at 400 x mag.

Discussion.

The concentration of PAI-1 in the plasma of rabbits (51), rats (123), and man (125) increases during endotoxemia. Endotoxin treatment induces PAI-1 mRNA in the heart, lung, kidney and liver of the rat (123), and in virtually all tissues of the mouse, including the kidney ((122) ; see also Fig. 1). These results suggest that plasma PAI-1 may originate from multiple tissues in the endotoxemic animal. In spite of this, little is known about the nature of the cells that produce PAI-1 in the various tissues. The wide distribution of PAI-1 mRNA in the endotoxin-treated animals suggests that common cells of the vascular wall may be involved and cell culture studies demonstrate that cultured endothelial cells can be induced to synthesize PAI-1 in response to LPS (48,85). Moreover, analysis of cell populations obtained from the LPS-treated rat by cell separation techniques suggests that hepatic PAI-1 mRNA may be derived primarily from hepatic endothelial cells (123) in response to LPS. However, the cellular localization of renal PAI-1 mRNA is unknown and the origin of PAI-1 *in vivo* remains speculative.

In this study, we attempt to identify the specific cells within the kidney that produce PAI-1 since the kidney is sensitive to the effects of endotoxemia. For example, endotoxemia is believed to be a critical factor in the HUS (126-128), a disease in which increased plasma PAI-1 has been demonstrated (113). This disorder is also characterized by focal renal lesions of fibrin deposition in glomerular arterioles

and capillaries (129,130). Northern blot analysis revealed that the untreated control kidney produces low, but significant levels of PAI-1 mRNA (Fig.1 A). *In situ* hybridization analysis demonstrated that the PAI-1 mRNA present in the normal kidney is restricted to the media of renal vessels (Fig.6 A) and to the renal papilla (Fig.5 A). The location of PAI-1 positive cells within the media of control renal vessels suggests that it is being produced by smooth muscle cells since they are the predominant cell type in this location (131). Analysis of other untreated control tissues by *in situ* hybridization reveals a similar localization of PAI-1 positive cells to the media of large vessels (data not shown). These results raise the possibility that vascular smooth muscle cells in a variety of tissues may contribute to the PAI-1 in plasma of control mice. The identity of the PAI-1 producing cells in the renal papilla remains to be determined.

Treatment of mice with LPS caused marked increases in renal PAI-1 mRNA as seen by Northern blotting (Fig.1, lane B) and by *in situ* hybridization (Fig.2-6). Increased antigen staining was also observed throughout the kidney (Fig.2-6). This response has been previously quantitated (122) and reaches a maximum of 93-fold induction 3 hours after administration of 50ug of LPS. The specificity of the PAI-1 response has also been previously investigated using nuclear run on assays to compare the rate of transcription of the PAI-1, vWF and ChoB genes in response to LPS (48). It was demonstrated that while the rate of PAI-1 transcription increases more than 30-fold, vWF and ChoB did not change or increased only slightly. My

localization studies in endotoxemic mice demonstrate that the primary site of renal PAI-1 synthesis is in endothelial cells. In the glomeruli the appearances and positions of the positive cells suggested that they were endothelial cells since in many cases the nucleus of the positive cell was situated within a well defined capillary (Fig.2 C and F). The endothelial cell localization of PAI-1 was confirmed by immunoelectron microscopy for PAI-1 antigen (Fig.3 A and B) which showed positive staining in the cytoplasm of endothelial cells. Outside of the glomerulus, the positive cells of the cortex (Fig.2 B, C) and the medulla (Fig.4 B, C) lay in close proximity to the distal and proximal convoluted tubules and these could be identified, by virtue of their position and appearance, as peritubular endothelial cells. To confirm the hypothesis that endothelial cells are the primary PAI-1 producing cells in renal tissue from the endotoxemic mouse, serial sections were stained with an antibody to vWF, an endothelial specific marker. The position and appearance of vWF positive cells coincided with that of PAI-1 positive cells (Fig.2 G,). In addition, analysis of the renal vasculature in endotoxemic mice demonstrates that in all instances, the PAI-1 producing cells were primarily on the luminal side of the vessels and could be clearly identified as endothelial cells (Fig.6 B). Activated leukocytes adherent to the vessel wall could also account for this pattern of localization but the wide distribution of the signal and the lack of any adherent cells seen in the positive sections (Fig.2 C, 2F, 3A, 5B and 5C) show that this was not the case. Furthermore, this staining pattern was observed even after prolonged perfusion of the vascular system with paraformalderhyde, a treatment which clearly washes most of the red blood cells and

leukocytes from the blood vessels (Fig.2 C and 2F).

Many cell types studied in tissue culture have been shown to synthesize PAI-1, including mesangial cells (132), glomerular epithelial cells (133), renal fibroblasts (134) and endothelial cells from many different sources (87,135-137). The observations that a wide spectrum of renal cells and endothelial cells produce PAI-1 *in vitro*, is in contrast to my *in vivo* findings with control mice in which we can only detect PAI-1 in the media of vessels and in the renal papilla. Even though the kidney can be induced to produce large amounts of PAI-1 mRNA and antigen by LPS, the majority of the PAI-1 response appeared to be restricted primarily to a subset of cells (i.e., endothelial cells). Epithelial cells in renal tissue from control and LPS-treated animals were entirely negative in these studies (Fig.2, 4). These results indicate that the cell types that produce PAI-1 *in vitro* may not necessarily account for the majority of the PAI-1 synthesis *in vivo.* A number of factors may account for these differences. For example, PAI-1 is a serum response gene (85,138) suggesting that the production of this inhibitor by a variety of cultured renal cells may be in response to the serum in the growth media. It is also possible that control mechanisms which govern normal growth *in vivo* may be compromised *in vitro*, resulting in the inappropriate expression of PAI-1 in the cultured cells. These differences may also reflect a species difference since the above cell culture studies were not performed with murine cells. Whatever the reason, these differences indicate that caution should be used in the interpretation of results derived solely from *in vitro* studies.

PAI-1 is an important antifibrinolytic molecule (139), and may function in matrix stabilization (40,132) and tissue remodelling (140). Inappropriate expression of PAI-1 during these processes may thus contribute to the pathogenesis of renal disease. For example, in the anti-GBM antibody model of GN in the rat (82), increased plasma PAI-1 was observed and thrombi were shown to accumulate in the glomeruli. TNFα, the cytokine which is thought to play a major role in the injury that takes place in this model, caused increased numbers of fibrin thrombi and a concurrent increase in the level of plasma PAI-1 (82). TNFα is also one of the primary mediators of the LPS reaction with a plasma peak at 45-100 minutes after administration of LPS (141). This time course of expression precedes the peak of PAI-1 expression at 180 minutes (122), suggesting that a common cell type may synthesize PAI-1 in both of these models in response to TNFα. My observations showing that LPS caused a marked increase in PAI-1 in ECs at all levels of the renal vasculature, including those in the glomerulus, suggests that ECs may also synthesize PAI-1 in the glomerulus during the progression of disease in the anti-GBM model. If so, these data imply that during the initial injury phase of the disease the balance between coagulation and fibrinolysis may have shifted in favor of coagulation. Raised local concentrations of PAI-1 in the endothelial cells of the glomerulus would be expected to contribute to this shift by inhibiting the normal processes responsible for the removal of fibrin.

In the later phases of renal damage leading to GN, there is a strong component of cellular proliferation and matrix accumulation (142). A variety of observations

indicate that PAI-1 can protect matrix from proteolytic degradation (111), suggesting that it may also play a role in the matrix accumulation that takes place during the progression of GN. Further support for this hypothesis comes from studies of the role of TGFß in matrix accumulation in a rat anti-thymocyte model of GN (143). In these studies anti-TGFß antibodies not only reduced the amount of matrix accumulation but also reduced the histological evidence of the disease. These results suggest that TGFß promotes matrix accumulation in this model. TGFß is a potent inducer of PAI-1 synthesis with doses as low as 1ng/ml inducing PAI-1 by 50-fold or more (48). Thus, the PAI-1 gene may be induced by increased local concentrations of TGFß, and the increased PAI-1 may in turn protect the matrix from normal degradation thus leading to ongoing pathology. This protection of matrix in response to TGFß has been demonstrated *in vitro* studies using human fibrosarcoma HT1080 cells (111). Further support for this mechanism of action comes from work using a rat model of GN which shows increases in renal TGFß activity and mRNA up to 14 days after the initial injury (144). My study demonstrates, that in endotoxemia, PAI-1 is synthesized in the glomerulus during the initial phase of the disease and we speculate that PAI-1 may also be chronically elevated in the glomerulus in response to other mediators like TGFß in the later phases of ongoing renal disease. This possibility is under investigation.

This work has been submitted to the American Journal of Pathology.

Title: CELLULAR LOCALIZATION OF TYPE-1 PLASMINOGEN ACTIVATOR INHIBITOR mRNA AND PROTEIN IN MURINE RENAL TISSUE.

Authors:M. Keeton, Y. Eguchi, M. Sawdey, C. Ahn and D. Loskutoff.

Acknowledgements. I would like to thank Dr C. Wilcox for initial help with *in situ* hybridization, Dr. C.B. Wilson for helpful discussions and advice, M. Pagels for expert histology assistance.

CHAPTER 6: INAPPROPRIATE EXPRESSION OF TYPE 1 PLASMINOGEN ACTIVATOR INHIBITOR IN RENAL TISSUE IN MURINE LUPUS.

Introduction. Systemic Lupus Erythematosus (SLE) is an autoimmune disorder in which 70% of the patients develop glomerulonephritis (GN). An interesting feature of lupus nephritis (LN) is the endothelial cell activation and proliferation, with subsequent intravascular coagulation that accompanies the disease (145-147). These pathogenic features suggest that endothelial cells may play a central role in the process of coagulation since I have recently shown that they produce large amounts of PAI-1 in response to lipopolysaccharide (LPS) (148), and it is known that LPS can accelerate the progress of LN in susceptible mice (149,150). PAI-1 is a potent anti-fibrinolytic molecule by virtue of its ability to inhibit both tissue type plasminogen activator (t-PA) and urokinase-type plasminogen activator (u-PA) (46), and local increases in PAI-1 may be expected to inhibit the clearance of fibrin at sites of coagulation. The inappropriate expression of PAI-1 by renal cells in response to LPS or cytokines released in the inflammatory stage of LN may contribute to the progression of the disease.

We have been interested in the role of PAI-1 in renal disease since increased plasma PAI-1 levels also correlate with the active phase of a variety of human renal disorders, including the nephrotic syndrome (112) and the hemolytic uraemic syndrome (113). Moreover, a large increase in plasma PAI-1 was observed in an

experimental model of GN in which rats were injected with anti-glomerular basement membrane (anti-GBM) antibodies (82). Microscopic examination of renal tissue from these animals revealed the presence of fibrin thrombi within glomeruli. Moreover, direct administration of TNFα also caused large increases in plasma PAI-1, and concomitant administration of both the nephrotoxic antibody (Ab) and TNFα caused superinduction of plasma PAI-1 levels. The increase in PAI-1 was again associated with an increase in fibrin thrombi. Although the expression of PAI-1 during the acute phase of these diseases could account for early decreases in fibrinolysis, the role of PAI-1 in ongoing chronic glomerulonephritis remains to be determined.

In this report, we investigate changes in renal PAI-1 in a murine model (151-153) of SLE in MRL/lpr female mice. We show that local increases in PAI-1 can be detected at sites of active disease including the glomerular tufts and crescents as well in areas of interstitial nephritis. PAI-1 expression was localized to endothelial cells, parietal epithelial cells, tubular epithelial cells and in mononuclear cells in the tubular interstitium. None of these cells appear to express PAI-1 in the normal kidney suggesting that these local increases in PAI-1 expression may contribute to the increased fibrin deposition associatiated with lupus nephritis.

Materials and methods.

Tissue preparation. 34 Female diseased mice (MRL/lpr; 4 months to 7 months) and 9 female control mice (MRL/scr or CB6 mice (BalbC/ByJ x C57Bl6/J; 4 months to 18 months; Scripps Clinic Rodent Breeding Colony) were sacrificed by overdose inhalation anaesthesia using metofane. Blood was drawn from the left ventricle and anticoagulated with 0.01M Citrate. The anticoagulated blood was then centrifuged at 4000g for 15 minutes and the plasma removed and stored at -70°C. Various organs were then removed and immersed in freshly prepared 4% cold paraformaldehyde at 4°C overnight, embedded in paraffin blocks,and sectioned at 2-5um thickness using a microtome. The tissue sections were mounted onto polylysine slides and stored at room temperature. PAS stains were performed using standard techniques.

ELISA assays. The substrates for the ELISA were made from calf thymus (Pel Freeze, Rogers, AK) exactly as previously described (154). Briefly, long soluble chromatin stripped of histone H1 and non histone proteins and thus consisting essentially of DNA wrapped around the $(H2A\text{-}H2B\text{-}H3\text{-}H4)_2$ histone octamer, was made by washing chromatin in 0.5 M NaCl (155). The native histone octamer was prepared by salt extraction of chromatin (156), and DNA (Calbiochem, La Jolla, CA) was further processed by proteinase K digestion, extraction with phenol, and digestion with S1 nuclease as described (154,157). Single stranded DNA was made by placing

this DNA into a boiling water bath for 15 minutes and then cooling rapidly in ice water.

The ELISA was performed as described in detail previously (154,157) except that the plates were coated with 100 μl instead of 200 μl of antigen in each well. In addition, methylated BSA was pre-coated on the ELISA plate before binding both double-stranded and single-stranded DNA. Sera were diluted 1:300 in serum diluent (1% gelatin, 1% BSA, 0.75% BGG, 0.05% tween-20, in 0.14 M NaCl, 0.01 M sodium phosphate, pH 7.4) and 100 μl was incubated in duplicate in the ELISA at room temperature for two hours. After washing, the plates were incubated for two hours with goat anti-mouse class specific antibodies conjugated with horseradish peroxidase (Caltag, South San Francisco, CA). The detecting antibody was quantified with the 2,2'-azino-di-[3-ethylbenzthiazolinsulfonate] (Boehringer Mannheim, Germany) colorimetric reagent as described (157).

Riboprobe preparation. A full length mouse PAI-1 cDNA (114) subcloned into the vector pBS+ (Stratagene) was provided by Drs. L.Diamond and M. Cole (Princeton University). An EcoRI/SphI fragment containing from nucleotide 1 to nucleotide 1085 of the mouse PAI-1 cDNA was cloned into pGEM -3Z (Promega). This vector was linearized with the restriction enzyme EcoRI and used to make an antisense riboprobe labelled with ^{35}S-labeled UTP (specific activity ,1200 Ci/mmol; Amersham) by in vitro transcription using SP6 RNA polymerase (Promega). The DNA template was removed by digestion using RQ1 DNAse for 15 minutes at 37°C and the

riboprobe purified by phenol extraction and ethanol precipitation. This vector was also used to make a sense control probe by *in vitro* transcription using T7 RNA polymerase following linearization with the restriction enzyme HindIII.

***In situ* hybridization.** *In situ* hybridizations were carried out essentially as described in Chapter 5 (115).

Immunohistochemistry. Immunohistochemistry was performed on cryostat sections using an immunoperoxidase technique. Kidneys were embedded in OTC, frozen in liquid nitrogen and four micron sections were cut using a cryostat. The sections were fixed with cold, 4% paraformaldehyde for 5 minutes, washed with PBS (5 min) and PBS-0.1% glycine (5 min), and then incubated sequentially in avidin (10 U/ml) and d-biotin (1 mg/ml) for 40 minutes each. The sections were blocked in blocking solution (reagent diluent; 2.5% heat inactivated horse serum in PBS, pH 7.5) for 20 minutes and then incubated with primary antibody (Rabbit anti-mouse PAI-1 [ ], 40 lg/ml in reagent diluent) in humidified chambers at RT for 2 hours. Tissue sections were further incubated with peroxidase conjugated goat anti-rabbit IgG (Jackson Immunology, 1:200 in reagent diluent) for 1 hour at room temperature (RT). Color reactions were developed with aminoethyl carbozole (AEC) for 30 min, counterstained with Mayor's hematoxylin, rinsed, and mounted with Gel-mount (Biomeda), and the results observed under light microscope.

In control experiments, tissue sections were stained with antisera previously depleted of the specific antibodies. In the case of PAI-1, immunoadsorption was performed by adding to the immunopurified rabbit anti-mouse PAI-1 solution, a 20-fold molar excess of PAI-1 antigen over antibody and the mixture was incubated overnight at 4°C. This mixture was then used instead of the primary antibody for immunohistochemical staining. No staining was apparent in these control experiments.

Immunoelectron microscopy. Staining for PAI-1 antigen and immunoelectron microscopy was performed as described in Chapter 5.

Results.

Histopathology: Periodic Schiff Acid (PAS) staining was performed on renal tissue from both diseased and control mice. The glomerular lesions were graded from 0 to IV as previously described (158). In this grading system, a grade I lesion shows minimal mesangial thickening, while II lesions contain noticable increases in both mesangium and glomerular cellularity. Grade III lesions are characterized by the preceding features plus superimposed inflammatory exudates and/or capsular adhesions, and grade IV lesions are characterized by obliteration of glomerular architecture involving > 70% of the glomeruli. A grade 0 is given to all specimens with no glomerular lesions. The control mice (C1 to C6 = CB6 and C7 to C9 = MRL/scr) showed no evidence of renal disease (Grade 0-I; Table 1) at all ages

examined, whereas the diseased mice (D1 to D35 = MRL/lpr) showed severe grades of LN (Grade II to IV; Table 1).

No	Age	Grade	Glom	Cres	Int	Poly	No	Age	Grad	Glom	Cres	Int	Poly
1	4	0	0	0	0	0	D14	5	III	3+	0	2+	2+
C2	6	0	0	0	0	0	D15	5	III	4+	0	2+	0
C3	8	0	0	0	0	0	D16	7	III	3+	+	3+	3+
C4	8	0	0	0	0	0	D17	6	III	3+	0	2+	4+
C5	12	0	0	0	0	0	D18	7	III	3+	2+	2+	3+
C6	18	0	0	0	0	0	D19	7	III	3+	+	0	2+
C7	2	0	0	0	0	0	D20	7	III	3+	+	2+	3+
C8	4	0	0	0	0	0	D21	7	III	3+	+	+	2+
C9	6	I	0	0	0	0	D22	7	III	3+	+	2+	2+
D1	2	0	0	0	0	0	D23	7	III	4+	0	3+	2+
D2	4	0	0	0	0	0	D24	7	III	3+	0	+	3+
D3	6	II	3+	0	2+	+	D25	5	III	4+	0	+	2+
D4	6	II	0	0	0	0	D26	7	III	4+	0	+	3+
D5	5	II	3+	0	+	3+	D27	5	III	3+	+	2+	+
D6	7	II	3+	0	2+	2+	D28	5	IV	4+	2+	3+	3+
D7	7	II	3+	0	+	2+	D29	5	IV	0	+	+	0
D8	7	II	2+	+	+	3+	D30	7	IV	4+	3+	2+	2+
D9	7	II	3+	0	2+	2+	D31	7	IV	4+	3+	3+	3+
D10	7	II	3+	0	+	2+	D32	7	IV	4+	+	+	0
D11	7	II	2+	0	+	2+	D33	6	IV	4+	3+	4+	4+
D12	5	II	3+	+	+	0	D34	6	IV	3+	3+	3+	3+
D13	6	II	3+	+	+	0	D35	5	IV	4+	2+	3+	2+

TABLE 1: Summary of the histological findings and the in-situ hybidization results for each region of the kidney in both the control mice (C1 to C6 = CB6 mice and C7 to C9 = MRL/scr mice) and the diseased mice (D4 to D38 = MRL/lpr). The age of the mice in months is indicated in the second column and the grade of renal disease from 0 to IV (as outlined in the results) is indicated in the third column. Each sample was also evaluated for the extent of glomerular proliferation and sclerosis (Glom), the extent of crescent formation (Cres), the extent of interstial nephritis (Int) and the extent of polyarteritis (Poly) and these results are expressed on a scale from 0 to 4+ as indicated in the appropriate columns. Sections of the same slides were graded for the presence or absence of PAI-1 mRNA in these same regions by in situ hybridization after 12 weeks exposure of the slides. The presence of PAI-1 mRNA in a specific region is indicated by a shaded block in the table.

The glomerular lesions were characterized by cell proliferation and inflammatory exudation accompanied by membrane thickening, crescent formation and fibrinoid deposits (Fig.1 A). Interstitial nephritis with inflammatory mononuclear cells surrounding the tubules was also frequently detected (Fig.1 B) and in many instances, severe polyarteritis involving the renal arteries was observed (Fig.1 C).

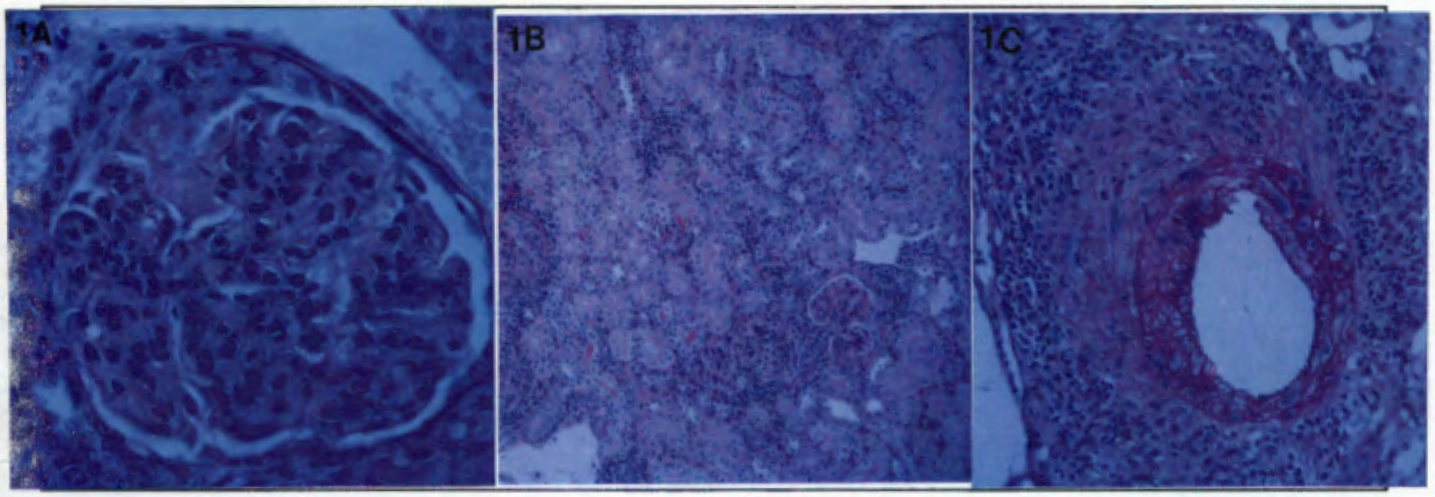

Figure 1. Histologic appearance of renal tissue from an MRL/lpr mouse. Panels A-C show paraffin sections from the kidney of a MRL/lpr mouse stained with PAS as described in the methods. Panel A (200x mag) shows a glomerular tuft with crescent formation and hypercellularity (Arrow denotes a crescent). Panel B (100x mag) shows tubules with surrounding interstitial nephritis. Panel C (200x mag) shows an artery with arteritis. Photographs were taken using bright field microscopy.

Disease markers: ELISA assays for autoantibodies including anti-ds DNA, anti-ssDNA, anti-chromatin and anti-histone were performed as described in the materials and methods (160). MRL/lpr mice had an increase in all parameters compared to control mice (Table 2) indicating that the MRL/lpr mice had autoimmune disease. We also examined creatinine levels but found no significant difference between the control and the disease group (0.4 vs 0.3) indicating that the mice did not have end stage renal failure.

ASSAY	Control OD (n=9)	Disease OD (n=15)
Anti-ds DNA Ab.	0.02±0.02	1.19±1.17
Anti-ss DNA Ab.	0.20±.056	5.08±2.03
Anti-chromatin Ab.	0.003±0.009	4.06±2.06
Anti-histone Ab.	0.29±0.16	1.83±2.06

TABLE 2: ELISA assays to measure markers of disease activity in both control mice (numbers C1 to C9) and in diseased mice (numbers D4 to D8 and D18 to 27). The ELISA assays were performed as described in the material and methods and the results are expressed as the average optical density (OD) reading (± SD) for each group after background subtraction.

Localization of PAI-1 by in situ hybridization and immunohistochemistry. All regions of the kidney were examined for PAI-1 mRNA using in situ hybridization and for PAI-1 antigen using immunohistochemistry. As previously observed (148), the muscular wall of renal vessels in the control animals showed a weak but specific signal for PAI-1 mRNA and antigen as did the renal papillae (data not shown). Although, the positive papillary cell type has not been determined, the hybridization signal was relatively weak and was only apparent after 12 weeks exposure of the slides. All other regions of the kidney including the glomeruli, were negative for both PAI-1 mRNA (12 weeks exposure) and antigen, regardless of the age of the animals (Fig.2 A).

In contrast to the weak signal detected in control animals, large amounts of PAI-1 mRNA (Fig.2 B and C) and PAI-1 antigen (Fig.2 D) were detected in kidneys of MRL/lpr mice. In this case,

the hybridization signal was apparent after only 2 weeks exposure of the slides (not shown). PAI-1 positive cells were found in four main areas of disease, including the tufts of glomeruli, the crescents of glomeruli, in areas with interstitial nephritis and finally also in vessels with vasculitis:

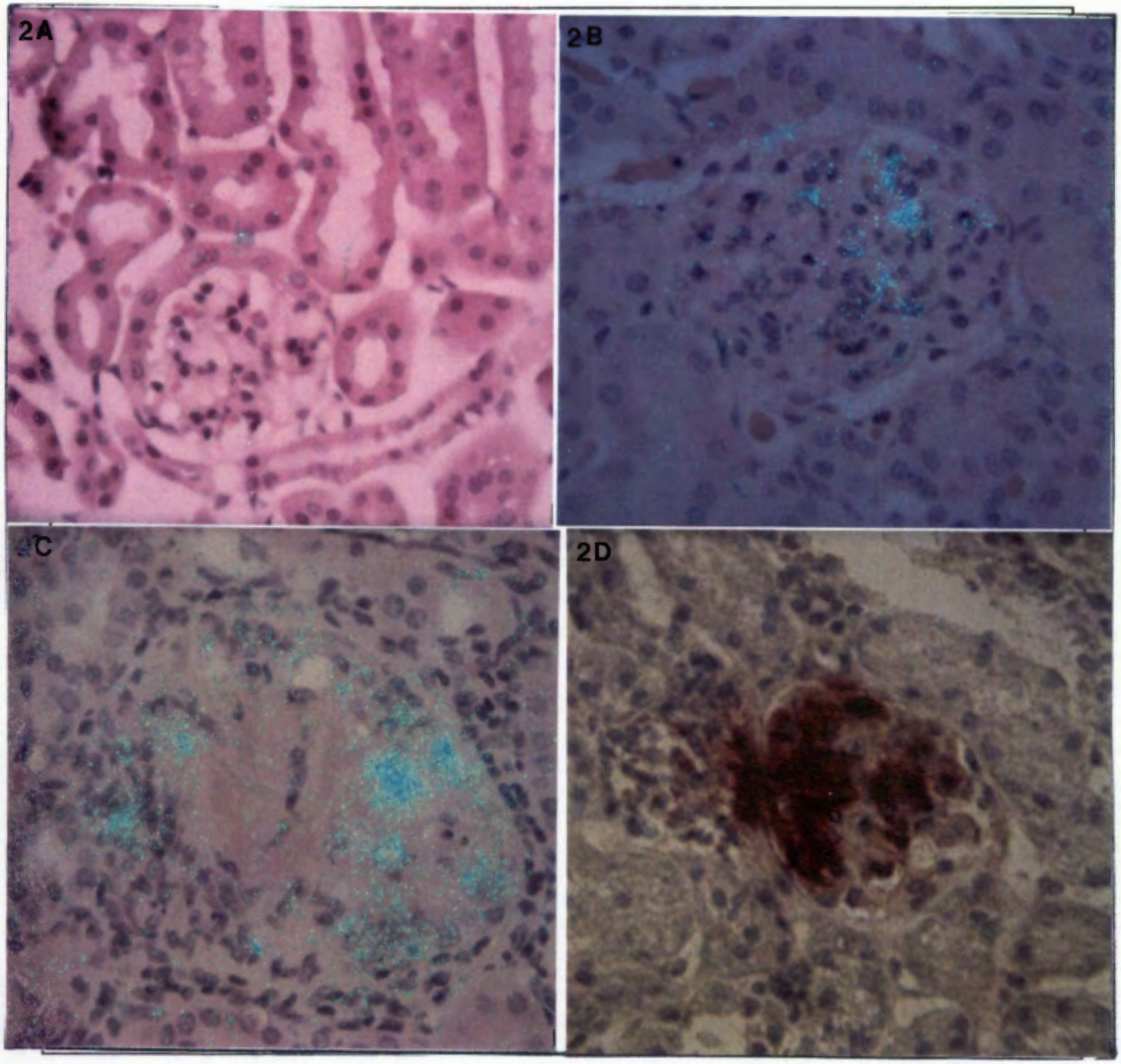

Figure 2. Cortical localization of PAI-1 mRNA in the kidneys of a normal and LN mice. Panel A (400x mag) shows renal cortex from a control mouse and Panels B-D (400x mag) show sections from the renal cortex of a MRL/lpr mouse after they were analyzed by in situ hybridization as described in the methods using a ^{35}S labelled mouse PAI-1 antisense riboprobe. Slides were exposed for 6 weeks at $4^{o}C$ and then stained with hematoxylin and eosin. Panel A: the glomerulus of a control mouse; Panel B: glomerulus of LN mouse with an early lesion (grade II) showing hypercellularity; Panel C: glomerulus from an advanced lesion (grade IV) showing necrosis; Panel D: (400x mag) a section of a glomerulus from an advanced lesion processed by immunohistochemistry for PAI-1 antigen.

Localization of PAI-1 mRNA in the glomerulus: Close examination of the glomeruli revealed that PAI-1 positive cells were frequently located within the proliferative areas of the glomerular tuft of both early and late lesions (Fig.2 C). These cells were mononuclear and could represent either mesangial cells or infiltrating inflammatory cells. These same regions of the glomerulus were also positive for PAI-1 antigen (Fig.2 D). Some of the postive cells had the appearance of capillary endothelial cells, a possibility confirmed by immunoelectron microscopy. For example, a low power EM view of a similar area shows an activated endothelial cell (Fig. 3 A; 2000x mag) stained for PAI-1 antigen (the arrow heads indicate positive DAB staining) which when examined at a higher power (Fig.3 B; 7000x mag, arrow heads indicate these areas) shows the presence of intracytoplasmic vessicles stained for PAI-1 antigen.

Figure 3: Panel A.

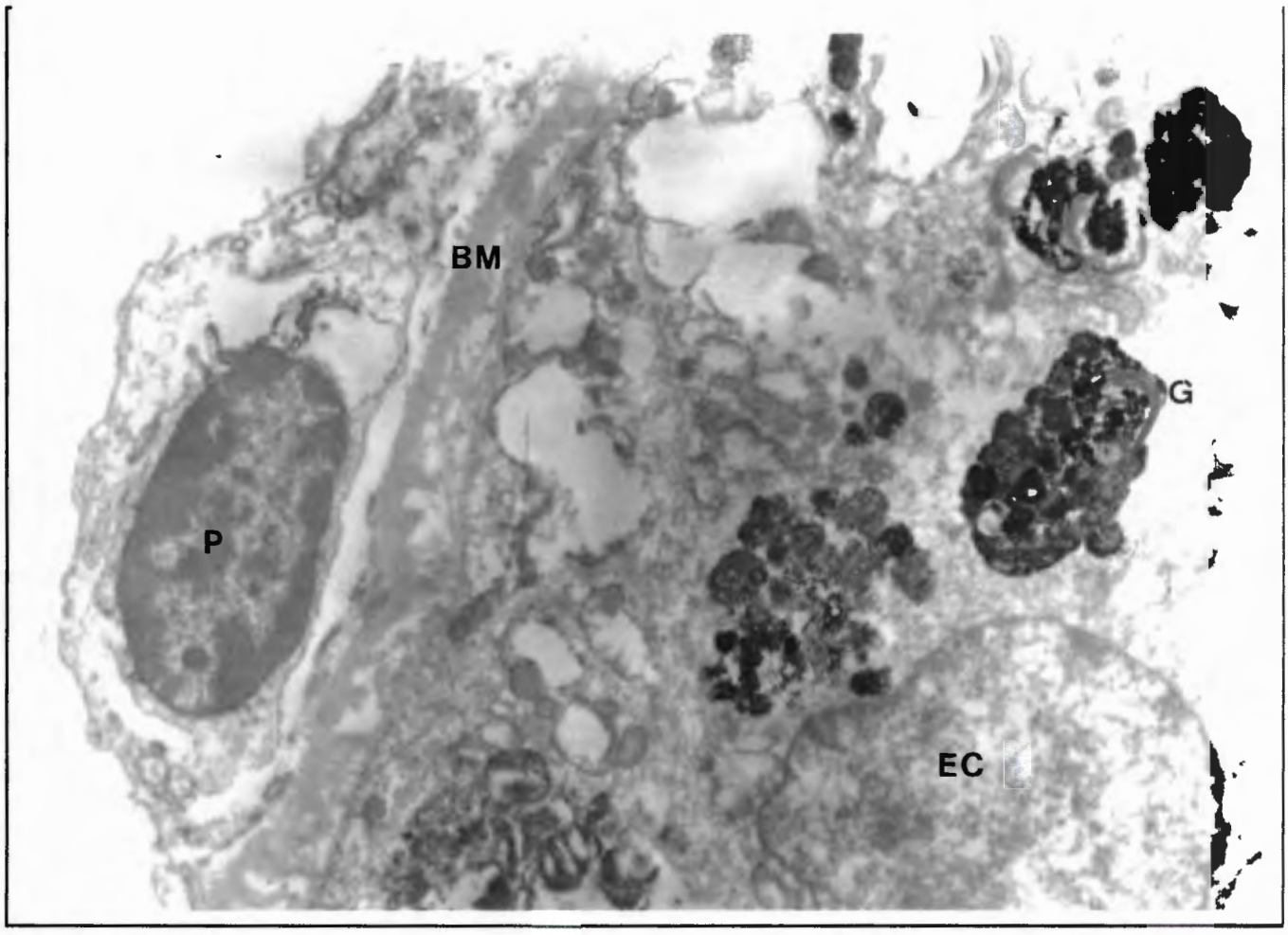

Figure 3: Panel B.

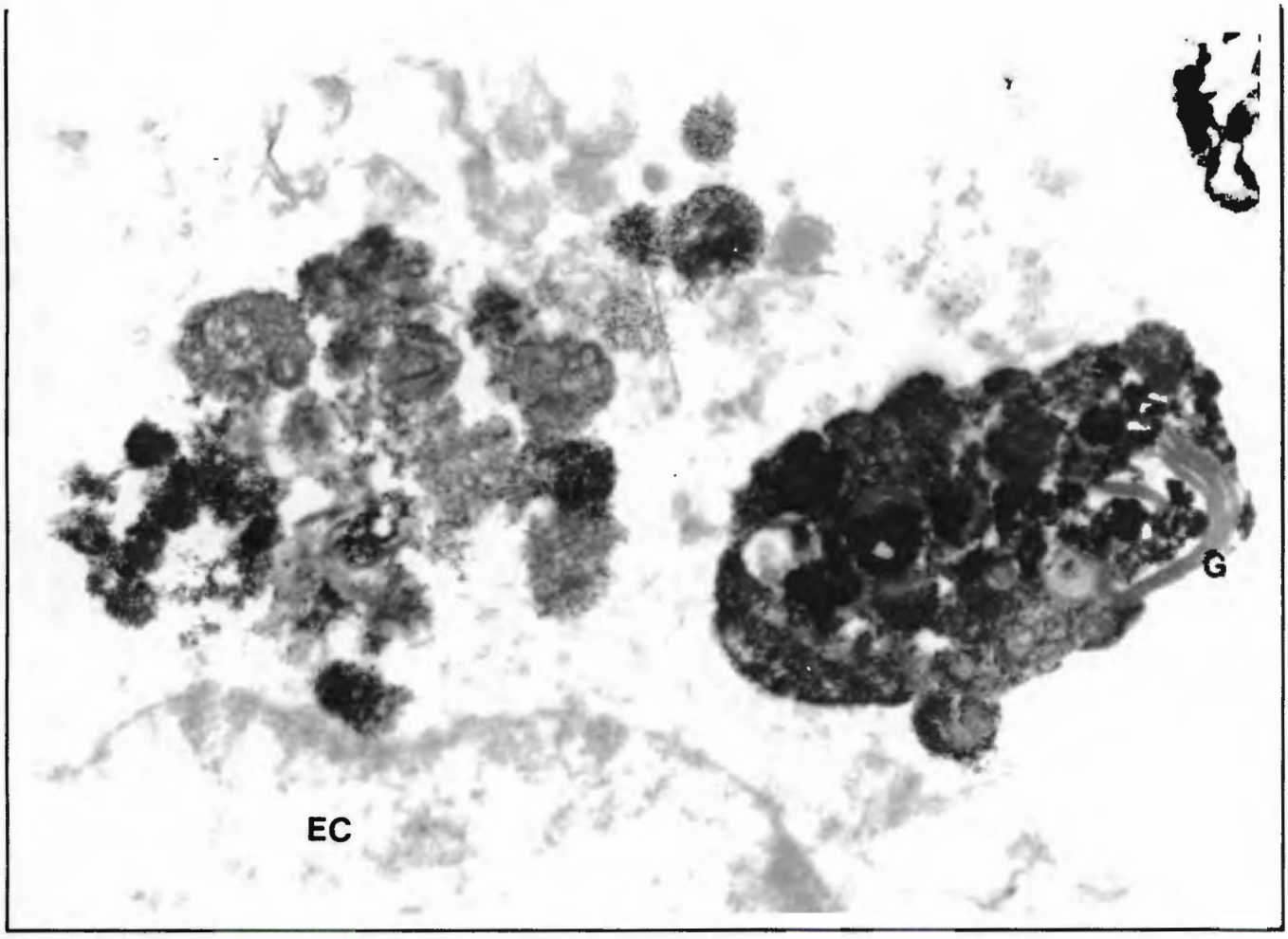

Figure 3: Immunoelectron microscopy for PAI-1 antigen. Sections were processed by the immunoperoxidase technique for PAI-1 antigen using DAB substrate as described in the methods. Panel A shows a low power view of the glomerulus with an activated endothelial cell (2000x mag; EC denotes the endothelial cells, L denotes the capillary lumen and arrows indicate positive DAB staining). Panel B shows a high power view of the same cell as shown in panel A in which intracytoplasmic deposits of PAI-1 antigen were visualized (7000x mag; EC denotes the endothelial cell and arrows indicate positive DAB staining).

A positive signal for PAI-1 mRNA was also detected in areas of crescent formation and in the early stages of the disease, we were able to identify parietal epithelial cells stained for PAI-1 mRNA (Fig.4 A) since these cells lay on the luminal side of bowmans capsule However, in later lesions

we were unable to identify the cell type due to the increased amount of inflammatory mononuclear cells present (Fig.4 B). Once again the presence of PAI-1 antigen was detected in these same areas (Fig.4 C).

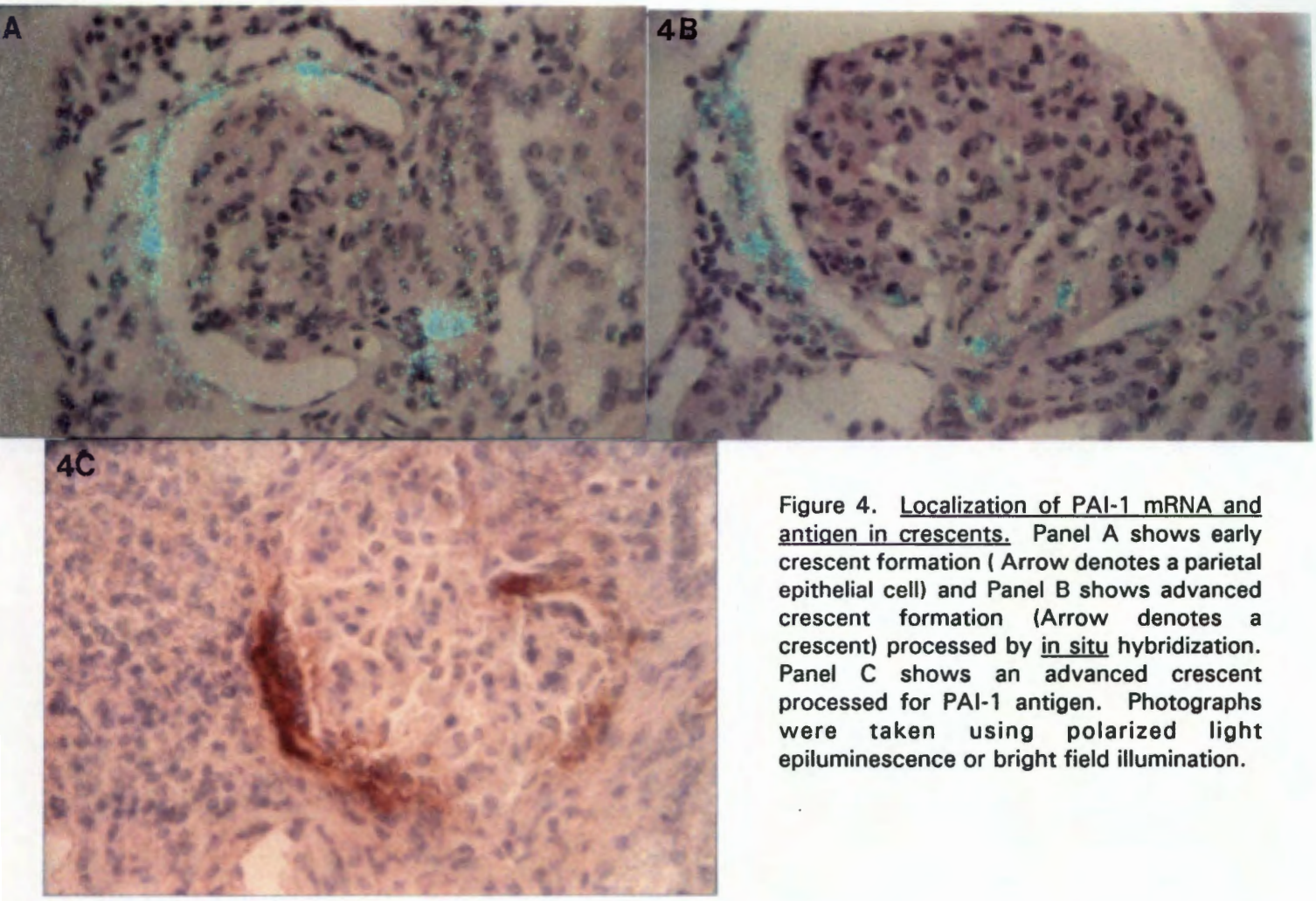

Figure 4. Localization of PAI-1 mRNA and antigen in crescents. Panel A shows early crescent formation (Arrow denotes a parietal epithelial cell) and Panel B shows advanced crescent formation (Arrow denotes a crescent) processed by in situ hybridization. Panel C shows an advanced crescent processed for PAI-1 antigen. Photographs were taken using polarized light epiluminescence or bright field illumination.

Localization of PAI-1 mRNA in the tubules: A number of mice also showed signs of inflammatory interstitial nephritis. These lesions were characterized by a large cuff of inflammatory mononuclear cells surrounding the tubular epithelial cells. PAI-1 mRNA was found both within the surrounding inflammatroy cells (Fig.5 A) and in the tubular epithelial cells themselves (Fig.5 B).

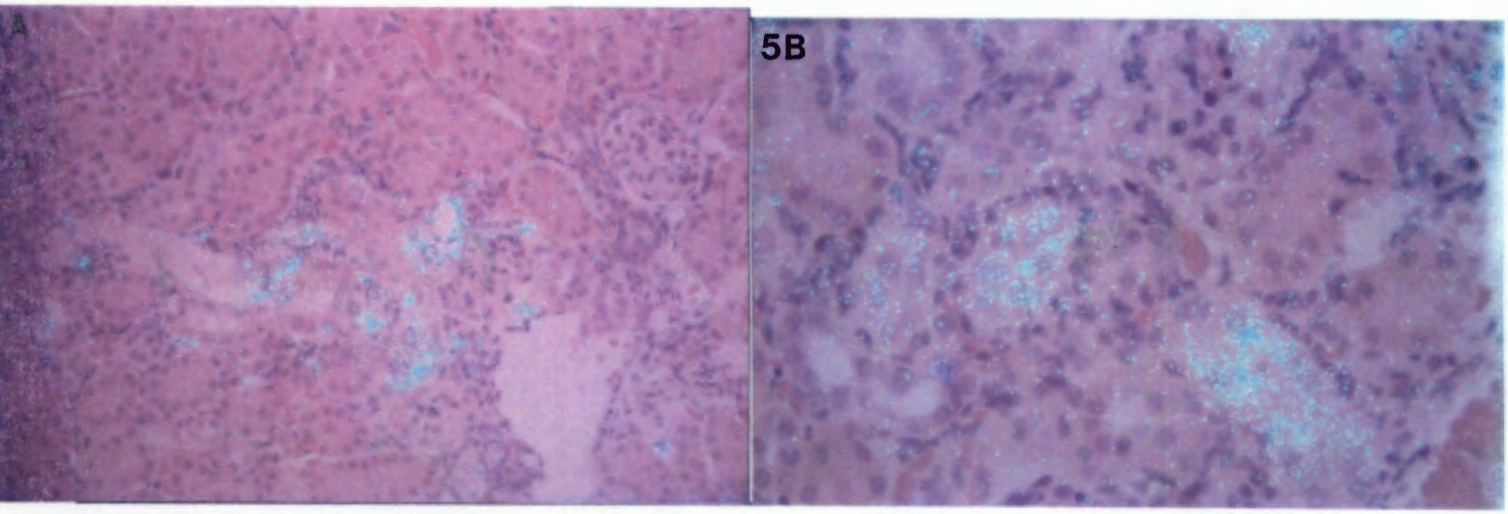

Figure 5. Localization of PAI-1 in the renal medulla. Renal medullary sections were processed by in situ hybridization for PAI-1 as described in Fig.2 in MRL/lpr mice. Panel A shows interstitial nephritis with inflammatory mononuclear cells and Panel B shows a tubule with positive epithelial cells. Photographs were taken using polarized light epiluminescence.

The presence of PAI-1 antigen in the renal tubules was confirmed by immunoelectron microscopy. A low power EM view of a tubule (Fig.6 A; 2000x mag) shows positive staining of all the epithelial cells in that tubule and a high power view shows the brush border of the epithelial cell and postitive staining in vesicles within the cytoplasm of the tubular epithelial cell (Fig.6 B; 7000x mag).

Figure 6: Panel A.

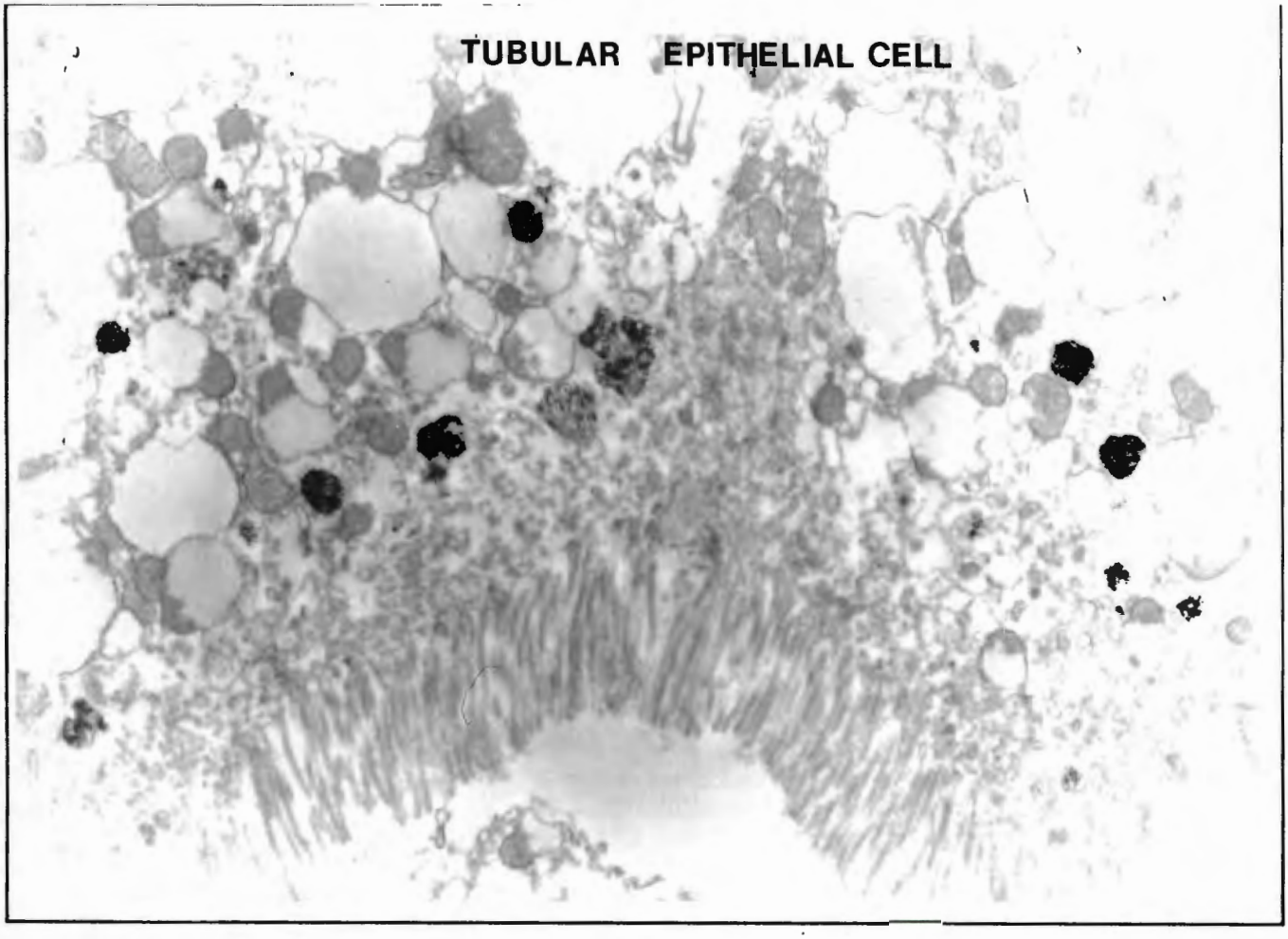

Figure 6: Panel B.

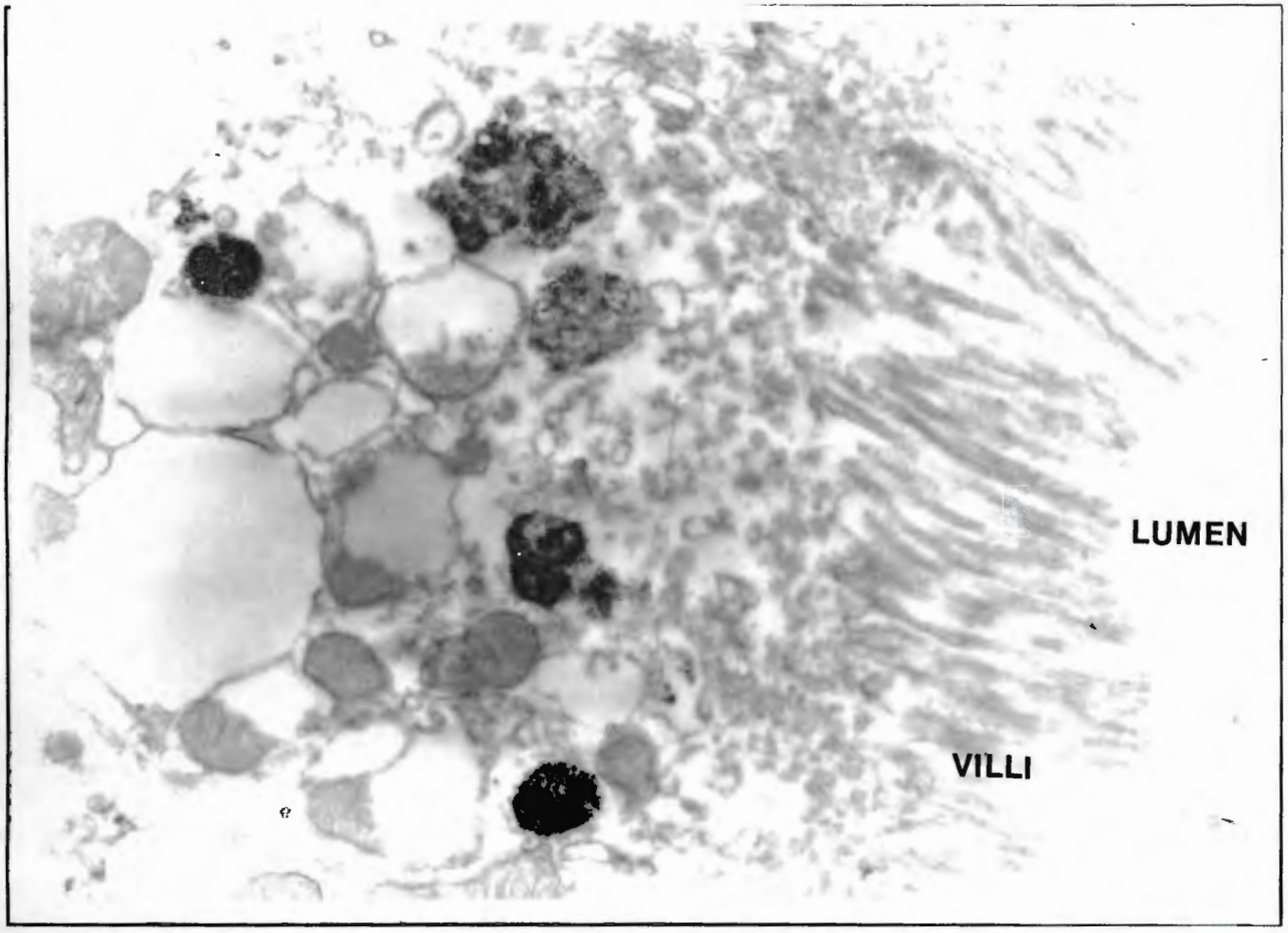

Figure 6. Immunoelectron microscopy for PAI-1 antigen. Sections were processed for immunoelectron microscopy as desribed in Figure 3. Panel A shows a low power view of a proximal convoluted tubule with positive PAI-1 antigen staining in the tubular epithelial cells (2000x mag). Panel B shows a high power view in which the brush border and the nucleus of the tubular epithelial cell are visualized (7000x mag; BB denotes the brush border). PAI-1 positive staining is indicated by the arrows.

Localization of PAI-1 mRNA in the blood vessels: A necrotizing inflammatory arteritis was observed in many large and medium size vessels. The media of these vessels was filled with inflammatory cells which had disrupted the normal vessel architecture but had not apparently affected the patency of the vessel. The media of these vessels had cells positive for PAI-1 mRNA (Fig.7 A and B). In other areas of the kidney in which there was marked inflammation with a

mononuclear cell infiltrate, smaller vessels were observed in which endothelial cells (identified by their position on the luminal side of the vessel wall) stained positively for PAI-1 mRNA (Fig.7 C). This result is in contrast to that for the normal kidney in which endothelial cells are entirely negative (Chapter 5).

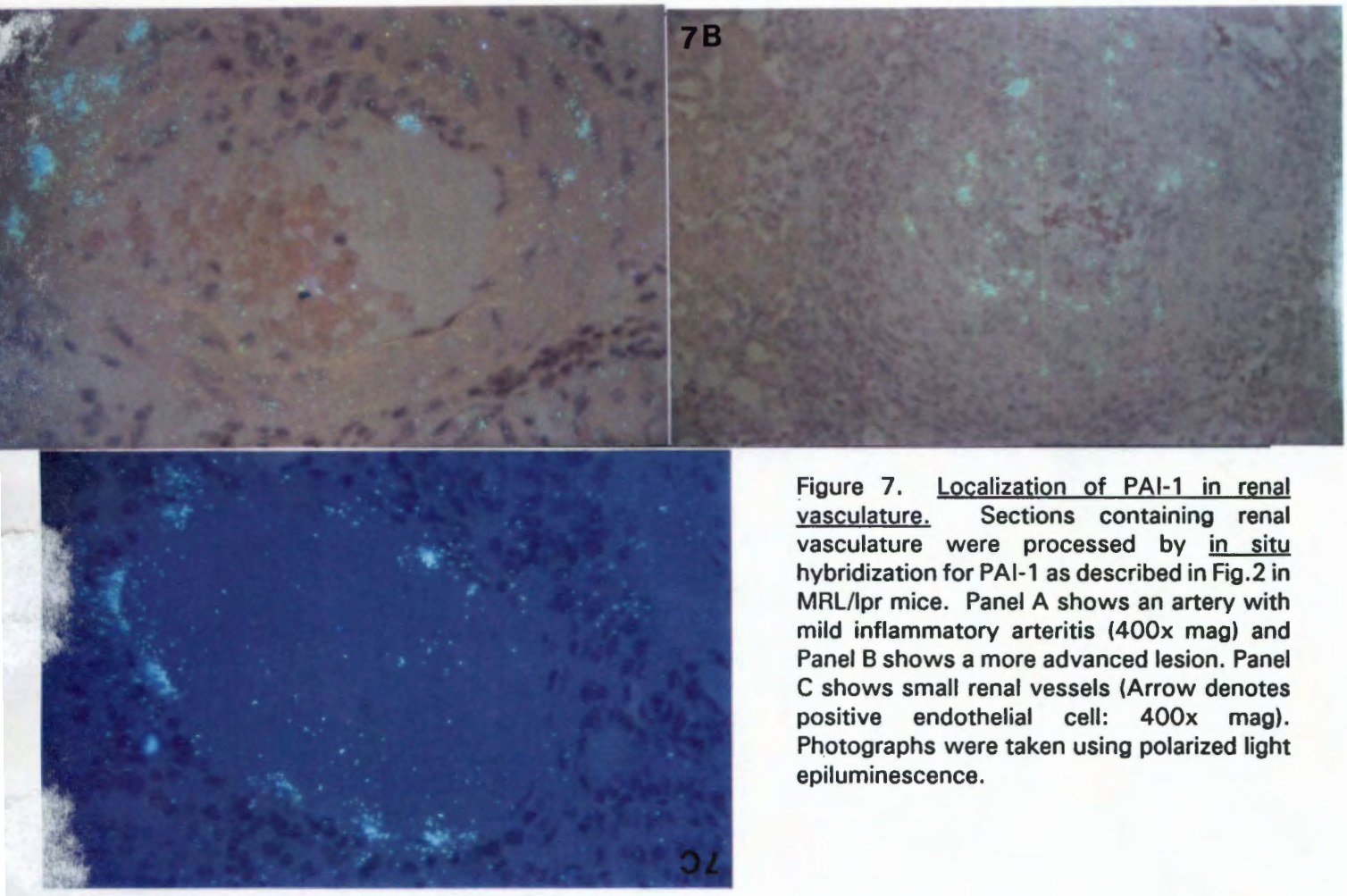

Figure 7. Localization of PAI-1 in renal vasculature. Sections containing renal vasculature were processed by in situ hybridization for PAI-1 as described in Fig.2 in MRL/lpr mice. Panel A shows an artery with mild inflammatory arteritis (400x mag) and Panel B shows a more advanced lesion. Panel C shows small renal vessels (Arrow denotes positive endothelial cell: 400x mag). Photographs were taken using polarized light epiluminescence.

Comparison between the histologic findings and the distribution of PAI-1 mRNA. Table 1 contains a summary of the ages of the mice, the histologic grading, the extent of disease in four separate regions of the kidney (namely the glomerulus, the crescents, the intersitium and the blood vessels) and whether these regions were positive for PAI-1 mRNA by in situ hybridization. Regions in which a positive in situ hybridization signal was seen are indicated by shading of the appropriate

blocks in Table 1. Control mice of the CB6 genetic background (C1 to C6) showed no histological evidence of renal disease and were negative for PAI-1 mRNA in the regions described above. Control mice with the MRL/scr genetic background were also negative for histologic evidence of disease except for the 6 month old mouse which showed grade I renal disease with minimal mesangial thickening. These mice were also negative by in situ hybridization for PAI-1 mRNA. In contrast to these findings in control mice, all MRL/lpr mice showed evidence of moderate to severe lupus nephritis (grade II to IV), and as can be seen in Table 1 most of the areas with severe disease were also positive for PAI-1 mRNA by in situ hybridization.

Discussion.

A striking feature of many acute and chronic forms of glomerulopathy is the formation of intravascular thrombi in the glomerulus (82,160-164). This behavior is particularly prominent in LN (145,146) where intravascular thrombosis together with endothelial cell and mesangial cell proliferation are also observed.

In spite of many studies which correlate abnormalities in some of the fibrinolytic factors with both acute and chronic renal diseases (82,112,113,146,147,165), little is known about the role of these factors in the progression of renal disease. A key molecule in this regard is PAI-1, a potent anti-fibrinolytic protein which inhibits both t-PA and u-PA. Increased levels of PAI-1 have been detected in the plasma of individuals with a variety of renal diseases ( ) and in that of an experimental model of GN (82,112,113). Although, the origin (site of synthesis) of this plasma PAI-1 is unknown, we have recently shown that both glomerular and peritubular endothelial cells in vivo have the capacity to synthesize large amounts of PAI-1 in response to endotoxin. This observation raises the possibility that chronic expression of PAI-1 in endothelial cells could predispose to the intravascular coagulation frequently associated with LN.

To see if PAI-1 was inappropriately expressed in ongoing renal disease, we chose to study LN in female MRL/lpr mice between the ages of 4 and 7 months. Mice with the MRL genetic background have a predisposition to develop autoimmune renal disease (151). A spontaneous recessive mutation, lpr (lymphoproliferation) in this genetic background leads to an early onset SLE

like syndrome. In my studies, I compared the expression of PAI-1 in the kidneys of normal mice (i.e., CB6 mice and MRL/scr mice without the disease) to the expression of PAI-1 in mice with LN (i.e., MRL/lpr). Histopathologic analysis of renal tissue from MRL/lpr mice confirmed that these animals had active LN (Fig.1 A to C and Table 1), whereas the control mice (MRL/scr and CB6, Table 1) did not. This histologic assessment was supported serologically by measurments of the concentrations of markers of active SLE in the plasma of these mice. MRL/lpr mice had significantly higher levels of anti-ds DNA Abs, anti-ssDNA Abs (159,166), anti-chromatin Ab and anti-histone Abs (166) than did the control groups (Table 2). Although we also measured serum creatine levels, no significant difference was found between the control group and the disease group. Thus, the mice with LN did not seem to be in terminal renal failure.

Low levels of PAI-1 mRNA in normal mice were detected specifically in the SMCs of medium size vessels and in an unidentified cell type in the renal papilla (data not shown), consistent with my previous findings (148). However, in marked contrast to this, mice with LN had high levels of PAI-1 mRNA at many sites of active disease. We identified PAI-1 positive endothelial cells by virtue of their characteristic position on the luminal side of the vessel wall, both in the glomerular tuft (Fig.2 C and Fig.3 A and B) and in small blood vessels (Fig.7 B) at sites of active disease. PAI-1 positive cells were also found in the glomerular crescents (Fig.4 A,B and C). In early crescent formation it was possible to identify PAI-1 positive parietal epithelial cells by their position on the luminal side of Bowmans capsule. (Fig.4 A). In more advanced lesions, we were not able to identify the positive cells because of the high density of inflammatory monocytes within the crescents (Fig.4 B and C). At sites of interstitial nephritis we were also able to identify tubular

epithelial cells expressing PAI-1 (Fig.5 B and Fig.6 A and B) as well as an unidentified cell type in the surrounding inflammatory cells (Fig.5 A). Finally, large vessels with infiltrating inflammatory cells were also positive for PAI-1 in the media (Fig.7 A). This signal was seen at shorter exposures compared to normal mice (2 weeks compared to 12 weeks).

The wide spectrum of cells expressing PAI-1 in the kidneys of mice with LN suggests a common underlying mechanism directing this expression. In my study, PAI-1 producing cells were found in areas of active disease and it is possible that the macrophages at these sites (167,168) released a cytokine that induced PAI-1 expression in a variety of renal cells. Studies of LN in MRL/lpr mice have shown that TNFα is expressed in the cortex of diseased kidneys but not in normal kidneys (169). Moreover, administration of TNFα at 4 months of age can exacerbate the disease (170). Macrophages isolated from mice with LN synthesize TNFα in vitro (169) thus suggesting that TNFα may be an important cytokine in the progression of LN. Other indirect evidence to involve TNFα in the pathogenesis of LN comes from studies on the role of LPS in renal disease. Hang et al showed that, in response to the mitogenic principle of endotoxin (R595), all the strains of mice which they studied developed low levels of autoimmune GN (2+) except for endotoxin-resistant C3H/HeJ mice (158). In addition,MLR/lpr male mice, and other mice that develop late onset LN, had greatly accelerated renal disease in response to R595 compared to their untreated counterparts. The primary mediator of the LPS response is TNFα (141) and C3H/HeJ mice, which do not make TNFα in response to LPS due to a defect in the signal pathway (171), do not develop autoimmune GN. This data again suggests that TNFα may be a crucial cytokine in the pathogenesis of LN.

It is interesting to compare the differences between PAI-1 mRNA expression in LN to that seen after LPS administration. In LN there is chronic expression of PAI-1 over long periods of time (weeks to months) since almost all the diseased mice show some degree of PAI-1 expression. In contrast, in mice treated with LPS there is a much more transient expression of renal PAI-1, with a peak at 3 hours and a return to background levels by 24 hours (122). In addition to this difference, the repertoire of cells that express PAI-1 mRNA in these models is also different. After LPS administration, the majority of the PAI-1 expression is by endothelial cells at all levels of the renal vasculature. This is in contrast to LN where many different cells types express PAI-1 including endothelial cells, parietal epithelial cells, tubular epithelial cells and also unidentified cells in areas of inflammatory infiltrates. These findings suggest that LPS may mediate the PAI-1 response via a direct action on endothelial cells. For example, there may be a direct affect of LPS in vivo which causes a transient peak of PAI-1 expression primarily in endothelial cells, followed by secondary more chronic effects related to the induction of TNFα. Furthermore, mononuclear cells in areas of inflammation may also express TNFα and other cytokines which may account for the much more widespread expression of PAI-1 seen in LN compared to endotoxaemia.

In summary, this study of LN has demonstrated a number of unique features about the expression of PAI-1 in vivo. First of all, we find the chronic expression of PAI-1 in a disease in which coagulation is a prominent feature. We show that many cell types express PAI-1, a fact that had been suggested by in vitro studies (132-134) but not previously demonstrated in vivo. Finally, we demonstrate that the PAI-1 expression is localized to sites of active disease. All of this data is suggestive of a role for this potent anti-fibrinolytic molecule in the ongoing pathology of LN. This

possibility is under investigation.

This work is in preparation for submission to Kidney International.

Title: INAPPROPRIATE EXPRESSION OF TYPE 1 PLASMINOGEN ACTIVATOR INHIBITOR (PAI-1) IN RENAL TISSUE IN MURINE LUPUS.

Authors: M. Keeton, C. Ahn, Y. Eguchi, R. Burlingame & D. J. Loskutoff.

Acknowledgements. I would like to thank Dr C. Chang for help with the electron microscopy, and T. Thinnes and K. Roegner for help with the *in situ* hybridization experiments.

CHAPTER 7: SUMMARY.

1. The experiments described in Chapter 1 showed that, in the K562 system at least, differentiation-linked changes in t-PA activity were incidental to PAI-1 synthesis and release and that the inhibitor is a critical regulatory protein. Whether or not the increase in PAI-1 secretion is due to a direct effect of PMA is uncertain, since phorbol ester is known to increase TGFß and PDGF levels in these cells (70,78) and TGFß causes large increases in PAI-1 synthesis by a variety of cultured cell types (48,79,80).

2. The transfection studies described in Chapter 2 showed that two sequences were important in the TGFß response of the PAI-1 promoter and 5' flanking region. The first of these was located in the proximal promoter (-49 to -87) and mediated an 11-fold induction with TGFß, while the second more distal region (-636 to -740) contained two sequences which together mediated a 50-fold or greater response. Sequence comparison indicated that both of the responsive regions contained sequences with high homology to the AP-1 consensus binding site. Moreover, gel retardation analysis experiments demonstrated that both sequences bound a common nuclear protein, and that an oligonucleotide containing a consensus AP-1 site was able to compete for the binding of this protein. Thus the response of the PAI-1 gene to TGFß is mediated by at least two separate regions, and both of these regions contain DNA sequences with homology to the AP-1 binding site. Furthermore these experiments also demonstrated that NF-1-like binding sites located in the promoter and 5' flanking sequence were not responsible for the TGFß induction in this system.

3. One TGFß responsive region of the PAI-1 promoter (-708 to -732) was examined to determine the role of the AP-1-like site in this response. My data indicates that the full TGFß response of this region was dependent on the interaction of two distinct binding sites. Although the first site has homology to the AP-1 site, it does not appear to bind AP-1. Although this site does not appear to be essential, it is required for the full TGFß response of this region. The second site, located 5' to the AP-1 site, appears to be critical in the TGFß response. This site is 15bp in size and contains a motif that is present in both active regions of the PAI-1 promoter as well as in the most responsive region of the TGFß promoter. This novel sequence does not appear to correspond to any previously described transcription factor binding sites and may represent a new and specific binding site which is critical for a strong TGFß response.

4. I also examined the <u>in vivo</u> localization of PAI-1 in both an acute phase model and during a model of chronic renal disease. <u>In situ</u> hybridization was performed to determine the cellular localization of PAI-1 mRNA within renal tissues. In control kidneys, low levels of PAI-1 mRNA were detected in the renal papilla, and in the muscular walls of renal arteries. However, in the endotoxaemic mice, an intense hybridization signal for PAI-1 mRNA was observed in glomerular and peritubular cells. These cells also stained positively for von Willebrand factor antigen, an endothelial cell-specific marker.The PAI-1 mRNA hybridization signal could further be observed in peri-tubular endothelial cells in the medulla, and in endothelial cells of veins and arteries throughout the kidney. Immunochemical staining revealed that PAI-1 antigen colocalized to cytoplasm of the cells expressing PAI-1

mRNA. These results provide the first direct evidence that PAI-1 is induced in endothelial cells of the kidney during endotoxaemia in vivo, and suggests a role for PAI-1 in the pathogenesis of renal disease.

5. To examine the role of PAI-1 in the pathogenesis of renal disease characterized by thrombosis, I chose to study a model of lupus nephritis. I compared the expression of PAI-1 in the kidneys of normal mice to the expression of PAI-1 in mice with LN. Histopathologic analysis of renal tissue confirmed that the LN animals had active renal disease. This was confirmed by serology which showed that the diseased mice had significantly higher levels of anti-ds DNA Abs, anti-ss DNA Abs, anti-chromatin Abs and anti-histone Abs than did the control group. Low levels of PAI-1 mRNA in normal mice was detected specifically in the SMCs of medium size vessels and in the renal papilla, consistent with my previous findings. However, in contrast to this, mice with LN had high levels of PAI-1 mRNA at many sites of active disease. I identified PAI-1 positive endothelial cells both in the glomerular tuft and in small blood vessels at sites active disease. PAI-1 positive parietal epithelial cells were also identified in Bowmans capsule. At sites of interstitial nephritis PAI-1 positive tubular epithelial cells were also identified. Finally large vessels with infiltrating inflammatory cells were also positive for PAI-1 in the media. This study showed that many cell types express PAI-1, a fact that had been suggested by in vitro studies but not previously demonstrated in vivo. This data is suggestive of a role for this potent anti-fibrinolytic molecule in the ongoing pathology of LN.

REFERENCES.

1. Astrup, T. 1978. Fibrinolysis. An overview. In Progress in Chemical Fibrinolysis and Thrombolysis. J.F. Davidson, R.M. Rowan, M.M. Samama, and P.C. Desnoyers, editors. Raven Press, New York. 1-89.

2. Hekman, C.M. and D.J. Loskutoff. 1987. Fibrinolytic pathways and the endothelium. Sem. Thromb. Hemost. 13:514-527.

3. Pillemer, E., R.R. Schleef, D.J. Loskutoff, D. Higgins, and L.J. Levitt. 1987. Bleeding diathesis with decreased functional activity of plasminogen activator inhibitor (PAI-1). Blood 70:1-378a.

4. Estelles, A., J. Gilabert, J. Azner, D.J. Loskutoff, and R.R. Schleef. 1989. Changes in the plasma levels of type 1 and type 2 plasminogen activator inhibitors in normal pregnancy and in patients with severe preeclampsia. Blood 74:1332-1338.

5. Schleef, R.R., D.L. Higgins, E. Pillemer, and J.J. Levitt. 1989. Bleeding diathesis due to decreased functional activity of type 1 plasminogen activator inhibitor. J. Clin. Invest. 83:1747-1752.

6. Wing, L.R., B. Bennett, and N.A. Booth. 1991. The receptor for tissue plasminogen activator (t-PA) in complex with its inhibitor, PAI-1, on human hepatocytes. FEBs Letters 278:95-97.

7. Appella, E., E.A. Robinson, S.J. Ullrich, M.P. Stoppelli, A. Corti, G. Cassani, and F. Blasi. 1987. The receptor-binding sequence of urokinase. J. Biol. Chem. 262:4437-4440.

8. Behrendt, N., E. Renne, M. Ploug, T. Petri, D. Lober, L.S. Nielsen, W-D. Schleuning, F. Blasi, E. Appella, and K. Dano. 1990. The human receptor for urokinase plasminogen activator. J. Biol. Chem. 265:6453-6460.

9. Cubellis, M.V., T-C. Wun, and F. Blasi. 1990. Receptor-mediated internalization and degradation of urokinase is caused by its specific inhibitor PAI-1. EMBO J. 9:1079-1085.

10. Plow, E.F., D. Freaney, J. Plescia, and L.A. Miles. 1986. The plasminogen system and cell surfaces: evidence for plasminogen and urokinase receptors on the same cell type. J. Cell Biol. 103:2411-2420.

11. Salonen, E.M., O. Saksela, T. Vartio, A. Vaheri, L. Nielsen, and J. Zeuthen. 1985. Plasminogen and tissue-type plasminogen activator bind to immobilized fibronectin. J. Biol. Chem. 260:12302-12307.

12. Knudsen, B.S., R. Silverstein, L. Leung, P.C. Harpel, and R.L. Nachman. 1986. Binding of plasminogen to extracellular matrix. J. Biol. Chem. 261:10765-10771.

13. Sprengers, E.D. and C. Kluft. 1987. Plasminogen activator inhibitors.

Blood 69:381-387.

14. Levin, E.G. 1983. Latent tissue plasminogen activator produced by human endothelial cells in culture: Evidence for an enzyme-inhibitor complex. Proc. Natl. Acad. Sci. USA 80:6804-6808.

15. Kopitar, M., B. Rozman, J. Babnik, V. Turk, D.E. Mullins, and T-C. Wun. 1985. Human leukocyte urokinase inhibitor-purification, characterization and comparative studies against different plasminogen activators. Thromb. Haemost. 54:750-755.

16. Baker, J.B., D.A. Low, R.L. Simmer, and D.D. Cunningham. 1980. Protease-Nexin: a cellular component that links thrombin and plasminogen activator and mediates their binding to cells. Cell 21:37-45.

17. Loskutoff, D.J., M. Sawdey, and J. Mimuro. 1988. Type 1 plasminogen activator inhibitor. In Progress in Hemostas. Thromb. B. Coller, editor. 87-115.

18. Ginsburg, D., R. Zeheb, A.V. Yang, U.M. Rafferty, P.A. Andreasen, L. Nielsen, K. Dano, R.V. Lebo, and T.D. Gelehrter. 1986. cDNA cloning of human plasminogen activator-inhibitor from endothelial cells. J. Clin. Invest. 78:1673-1680.

19. Klinger, K.W., R. Winqvist, A. Riccio, P.A. Andreasen, R. Sartorio, L.S. Nielsen, N. Stuart, P. Stanislovitis, P. Watkins, R. Douglas, K-H. Grzeschik, K. Alitalo, F. Blasi, and K. Dano. 1987. Plasminogen activator inhibitor type 1 gene is located at region q21.3-q22 of chromosome 7 and genetically linked with cystic fibrosis. Proc. Natl. Acad. Sci. USA 84:8548-8552.

20. Loskutoff, D.J., M. Linders, J. Keijer, H. Veerman, H. van Heerikhuizen, and H. Pannekoek. 1987. The structure of the human plasminogen activator inhibitor 1 gene: Non-random distribution of introns. Biochem. 26:3763-3768.

21. Ny, T., M. Sawdey, D.A. Lawrence, J.L. Millan, and D.J. Loskutoff. 1986. Cloning and sequence of a cDNA coding for the human β-migrating endothelial-cell-type plasminogen activator inhibitor. Proc. Natl. Acad. Sci. USA 83:6776-6780.

22. Pannekoek, H., H. Veerman, H. Lambers, P. Diergaarde, C.L. Verweij, A.J. van Zonneveld, and J.A. van Mourik. 1986. Endothelial plasminogen activator inhibitor (PAI): A new member of Serpin gene family. EMBO J. 5:2539-2544.

23. Andreasen, P.A., A. Riccio, K.G. Welinder, R. Douglas, R. Sartorio, L.S. Nielsen, C. Oppenheimer, F. Blasi, and K. Dano. 1986. Plasminogen activator inhibitor type-1: reactive center and amino-terminal heterogeneity determined by protein and cDNA sequencing. FEBs Letters 209:213-218.

24. Erickson, L.A., C.M. Hekman, and D.J. Loskutoff. 1986. Denaturant-induced stimulation of the B-migrating plasminogen activator

inhibitor in endothelial cells and serum. Blood 68:1298-1305.

25. van Mourik, J.A., D.A. Lawrence, and D.J. Loskutoff. 1984. Purification of an inhibitor of plasminogen activators (antiactivator) synthesized by endothelial cells. J. Biol. Chem. 259:14914-14921.

26. Lawrence, D.A. and D.J. Loskutoff. 1986. Inactivation of plasminogen activator inhibitor by oxidants. Biochem. 25:6351-6355.

27. Booth, N.A., J.A. Anderson, and B. Bennett. 1985. Platelet release protein which inhibits plasminogen activators. J. Clin. Pathol. 38:825-830.

28. Hekman, C.M. and D.J. Loskutoff. 1985. Endothelial cells produce a latent inhibitor of plasminogen activators that can be activated by denaturants. J. Biol. Chem. 260:11581-11587.

29. Katagiri, K., K. Okada, H. Hattori, and M. Yano. 1988. Bovine endothelial cell plasminogen activator inhibitor. Purification and heat activation. Eur. J. Biochem. 176:81-87.

30. Lambers, J.W.J., M. Cammenga, B. Konig, H. Pannekoek, and J.A. van Mourik. 1987. Activation of human endothelial type plasminogen activator inhibitor (PAI-1) by negatively charged phospholipids. J. Biol. Chem. 262:17492-17496.

31. Wun, T-C., M.O. Palmier, N.R. Siegel, and C.E. Smith. 1989. Affinity purification of active plasminogen activator inhibitor-1 (PAI-1) using immobilized anhydrourokinase. J. Biol. Chem. 264:7862-7868.

32. Levin, E.G. and L. Santell. 1987. Conversion of the active to latent plasminogen activator inhibitor from human endothelial cells. Blood 70:1090-1098.

33. Kooistra, T., E.D. Sprengers, and V.W.M. van Hinsbergh. 1986. Rapid inactivation of the plasminogen-activator inhibitor upon secretion from cultured human endothelial cells. Biochem. J. 239:497-503.

34. Hekman, C.M. and D.J. Loskutoff. 1988. Bovine plasminogen activator inhibitor 1: Specificity determinations and comparison of the active, latent and guanidine-activated forms. Biochem. 27:2911-2918.

35. Laiho, M., O. Saksela, P.A. Andreasen, and J. Keski-Oja. 1986. Enhanced production and extracellular deposition of the endothelial-type plasminogen activator inhibitor in cultured human lung fibroblasts by transforming growth factor-β. J. Cell Biol. 103:2403-2410.

36. Knudsen, B.S., P.C. Hapel, and R.L. Nachman. 1987. Plasminogen activator inhibitor is associated with the extracellular matrix of cultured bovine smooth muscle cells. J. Clin. Invest. 80:1082-1089.

37. Levin, E.G. and L. Santell. 1987. Association of plasminogen activator

inhibitor (PAI-1) with the growth substratum and membrane of human endothelial cells. J. Cell Biol. 105:2543-2549.

38. Pollanen, J., O. Saksela, E.M. Salonen, P.A. Andreasen, L. Nielsen, K. Dano, and A. Vaheri. 1987. Distinct localizations of urokinase-type plasminogen activator and its type 1 inhibitor under cultured human fibroblast and sarcoma cells. J. Cell. Biol. 104:1085-1096.

39. Mimuro, J., R.R. Schleef, and D.J. Loskutoff. 1987. The extracellular matrix of cultured bovine aortic endothelial cells contains functionally active type 1 plasminogen activator inhibitor. Blood 70:721-728.

40. Mimuro, J. and D.J. Loskutoff. 1989. Binding of type 1 plasminogen activator inhibitor to the extracellular matrix of cultured bovine endothelial cells. J. Biol. Chem. 264:5058-5063.

41. Declerck, P.J., M. De Mol, M-C. Alessi, S. Baudner, E-P. Paques, K.T. Preissner, G. Muller-Berghaus, and D. Collen. 1988. Purification and characterization of a plasminogen activator inhibitor 1 binding protein from human plasma. J. Biol. Chem. 263:15454-15461.

42. Mimuro, J. and D.J. Loskutoff. 1989. Purification of a protein from bovine plasma that binds to type 1 plasminogen activator inhibitor and prevents its interaction with extracellular matrix. J. Biol. Chem. 264:936-939.

43. Emeis, J.J. 1985. Fast hepatic clearance of plasminogen activator inhibitor. Thromb. Haemost. 54:230.

44. Hanss, M. and D. Collen. 1987. Secretion of tissue type plasminogen activator and plasminogen activator inhibitor by cultured human endothelial cells, modulation by thrombin, endotoxin, and histamine. J. Lab. Clin. Med. 109:97-104.

45. Colucci, M., J.A. Paramo, and D. Collen. 1986. Inhibition of one-chain and two-chain forms of human tissue-type plasminogen activator by the fast-acting inhibitor of plasminogen activator in vitro and in vivo. J. Lab. Clin. Med. 108:53-59.

46. Hekman, C.M. and D.J. Loskutoff. 1987. Kinetic analysis of the interactions between plasminogen activator inhibitor 1 and both urokinase and tissue plasminogen activator. Archives Biochem. Biophys. 262:199-210.

47. Loskutoff, D.J., M. Sawdey, and J. Mimuro. 1989. Type 1 plasminogen activator inhibitor. In Progress in Hemostasis and Thrombosis. B. Coller, editor. Bermedica Production, Columbia, Maryland. 87-115.

48. Sawdey, M., T.J. Podor, and D.J. Loskutoff. 1989. Regulation of type 1 plasminogen activator inhibitor gene expression in cultured bovine aortic endothelial cells: Induction by transforming growth factor-β, lipopolysaccharide, and tumor necrosis factor-α. J. Biol. Chem.

264:10396-10401.

49. van Zonneveld, A-J., S.A. Curriden, and D.J. Loskutoff. 1988. Type 1 plasminogen activator inhibitor gene: Functional analysis and glucocorticoid regulation of its promoter. Proc. Natl. Acad. Sci. USA 85:5525-5529.

50. Westerhausen, D.R., W.E. Hopkins, and J.J. Billadello. 1991. Multiple transforming growth factor-β-inducible elements regulate expression of the plasminogen activator inhibitor type-1 gene in hep G2 cells. J. Biol. Chem. 266:1092-1100.

51. Colucci, M., J.A. Paramo, and D. Collen. 1985. Generation in plasma of a fast-acting inhibitor of plasminogen activator in response to endotoxin stimulation. J. Clin. Invest. 75:818-824.

52. Paramo, J.A., A. DeBoer, M. Colucci, J.J.C. Jonker, and D. Collen. 1985. Plasminogen activator inhibitor (PA-inhibitor) activity in the blood of patients with deep vein thrombosis. Thromb. Haemost. 54:725.

53. Almer, L. and H. Ohlin. 1987. Elevated levels of rapid inhibitor of plasminogen activator (t-PAI) in acute myocardial infarction. Thromb. Res. 47:335-339.

54. Hamsten, A., B. Wiman, U. deFaire, and M. Blomback. 1985. Increased plasma levels of a rapid inhibitor of tissue plasminogen activator in young survivors of myocardial infarction. N. Engl. J. Med. 313:1557-1563.

55. Kruithof, E.K.O., C. Tran-Thang, A. Gudinchet, J. Hauert, G. Nicoloso, C. Genton, H. Welti, and F.W. Bachmann. 1987. Fibrinolysis in pregnancy. A study of plasminogen activator inhibitors. Blood 69:460-466.

56. Oseroff, A., C. Krishnamurti, A. Hassett, D. Tang, and B. Alving. 1989. Plasminogen activator and plasminogen activator inhibitor activities in men with coronary artery disease. J. Lab. Clin. Med. 113:88-93.

57. Hamsten, A., U. De Faire, G. Walldius, G. Dahlen, A. Szamosi, C. Landou, M. Blomback, and B. Wiman. 1987. Plasminogen activator inhibitor in plasma: Risk factor for recurrent myocardial infarction. Lancet 2:3-9.

58. Juhan-Vague, I., B. Moerman, F. De Cock, M.F. Aillaud, and D. Collen. 1984. Plasma levels of a specific inhibitor of tissue-type plasminogen activator (and urokinase) in normal and pathological conditions. Thromb. Res. 33:523-530.

59. Sprengers, E.D., H.M.G. Princen, T. Kooistra, and V.W.M. van Hinsbergh. 1985. Inhibition of plasminogen activators by conditioned medium of human hepatocytes and hepatoma cell line hep G2. J. Lab. Clin. Med. 105:751-758.

60. Risberg, B., G.K. Hansson, E. Eriksson, and B. Wiman. 1987. Immunohistochemical localization of plasminogen activator inhibitor (PAI) in tissue. Thromb. Haemost. 58:446.

61. Vague, P.H., I. Juhan-Vague, M.C. Alessi, C. Badier, and J. Valadier. 1987. Metformin decreases the high plasminogen activator inhibition capacity, plasma insulin and triglyceride levels in non-diabetic obese subjects. Thromb. Haemost. 58:326-328.

62. Alessi, M.C., I. Juhan-Vague, T. Kooistra, P.J. Declerck, and D. Collen. 1988. Insulin stimulates the synthesis of plasminogen activator inhibitor 1 by the human hepatocellular cell line Hep G2. Thromb. Haemost. 60:491-494.

63. Kluft, C., J.H. Verheijen, A.F.H. Jie, D.C. Rijken, F.E. Preston, H.M. Sue-Ling, J. Jespersen, and A.D. Aasen. 1985. The postoperative fibrinolytic shutdown: a rapidly reverting acute phase pattern for the fast-acting inhibitor of tissue-type plasminogen activator after trauma. Scand. J. Clin. Lab. Invest. 45:605-610.

64. de Boer, J.P., J.J. Abbink, M.C. Brouwer, C. Meijer, D. Roem, G.P. Voorn, J.W.J. Lambers, J.A. van Mourik, and C.E. Hack. 1991. PAI-1 synthesis in the human hepatoma cell line Hep G2 is increased by cytokines - Evidence that the liver contributes to acute phase behaviour of PAI-1. Thromb. Haemostas. 65:181-185.

65. Saito, H., L.T. Goodnough, B.B. Knowles, and D.D. Aden. 1982. Synthesis and secretion of plasmin inhibitor by established human liver cell lines. Proc. Natl. Acad. Sci. USA 79:5684-5687.

66. Francis, R.B.,Jr., H. Liebman, S. Koehler, and D.I. Feinstein. 1986. Accelerated fibrinolysis in amyloidosis. Specific binding of tissue plasminogen activator inhibitor by an amyloidogenic monoclonal IgG. Blood 68:333a.

67. Wilson, E.L., P. Jacobs, and E.B. Dowdle. 1983. The secretion of plasminogen activators by human myeloid leukemic cells in vitro. Blood 61:568.

68. Wilson, E.L. and G.E. Francis. 1987. Differentiation linked secretion of urokinase and tissue plasminogen activator by normal human haemepoistic cells. J. Exp. Med. 165:1609.

69. Lozzio, C.B. and B.B. Lozzio. 1975. Human chronic myelogenous leukemia cell line with positive Philadelphia chromosome. Blood 45:321.

70. Tetteroo, P.A., F. Massaro, A. Mulder, R. Schreuder-van Gelder, and A.E.G. von dem Borne. 1984. Megakaryoblastic differentiation of proerythroblastic K562 cell-line cells. Leuk. Res. 8:197.

71. Wilson, E.L. and E.B. Dowdle. 1978. Secretion of plasminogen activator by normal, reactive and neoplastic human tissues cultured in vitro. Int. J. Cancer 22:390.

72. Granelli-Piperno, A. and E. Reich. 1978. A study of proteases and

protease-inhibitor complexes in biological fluids. J. Exp. Med. 148:223-234.

73. Erickson, L.A., D.A. Lawrence, and D.J. Loskutoff. 1984. Reverse fibrin autography: A method to detect and partially characterize protease inhibitors after sodium dodecyl sulfate-polyacrylamide gel electrophoresis. Anal. Biochem. 137:454-463.

74. Chomczynski, P. and N. Sacchi. 1987. Single-step method of RNA isolation by acid guanidinium thyiocynate-phenol-chloroform extraction. Anal. Biochem. 162:156-159.

75. Feinberg, A.P. and B. Vogelstein. 1983. A technique for radiolabeling DNA restriction endonuclease fragments to high specific activity. Anal. Biochem. 132:6-13.

76. Andreasen, P.A., L.S. Nielsen, P. Kristensen, J. Grondahl-Hansen, L. Skriver, and K. Dano. 1986. Plasminogen activator inhibitor from human fibrosarcoma cells binds urokinase-type plasminogen activator, but not its proenzyme. J. Biol. Chem. 261:7644-7651.

77. Andreasen, P.A., T.H. Christensen, J-Y. Huang, L.S. Nielsen, E.L. Wilson, and K. Dano. 1986. Hormonal regulation of extracellular plasminogen activators and Mrs 54000 plasminogen activator inhibitor in human neoplastic cell lines, studied with monoclonal antibodies. Mol. Cell. Endocrinol. 45:137-147.

78. Alitalo, R., T.P. Makela, P. Koskinen, L.C. Andersson, and K. Alitalo. 1988. Enhanced expression of transforming growth factor β during megakaryoblastic differentiation of K562 leukemia cells. Blood 71:899.

79. O'Shea, K.S., L-H.J. Liu, L.H. Kinnunen, and V.M. Dixit. 1990. Role of the extracellular matrix protein thrombospondin in the early development of the mouse embryo. J. Cell Biol. 111:2713-2723.

80. Fujii, S. and B.E. Sobel. 1990. Induction of plasminogen activator inhibitor by products released from platelets. Circulation 82:1485-1493.

81. Schleef, R.R., M.P. Bevilacqua, M. Sawdey, M.A. Gimbrone,Jr., and D.J. Loskutoff. 1988. Interleukin 1 (IL-1) and tumor necrosis factor (TNF) activation of vascular endothelium: Effects on plasminogen activator inhibitor (PAI-1) and tissue type plasminogen activator (tPA). J. Biol. Chem. 263:5797-5803.

82. Tomosugi, N., T. Naito, K. Ikeda, H. Yokoyama, K. Kobayashi, and H. Kida. 1990. The role of plasminogen activator inhibitor (PAI) on anti-glomerular basement membrane antibody-mediated glomerular injury and its modulation by tumor necrosis factor (TNF). Kidney Int. 37:435.

83. Saksela, O., D. Moscatelli, and D.B. Rifkin. 1987. The opposing effects of basic fibroblast growth factor and transforming growth factor β on the regulation of plasminogen activator activity in capillary endothelial cells.

J. Cell Biol. 105:957-963.

84. Mimuro, J. and D.J. Loskutoff. 1987. Effect of transforming growth factor-β (TGFβ) on the fibrinolytic system of cultured bovine aortic endothelial cells (BAEs). Thromb. Haemost. 58:1647.

85. Emeis, J.J. and T. Kooistra. 1986. Interleukin 1 and lipopolysaccharide induce an inhibitor of tissue-type plasminogen activator in vivo and in cultured endothelial cells. J. Exp. Med. 163:1260-1266.

86. Thalacker, F.W. and M. Nilsen-Hamilton. 1987. Specific induction of secreted proteins by transforming growth factor-β and 12-0-tetradecanoylphorbol-13-acetate. J. Biol. Chem. 262:2283-2290.

87. Loskutoff, D.J. 1991. Regulation of PAI-1 gene expression. Fibrinolysis 5:197-206.

88. Barnard, J.A., R.M. Lyons, and H.L. Moses. 1990. The cell biology of transforming growth factor B. Biochim. Biophys. Acta 1032:79-87.

89. Slivka, S.R. and D.J. Loskutoff. 1991. Platelets stimulate endothelial cells to synthesize type 1 plasminogen activator inhibitor. Blood 77:1013-1019.

90. Kim, S-J., P. Angel, R. Lafyatis, K. Hattori, K.Y. Kim, M.B. Sporn, M. Karin, and A.B. Roberts. 1990. Autoinduction of transforming growth factor B1 is mediated by the AP-1 complex. Mol. Cell. Biol. 10:1492-1497.

91. Lee, W., P. Mitchell, and R. Tjian. 1987. Purified transcription factor AP-1 interacts with TPA-inducible enhancer elements. Cell 49:741-752.

92. Angel, P., M. Imagawa, R. Chiu, B. Stein, R.J. Imbra, H.J. Rahmsdorf, C. Jonat, P. Herrlich, and M. Karin. 1987. Phorbol ester-inducible genes contain a common Cis element recognized by a TPA-modulated trans-acting factor. Cell 49:729-739.

93. Rossi, P., G. Karsenty, A.B. Roberts, N.S. Roche, M.B. Sporn, and B. de Crumbrugghe. 1988. A nuclear factor 1 binding site mediates the transcriptional activation of a type 1 collagen promoter by transforming growth factor-b. Cell 52:405-414.

94. Shaul, Y., R. Ben-Levy, and T. De-Medina. 1986. High affinity binding site for nuclear factor I next to the hepatitis B virus S gene promoter. EMBO J. 5:1967-1971.

95. Miksicek, R., U. Borgmeyer, and J. Nowock. 1987. Interaction of the TGGCA-binding protein with upstream sequences is required for efficient transcription of mouse mammary tumor virus. EMBO J. 6:1355-1360.

96. Sippel, A.E., H.P. Fritton, M. Theisen, U. Borgmeyer, U. Strech-Jurk, and T. Igo-Kemenes. 1991. The TGGCA protein binds in vitro to DNA contained

in a nuclease-hypersensitive region that is present only in active chromatin of the lysozyme gene. Cancer Cells 4:155-162.

97. De Wet, J.R., K.V. Wood, M. DeLuca, D.R. Helinski, and S. Subramani. 1987. Firefly luciferase gene: structure and expression in mammalian cells. Mol. Cell Biol. 7:725-737.

98. Gorman, C.M., L.F. Moffat, and B.H. Howard. 1982. Recombinant genomes which express chloramphenicol acetyltransferase in mammalian cells. Mol. Cell Biol. 2:1044-1051.

99. Fried, M. and D.M. Crothers. 1981. Equilibria and kinetics of lac repressor-operator interactions by polyacrylamide gel electrophoresis. Nuc. Acids Res. 9:6505-6525.

100. Garner, M.M. and A. Revzin. 1981. A gel electrophoresis method for quantifying the binding of proteins to specific DNA regions: Application to components of the Escherichia coli lactose operon regulatory system. Nuc. Acids Res. 9:3047-3060.

101. Dignam, J.D., R.M. Lebovitz, and R.G. Roeder. 1983. Accurate transcription initiation by RNA polymerase II in a soluble extract from isolated mammalian nuclei. Nucleic Acids Res. 11:1475-1489.

102. Bucher, P. and E.N. Trifonov. 1986. Compilation and analysis of eukaryotic POL II promoter sequences. Nucleic Acids Res. 14:10009-10026.

103. Gaub, M-P., M. Bellard, I. Scheuer, P. Chambon, and P. Sassone-Cors. 1990. Activation of the ovalbumin gene by the estrogen receptor involves the fos-jun complex. Cell 63:1267-1276.

104. Roberts, A.B., M.A. Anzono, L.M. Wakefield, W. Roche, D.F. Stern, and M.B. Sporn. 1985. The β transforming growth factor: A bifunctional regulator of cellular growth. Proc. Natl. Acad. Sci. USA 82:119-123.

105. Roberts, A.B., M.B. Sporn, R.K. Assoian, J.M. Smith, N.S. Roche, L.M. Wakefield, U.I. Heine, L.A. Liotta, V. Falanga, J.H. Kehrl, and A.S. Fauci. 1986. Transforming growth factor type-β: Rapid induction of fibrosis and angiogenesis in vivo and stimulation of collagen formation in vitro. Proc. Natl. Acad. Sci. USA 83:4167-4171.

106. Bassols, A. and J. Massague. 1988. Transforming growth factor b regulates the expression and structure of extracellular matrix chondroitin/dermatan sulfate proteoglycans. J. Biol. Chem. 263:3039-3045.

107. Keeton, M., S.A. Curriden, A.J. van Zonneveld, and D.J. Loskutoff. 1991. Identification of regulatory sequences in the type 1 plasminogen activator inhibitor gene responsive to transforming growth factor β. J. Biol. Chem. 266:23048-23052.

108. Bruzdzinski, C.J., M. Riordan-Johnson, E.C. Nordby, S.M. Suter, and T.D.

Gelehrter. 1990. Isolation and characterization of the rat plasminogen activator inhibitor-1 gene. J. Biol. Chem. 265:2078-2085.

109. Schule, R., M. Muller, H. Otsuka-Murakami, and R. Renkawitz. 1988. Cooperativity of the glucocorticoid receptor and the CACCC-box binding factor. Nature 332:87-90.

110. Jang, I-K., H.K. Gold, A.A. Ziskind, J.T. Fallon, R.E. Holt, R.C. Leinbach, J.W. May, and D. Collen. 1989. Differential sensitivity of erythrocyte-rich and platelet-rich arterial thrombi to lysis with recombinant tissue-type plasminogen activator. A possible explanation for resistance to coronary thrombolysis. Circulation 79:920-923.

111. Cajot, J.F., J. Bamat, G.E. Bergonzelli, E.K.O. Kruithof, R.L. Medcalf, J. Testuz, and B. Sordat. 1990. Plasminogen-activator inhibitor type 1 is a potent natural inhibitor of extracellular matrix degradation by fibrosarcoma and colon carcinoma cells. Proc. Natl. Acad. Sci. USA 87:6939-6943.

112. Oliver, A., P. Barcelo, C. Fernandex, F. Rousand, O. Lopez, J.A. Ballarin, and F. Calero. 1990. Increased levels of plasminogen activator inhibitor in nephrotic syndrome. Kidney Int. 37:1590.

113. Bergstein, J.M. and N.U. Bang. 1990. Plasminogen activator inhibitor-1 (PAI-1) is the circulating inhibitor of fibrinolysis (PAI-HUS) in the hemolytic-uremic syndrome (HUS). Kidney Int. 37:254.

114. Prendergast, G.C., L.E. Diamond, D. Dahl, and M.D. Cole. 1990. The c-myc-regulated gene mr1 encodes plasminogen activator inhibitor 1. Mol. Cell Biol. 10:1265-1269.

115. Wilcox, J.N., K.M. Smith, S.M. Schwartz, and D. Gordon. 1989. Localization of tissue factor in the normal vessel wall and in the atherosclerotic plaque. Proc. Natl. Acad. Sci. USA 86:2839-2843.

116. Wilcox, J.N., C.E Gee, and J.L. Roberts. 1986. In situ cDNA:mRNA hybridization: Development of a technique to measure mRNA levels in individual cells. Methods in Enzymol. 124:510-533.

117. Ey, P.L., S.J. Prowse, and C.R. Jenkin. 1978. Isolation of pure IgG1, IgG2a and IgG2b immunoglobulins from mouse serum using protein A-sepharose. Biochem. 15:429-436.

118. Ruggeri, Z.M. and T.S. Zimmerman. 1980. Variant von Willebrand's disease: Characterization of two subtypes by analysis of multimeric composition of Factor VIII/von Willebrand factor in plasma and platelets. J. Clin. Invest. 65:1318-1325.

119. Ruggeri, Z.M. and T.S. Zimmerman. 1981. The complex multimeric composition of Factor VIII/von Willebrand factor. Blood 57:1140-1143.

120. Bevilacqua, M.P., R.R. Schleef, M.A. Gimbrone,Jr., and D.J. Loskutoff.

1986. Regulation of the fibrinolytic system of cultured human vascular endothelium by interleukin 1. J. Clin. Invest. 78:587-591.

121. Wagner, D.D., J.B. Olmsted, and V.J. Marder. 1982. Immunolocalization of von Willebrand protein in Wiebel-Palade bodies of human endothelial cells. J. Cell. Biol. 95:355-360.

122. Sawdey, M. and D.J. Loskutoff. 1991. Regulation of murine type 1 plasminogen activator inhibitor gene expression in vivo. Tissue specificity and induction by lipopolysaccharide, tumor necrosis factor-α, and transforming growth factor-β. J. Clin. Invest. 88:1346-1353.

123. Quax, P.H.A., C.M. van den Hoogen, J.H. Verheijen, T. Padro, R. Zeheb, T.D. Gelehrter, T.J.C. van Berkel, J. Kuiper, and J.J. Emeis. 1990. Endotoxin induction of plasminogen activator and plasminogen activator inhibitor type 1 mRNA in rat tissues in vivo. J. Biol. Chem. 265:15560-15563.

124. Jaffe, E.A., R.L. Nachman, C.G. Becker, and C.R. Minick. 1973. Culture of human endothelial cells derived from umbilical cord veins. Identification by morphologic and immunologic criteria. J. Clin. Invest. 52:2745-2756.

125. Suffredini, A.F., P.C. Harpel, and J.E. Parrillo. 1989. Promotion and subsequent inhibition of plasminogen activation after administration of intravenous endotoxin to normal subjects. N. Engl. J. Med. 320:1165-1172.

126. Martin, D.L., K.L. MacDonald, K.E. White, J.T. Soler, and M.T. Osterholm. 1990. The epidemiology and clinical aspects of the hemolytic uremic syndrome in Minnesota. N. Engl. J. Med. 323:1161-1167.

127. Chart, H., S.M. Scotland, and B. Rowe. 1989. Serum antibodies to Escherichia coli serotype 0157:H7 in patients with hemolytic uremic syndrome. J. Clin. Microbiol. 27:285-290.

128. Butler, T., H. Rahman, K.A. Al-Mahmud, M. Islam, P. Bardhan, I. Kabir, and M.M. Rahman. 1985. An animal model of haemolytic--uraemic syndrome in shigellosis: lipopolysaccharides of Shigella dysenteriae I and S. flexneri produce leucocyte-mediated renal cortical necrosis in rabbits. Br. J. Exp. Path. 66:7-15.

129. Bertani, T., M. Abbate, C. Zoja, D. Corna, and G. Remuzzi. 1989. Sequence of glomerular changes in experimental endotoxemia: A possible model of hemolytic uremic syndrome. Nephron. 53:330-337.

130. Kanost, M.R., S.V. Prasad, and M.A. Wells. 1989. Primary structure of a member of the serpin superfamily of proteinase inhibitors from an insect, manduca sexta. J. Biol. Chem. 264:965-972.

131. Simionescu, N. and M. Simionescu. 1977. The Cardiovascular System. In Histology. Cell and Tissue Biology. L. Weiss, editor. Elsevier, New York. 371-382.

132. Hagege, J., E. Rondeau, F. Delarue, R. Lacave, R. Medcalf, and J-D. Sraer. 1990. Plasminogen activator inhibitor 1 (PAI-1) is a component of the extracellular matrix (ECM) of human mesangial cells (HMC). Kidney Int. 37:219.

133. Iwamoto, T., Y. Nakashima, and K. Sueishi. 1990. Selection of plasminogen activator and its inhibitor by glomerular epithelial cells. Kid. Inter. 37:1466-1476.

134. Higgins, P.J., M.P. Ryan, R. Zeheb, T.G. Gelehrter, and P. Chaudhari. 1990. p52 Induction by cytochalasin D in rat kidney fibroblasts: Homologies between p52 and plasminogen activator inhibitor type-1. J. Cell. Physiol. 143:321-329.

135. van Mourik, J.A., D.A. Lawrence, and D.J. Loskutoff. 1983. Characterization of a novel fibrinolytic inhibitor synthesized by bovine aortic endothelial cells in culture. Thromb. Haemost. 50:281a.

136. Verheijen, J.H., G.T.G. Chang, and C. Kluft. 1984. Evidence for the occurrence of a fast-acting inhibitor for tissue-type plasminogen activator in human plasma. Thromb. Haemost. 51:392-395.

137. Sprengers, E.D., J.H. Verheijen, V.W.M. van Hinsbergh, and J.J. Emeis. 1984. Evidence for the presence of two different fibrinolytic inhibitors in human endothelial cell conditioned medium. Biochim. Biophys. Acta 801:163-170.

138. Sawdey, M., T. Ny, and D.J. Loskutoff. 1986. Messenger RNA for plasminogen activator inhibitor. Thromb. Res. 41:151-160.

139. Hekman, C.M. and D.J. Loskutoff. 1988. Kinetic analysis of the interactions between plasminogen activator inhibitor 1 and both urokinase and tissue plasminogen activator. Arch. Biochem. Biophys. 262:199-210.

140. Feinberg, R.F., L-C. Kao, J.E. Haimowitz, J.T. Queenan,Jr., T-C. Wun,Strauss,J.F.,III, and H.J. Kliman. 1989. Plasminogen activator inhibitor types 1 and 2 in human trophoblasts. PAI-1 is an immunocytochemical marker of invading trophoblasts. Lab. Invest. 61:20-26.

141. Mathison, J., E. Wolfson, and R. Ulevitch. 1988. Participation of tumor necrosis factor in the mediation of gram negative bacterial lipopolysaccharide-induced injury in rabbits. J. Clin. Invest. 81:1925-1937.

142. Diamond, J.R. and M.J. Karnovsky. 1988. Focal and segmental glomerulosclerosis: Analogies to atherosclerosis. Kidney Int. 33:917-924.

143. Border, W.A., S. Okuda, L.R. Languino, M.B. Sporn, and E. Ruoslahti. 1990. Suppression of experimental glomerulonephritis by antiserum against transforming growth factor β1. Nature 346:371-374.

144. Okuda, S., L.R. Languino, E. Ruoslahti, and W.A. Border. 1990. Elevated

expression of transforming growth factor-B and proteoglycan production in experimental glomerulonephritis. J. Clin. Invest. 86:453-462.

145. Kant, K.S., V.E. Pllak, and A. Dosekun. 1985. Lupus nephritis with thrombosis and abnormal fibrinolysis: Effect of ancrod. J. Lab. Clin. Med. 105:77-88.

146. Kant, K.S., V.E. Pollak, M.A. Weiss, H.I. Glueck, M.A. Miller, and E.V. Hess. 1981. Glomerular thrombosis in systemic lupus erythematosus: Prevalence and significance. Medicine 60:71.

147. Glas-Greenwalt, P., K.S. Kant, C. Allen, and V.E. Pollak. 1984. Fibrinolysis in health and disease: Severe abnormalities in systemic lupus erythematosus. J. Lab. Clin. Med. 104:962.

148. Keeton, M. and D.J. Loskutoff. 1991. Cellular localization of type 1 plasminogen activator inhibitor in renal tissue from normal and endotoxin-treated mice. J. Clin. Invest. submitted:

149. Granholm, N.A. and T. Cavallo. 1990. Prolonged circulation of immune complexes due to various altered immune functions contributes to nephritis in MRL/lpr mice. Clin. Exp. Immunol. 82:300-306.

150. Cavallo, T. and N.A. Granholm. 1990. Bacterial lipopolysaccharide transforms mesangial into proliferative lupus nephritis without interfering with processing of pathogenic immune complexes in NZB/W mice. Am. J. Path. 137:971-978.

151. Datta, S.K. 1988. Murine Lupus. Methods Enzymol. 162:385-412.

152. Theofilopoulos, A.N. and F.J. Dixon. 1985. Murine models of systemic lupus erythematogy. Adv. Immunol. 37:269-330.

153. Maher, J.J. and R.F. McGuire. 1990. Extracellular matrix gene expression increases preferentially in rat lipocytes and sinusoidal endothelial cells during hepatic fibrosis in vivo. J. Clin. Invest. 86:1641-1648.

154. Burlingame, R.W. and R.L. Rubin. 1990. Subnucleosome structures as substrates in enzyme-linked immunosorbent assays. J. Immunol. Meth. 134:187-199.

155. Lutter, L.C. 1978. Kinetic analysis of deoxyribonuclease I cleavages in the nucleosome core: evidence for a DNA superhelix. J. Mol. Biol. 124:391-405.

156. Godfrey, J.E., A.D. Baxevanis, A.D. Moudrianakis, and E.N. Moudrianakis. 1990. Spectropolarimetric analysis of the core histone octamer and its subunits. Biochem. 29:965-972.

157. Rubin, R.L. 1986. Anti-DNA antibodies. In Methods of Enzymatic Analysis. H. Bergmeyer, editor. Verlag Chemie, France. 175-194.

158. Hang, L., J.H. Slack, C. Amundson, S. Izui, A.N. Theofilopoulos, and F.J. Dixon. 1983. Induction of murine autoimmune disease by chronic polyclonal B cell activation. J. Exp. Med. 157:874-883.

159. Casali, P., S.E. Burastero, J.E. Balow, and A.L. Notkins. 1989. High-affinity antibodies to ssDNA are produced by CD-B cells in systemic lupus erythematosus patients. J. Immun. 143:3476-3483.

160. Holdsworth, S.R. and P.G. Tipping. 1985. Macrophage-induced glomerular fibrin deposition in experimental glomerulonephritis in the rabbit. J. Clin. Invest. 76:1376-1374.

161. Kamitsuji, H., S. Sakamoto, and T. Matsunaga. 1988. Intraglomerular deposition of fibrin/fibrinogen related antigen in children with various renal diseases. Am. J. Pathol. 133:61.

162. Prost, A.K.D., C.G.D. Nochy, and V.L. Floch. 1987. Enhanced glomerular procoagulant activity and fibrin deposition in rats with mercuric chloride-induced autoimmune nephritis. Lab. Invest. 57:138.

163. Robson, A.M., B.R. Cole, and R.A. Kiestra. 1977. Severe glomerulonephritis complicated by coagulophathy: treatment with anticoagulant and immunosuppressive drug. J. Pediatrics 90:881-892.

164. Takemura, T., K. Yoshioka, and N. Akano. 1987. Glomerular deposition of cross-linked fibrin in human kidney disease. Kid. Inter. 32:102-111.

165. Giroux, L., P. Verroust, L. Morel-Maroger, F. Delarue, M. Delauche, and J.D. Sraer. 1979. Glomerular fibrinolytic activity during nephrotoxic nephritis. Lab. Invest. 40:415-422.

166. Fournie, G.J. 1988. Circulating DNA and lupus nephritis. Kid. Inter. 33:487-497.

167. Cole, E.H., J. Sweet, and G.A. Levy. 1986. Expression of macrophage procoagulant activity in murine systemic lupus erythematosus. J. Clin. Invest. 78:887-893.

168. Cole, E.H., J. Schulman, and M. Urowitz. 1985. Monocyte procoagulant activity in glomerulonephritis associated with systemic lupus erythematosus. J. Clin. Invest. 75:861-868.

169. Boswell, J.M., M.A. Yui, D.W. Burt, and V.E. Kelley. 1988. Increased tumor necrosis factor and IL-1 β gene expression in the kidneys of mice with lupus nephritis. J. Immun. 141:3050-3054.

170. Brennan, D.C., M.A. Yui, R.P. Wuthrich, and V.E. Kelley. 1990. TNF and IL-1 in lupus nephritis: Enhanced gene expression and acceleration of disease. Kid. Inter. 38:409.

171. Beutler, B., N. Krochin, I.W. Milsark, C. Luedke, and A. Cerami. 1986. Control of cachectin (Tumor Necrosis Factor) synthesis: Mechanisms of endotoxin resistance. Science 232:977-980.